ISTANBUL TECHNICAL UNIVERSITY ★ GRADUATE SCHOOL OF SCIENCE ENGINEERING AND TECHNOLOGY

ELECTRO-MEMBRANE SALT SPLITTING PROCESS TO PRODUCE LITHIUM HYDROXIDE

Ph.D. THESIS

Abdullah Zahid TURAN

Department of Chemical Engineering

Chemical Engineering Program

AUGUST 2016

ISTANBUL TECHNICAL UNIVERSITY ★ GRADUATE SCHOOL OF SCIENCE ENGINEERING AND TECHNOLOGY

ELECTRO-MEMBRANE SALT SPLITTING PROCESS TO PRODUCE LITHIUM HYDROXIDE

Ph.D. THESIS

Abdullah Zahid TURAN
(506092003)

Department of Chemical Engineering

Chemical Engineering Program

Thesis Advisor: Prof. Dr. A. Nusret BULUTCU

AUGUST 2016

İSTANBUL TEKNİK ÜNİVERSİTESİ ★ FEN BİLİMLERİ ENSTİTÜSÜ

ELEKTRO-MEMBRAN TUZ AYRIŞTIRMA PROSESİ İLE LİTYUM HİDROKSİT ÜRETİMİ

DOKTORA TEZİ

Abdullah Zahid TURAN
(506092003)

Kimya Mühendisliği Bölümü

Kimya Mühendisliği Programı

Tez Danışmanı: Prof. Dr. A. Nusret BULUTCU

AĞUSTOS 2016

ABDULLAH ZAHİD TURAN, a Ph.D. student of ITU Graduate School of Science Engineering and Technology student ID 506092003, successfully defended the thesis entitled "ELECTRO-MEMBRANE SALT SPLITTING PROCESS TO PRODUCE LITHIUM HYDROXIDE", which he prepared after fulfilling the requirements specified in the associated legislations, before the jury whose signatures are below.

Thesis Advisor :	**Prof. Dr. A. Nusret BULUTCU** İstanbul Technical University	.....
Jury Members :	**Prof. Dr. Ahmet SİRKECİOĞLU** İstanbul Technical University	.....
	Prof. Dr. Hale GÜRBÜZ İstanbul Technical University	.....
	Prof. Dr. İ. Ersan KALAFATOĞLU Marmara University	.....
	Prof. Dr. Mehmet C. ÇAMURDAN Bogazici University	.....

Date of Submission : 30 June 2016
Date of Defense : 09 August 2016

In the name of The All-Knowing, The Wise
with endless gratitude
for every single blessing...

FOREWORD

I would like to thank my respected advisor, Prof. Dr. A. Nusret Bulutcu, for guiding and supporting me throughout the course of this study. I would like to express my special appreciation and thanks to Prof. Dr. İ. Ersan Kalafatoğlu, not only for his great effort for improving my thesis but also for his guidance in previous studies, which helped me to establish a background for the construction of this study. I am also thankful to Prof. Ahmet Sirkecioğlu for his kind assistance.
I gratefully acknowledge TÜBİTAK SAVTAG for the financial support of the project (No: 111A016) as well as the project supervisor Dr. Elif Ünveren for her valuable support since this study was performed as a part of the respective project. I would especially like to thank TÜBİTAK Marmara Research Centre Administration for making it possible for me to conduct this study at the laboratories of Institute of Chemical Technology.
I would like to express my deepest gratitude to my family for their constant love and support through all my life. …To my dear mother, Leyla Turan, who has devoted her life to me, Betül, Kevser and Mehmet being good people. …To my dear father, Prof. Dr. Mustafa Turan, who has always supported me in life with a great self-sacrifice. This study would not have been possible without his constant guidance and encouragement in my scientific research career.

August 2016

Abdullah Zahid TURAN
(Chemical Engineer)

TABLE OF CONTENTS

Page

FOREWORD ..... **ix**
TABLE OF CONTENTS ..... **xi**
ABBREVIATIONS ..... **xiii**
LIST OF TABLES ..... **xv**
LIST OF FIGURES ..... **xvii**
SUMMARY ..... **xix**
ÖZET ..... **xxiii**
1. INTRODUCTION **1**
1.1 Purpose of Thesis 4
1.2 Literature Review 4
1.3 Scope of Thesis 9
2. THEORETICAL BACKGROUND **11**
2.1 Electrochemistry Fundamentals 11
2.1.1 Electrochemical reactions 11
2.1.2 Electrochemistry thermodynamics 13
2.1.3 Electrochemistry kinetics 17
2.1.4 Faraday's law and reaction rate 19
2.1.5 Ionic conductivity and mobility 21
2.2 Electromembrane Process Fundamentals 28
2.2.1 Properties of ion-exchange membranes 28
2.2.1.1 General features 28
2.2.1.2 Preparation of ion-exchange membranes 30
2.2.1.3 Ion-exchange equilibrium 34
2.2.1.4 Electrochemical equilibrium and Donnan potential 35
2.2.2 Transport in ion-exchange membranes 39
2.2.2.1 Definition of the flux term 39
2.2.2.2 Transport number and membrane permselectivity 41
2.2.2.3 Water transport through membrane 43
2.2.2.4 Effect of membrane heterogeneity in transport 44
2.3 Electromembrane Process Applications 46
2.3.1 Electrodialysis 46
2.3.2 Electrosynthesis 48
2.3.3 Fuel cells 49
3. ELECTROMEMBRANE PROCESS for LIOH PRODUCTION **51**
3.1 Batch Process 51
3.1.1 Anolyte mass balance 52
3.1.2 Catholyte mass balance 54
3.2 Continuous Process 56
3.2.1 Anolyte mass balance 58
3.2.2 Catholyte mass balance 62

4. EXPERIMENTAL STUDIES 65
4.1 Overview of Experimental Studies 65
4.2 Materials and Equipment 66
4.3 Chemical Analysis Methods 67
4.4 Membrane Characterization 68
4.4.1 Experimental 69
4.4.1.1 Pre-treatment of membranes 69
4.4.1.2 Determination of water content 69
4.4.1.3 Determination of ion exchange capacity 69
4.4.2 Results 70
4.5 Anolyte preparation and purification 71
4.5.1 Purpose 71
4.5.2 Experimental 71
4.5.3 Results 72
4.6 Conductivity/pH v.s. Concentration Relation of Electrolytes 73
4.6.1 Purpose 73
4.6.2 Experimental 73
4.6.3 Results 75
4.7 General Membrane Behaviour in The Electrochemical Production of Lithium Hydroxide 82
4.7.1 Purpose 82
4.7.2 Experimental 82
4.7.3 Results 85
4.8 Determination and Regression Modelling of Transport Numbers 92
4.8.1 Purpose 92
4.8.2 Experimental 92
4.8.3 Results 96
4.8.3.1 Ion transport numbers 96
4.8.3.2 Water transport number 108
4.9 Comparison of the Transport Properties of Different Membranes 111
4.9.1 Purpose 111
4.9.2 Experimental 111
4.9.3 Results 112
4.9.3.1 Ion transport numbers 112
4.9.3.2 Water transport numbers 121
4.9.3.3 Comparison of membrane performances 123
5. CONCLUSIONS 131
REFERENCES 137
APPENDICES 145
CURRICULUM VITAE 149

ABBREVIATIONS

AEM	**:** Anion exchange membrane
ANOVA	**:** Analysis of variance
BV	**:** Bed volume
CE	**:** Current efficiency
CEM	**:** Cation exchange membrane
Cond	**:** Conductivity
DP	**:** Donnan potential
ED	**:** Electrodialysis
EDI	**:** Electrodeionization
EPR	**:** Electrolysis production rate
EPW	**:** Electrolysis unit power consumption
IEC	**:** Ion exchange capacity
RED	**:** Reverse electrodialysis

LIST OF TABLES

Page

Table 2.1 : Standard electrode (reduction) potentials of some reactions 16
Table 2.2 : Ionic conductivity values for some common solvent-electrolyte combinations 22
Table 4.1: Properties of the electromembrane cell (EC Electro MP-Cell)..... 67
Table 4.2: Membrane characterization results 70
Table 4.3: Results of anolyte ion exchange purification process..... 73
Table 4.4: Preliminary conductivity measurements..... 74
Table 4.5: Secondary conductivity measurements..... 77
Table 4.6: Comparison of the measured and predicted concentration values..... 78
Table 4.7: Anolyte concentration prediction according to Eq. 4.5-7. 79
Table 4.8: Anolyte concentration measurements in a larger concentration range 81
Table 4.9: Comparison of LiOH electro-membrane production costs..... 91
Table 4.10: Transport number results for N-424 membrane..... 97
Table 4.11: Multiple regression analysis comparison of two equations for T_{Li}..... 106
Table 4.12: Transport number results for N-438 and MK40 membranes..... 112
Table 4.13: Statistical test of proposed model equations..... 116
Table 4.14: The parameters of the experiments used for comparison 123

LIST OF FIGURES

Page

Figure 1.1 : Membrane electrolysis cell designs, (a) two-compartment (3) three-compartment. 2
Figure 2.1 : Common electrochemical reaction types. 13
Figure 2.2 : Process sub-steps of electrode reactions. 21
Figure 2.3 : Ions at rest (a), under electric field (b). 24
Figure 2.4 : The structure of a (a) homogeneous (b) heterogeneous cation-exchange membrane. 31
Figure 2.5 : The synthesis of a cross-linked homogeneous cation-exchange membrane. 32
Figure 2.6 : The cluster model used to describe the distribution of functional groups in perfluorocarbon-type cation exchange membranes. 32
Figure 2.7 : The chemical structure of strong (a) and weak (b) acid perfluorinated membranes. 33
Figure 2.8 : (a) The distribution of ions between membranes and solution, (b) Concentration change of ions between membranes and solution, (c) Donnan potential change between membranes and the adjacent solution. 37
Figure 2.9 : Mechanisms of ion transport through membrane. 39
Figure 2.10 : (a) Hydronium ion (b) Mechanism of proton transport through membrane. 42
Figure 2.11 : Transport mechanisms of ions in (a) homogeneous (b) heterogeneous membranes 45
Figure 2.12 : Electrodialysis process. 47
Figure 2.13 : Chlor-alkali process. 48
Figure 2.14 : Fuel cell. 50
Figure 3.1 : Mass balance of anolyte and catholyte solutions in batch process 52
Figure 3.2 : Mass balance of electrolyte solutions in continuous process. 57
Figure 4.1 : Membranes used in the experimental studies (a) N-424, (b) N-438, (c) MK-40. 68
Figure 4.2 : Anolyte preparation and pre-treatment procedure. 71
Figure 4.3 : Conductivity-concentration regression for catholyte (LiOH) solution. 76
Figure 4.4 : Conductivity-concentration regression for anolyte (Li_2SO_4) solution. 76
Figure 4.5 : The diagram of the experimental set-up for batch process (1: cell, 2-3: anolyte-catholyte reactors, 4-5: condensers, 6: power source, 7: computer, 8: cooling system, 9: heating system, 10: measuring devices). 82
Figure 4.6 : Experimental set-up for batch process, view1. 83
Figure 4.7 : Experimental set-up for batch process, view2. 83
Figure 4.8 : Current efficiency results (30°C) 86
Figure 4.9 : Current efficiency results (60°C) 86
Figure 4.10 : Electrolysis unit power consumption results (30°C). 88
Figure 4.11 : Electrolysis unit power consumption results (60°C) 88

Figure 4.12 : Current-potential relation. 89
Figure 4.13 : LiOH production rate results (30°C). 89
Figure 4.14 : LiOH production rate results (60°C). 90
Figure 4.15 : The diagram of the experimental set-up for continuous process (blue lines are unique to continuous process, 1: cell, 2-3: anolyte-catholyte reactors, 4: DC power source, 5: computer, 6: pH/conductivity measuring devices, 7: büchner funnel, 8: resin column, 9: water feed funnel). 94
Figure 4.16 : Experimental set-up (continuous process)..... 94
Figure 4.17 : (a) Main effects (b) Interaction plots for T_{Li}. 100
Figure 4.18 : Contour plots of x=OH^-, y=Li^+ (moles/kg) vs. T_{Li} at H_2SO_4 concent of a) 0% (continuous process), b) 0% (batch), c) 1%, d) 5%, e) 10%..... 102
Figure 4.19 : Contour plots of x=H^+, y=OH^- (moles/kg) vs. T_{Li} at Li_2SO_4 concentrations of a) 5%, b) 10%, c) 20%..... 103
Figure 4.20 : Contour plots of x=H^+, y=Li^+ (moles/kg) vs. T_{Li} at LiOH . concentrations of a) 1%, b) 3%, c) 7%..... 104
Figure 4.21 : Contour plots of permselectivity; a) x=Li^+, y=H^+ (moles/kg) vs. $P^{Li/H}$ (at 1% LiOH); b) x=Li^+, y=OH^- (moles/kg) vs. $P^{Li/OH}$ (at 5% H_2SO_4); c) x=H^+, y=OH^- (moles/kg) vs. $P^{H/OH}$ (at 20% Li_2SO_4). 108
Figure 4.22 : (a) Main effects (b) Interaction plots for T_{Li} (N-438)..... 113
Figure 4.23 : Contour plots of T_{Li} of N-438 membrane for x=OH^-, y=Li^+ (moles/kg) at H_2SO_4 concentrations of a) 0%, b) 5%; for x=H^+, y=OH^- (moles/kg) at Li_2SO_4 concentrations of c) 5%, d) 20%; for x=H^+, y=Li^+ (moles/kg) at LiOH concentrations of e) 1%, f) 7%..... 115
Figure 4.24 : (a) Main effects (b) Interaction plots for T_{Li} (MK-40)..... 118
Figure 4.25 : Contour plots of T_{Li} of MK-40 membrane for x=OH^-, y=Li^+ (moles/kg) at H_2SO_4 concentrations of a) 0%, b) 5%; for x=H^+, y=OH^-(moles/kg) at Li_2SO_4 concentrations of c) 5%, d) 20%; for x=H^+, y=Li^+ (moles/kg) at LiOH concentrations of e) 1%, f) 7%..... 119
Figure 4.26 : Lithium ion transport numbers (T_{Li}) of the three membranes. 124
Figure 4.27 : Hydrogen ion transport numbers (T_H) of the three membranes. 125
Figure 4.28 : Hydroxyl ion transport numbers (T_{OH}) of the three membranes. 125
Figure 4.29 : Water transport numbers (T_{H2O}) of the three membranes..... 126
Figure 4.30 : Lithium ion permselectivity against hydrogen ion ($P^{Li/H}$) of the three membranes. 127
Figure 4.31 : Lithium ion permselectivity against hydroxyl ion ($P^{Li/OH}$) of the three membranes. 127
Figure 4.32 : Hydrogen ion permselectivity against hydroxyl ion ($P^{H/OH}$) of the three membranes. 128
Figure 4.33 : Average cell voltage (V) during electrolysis..... 129

ELECTRO-MEMBRANE SALT SPLITTING PROCESS TO PRODUCE LITHIUM HYDROXIDE

SUMMARY

Electrochemical salt splitting is an important electromembrane application, which has come into prominence with the development of advanced membranes. In a salt splitting process, a salt is split to produce acid and/or alkali. The main reaction for this kind of process is water electrolysis at two electrodes.

Salt splitting process can be utilized for synthesis purposes. Lithium hydroxide can be synthesised this way as well by the electrochemical splitting of lithium sulphate. The process is superior over the conventional reaction/crystallisation process in terms of leaving no solid residue and acquiring higher purity levels. Thus, the determination of the parameters affecting on this process has to be investigated. More precisely, the investigation of the membrane transport behaviour is vital to understand this electromembrane process.

In this study, electro-membrane salt splitting process to produce lithium hydroxide using lithium sulphate in a two-compartment membrane electrolysis cell was investigated by means of determining significant parameters affecting on the process and understanding the membrane transport behaviour during electrolysis.

First, concentration-conductivity regression equations were determined in order to be able to predict instantaneous anolyte and catholyte concentrations during membrane electrolysis with the help of conductivity-pH values and without the need of analysing the electrolytes. The measured values were compared with the predicted values with the help of the established regression equation and it was found that anolyte concentration prediction gives average error values of 6.0% and 19.5% for lithium sulphate and sulphuric acid concentration, respectively. Lithium sulphate error was acceptable, yet sulphuric acid prediction led to relatively high error values, which was attributed to the logarithmic relation of pH with hydrogen ion concentration. On the other hand, lithium hydroxide could be predicted successfully with an average error value of 4.6%.

Then, general membrane behaviour was investigated in the electrochemical production of lithium hydroxide in a two-compartment membrane electrolysis cell under different process parameters (temperature, current density, catholyte concentration). The most important factor affecting on current efficiency was found to be LiOH concentration, the increase of which led to a reduction in current efficiency and that was attributed to the increasing back-transport of OH^- ions with the increase of LiOH concentration. Current density did not exhibit a significant effect on current efficiency for the current density range studied. This was possibly due to the fact that limiting current was not reached during the experiments. Temperature slightly improved current efficiency possibly due to increasing transport properties with increasing fluidity. Electrolysis unit power consumption (EPW) increased with the increase of current density due to the increasing potential with the increase of current according to Ohm's law. Power consumption also increased with

the increase of LiOH concentration due to low current efficiencies obtained at high LiOH concentrations. Furthermore, temperature increase, which led to the increase of conductivity, caused a decrease in cell potential, correspondingly a decrease in power consumption. A cost estimation targeting to obtain 10% LiOH solution revealed that the experiment with 60°C, 8% LiOH and 4 A/dm^2 operating conditions presented the optimum working parameters to produce lithium hydroxide within the studied range. This was due the fact high temperature and low current density lowers power costs while high LiOH concentration makes it possible to evaporate less water to obtain 10% LiOH solution.

In the next stage of the study, the effect of ion concentrations (Li^+ in anolyte, H^+ in anolyte and OH^- in catholyte) on transport numbers was further examined in order to examine the interactions between ions and to put forward a regression model equation, which will reflect the scientific reality observed in the membrane transport mechanism. In this step, batch and continuous membrane electrolysis experiments were carried out. The main findings were as below:

- A detailed analysis of the interactions between parameters revealed that -other than the individual concentrations terms (Li^+ and H^+ in anolyte, OH^- in catholyte)- the following critical factor pairs were effective in determining the significance of a specific ion concentration on the transport number of lithium; "$Li^+.H^+$ and Li^+/OH^-" ratios for Li^+ ion, "H^+/Li^+ and H^+/OH^-" ratios for H^+ ion and "$OH^-.Li^+$ and OH^-/H^+" ratios for OH^- ion.
- With this finding on interactions, a multiple regression equation adjusted by exponential forms of the critical factor pairs to reflect the effect of these interactions between individual terms was established. This equation gave an R-squared value of 0.953 and was helpful in predicting transport numbers of lithium with an average error value of 8.9%. The R-squared value of the equation increased even higher to 0.975 when only batch data was taken into consideration. This regression equation was also helpful in predicting transport numbers of H^+ and OH^- ions with an approximation. Transport number of water was fitted in a similar regression equation having an R-squared value of 0.912.Experiments, which were kept out of the model, were used to test these equations. The transport number of these tests could be successfully predicted with average error values of 7% and 3% for lithium and water respectively.
- It was found that the uniqueness in hydrogen ion transport mechanism affected both cation transport numbers as well as water transport number. Transport number of lithium reduced significantly with the increase of hydrogen ions. As for hydroxyl ions, the increase of its concentration also created a reduction in transport number of lithium (T_{Li}), yet much less compared to the effect of hydrogen ions due to ion exclusion. Water transport number increased with the increase of Li^+ concentration while decreased with the increase of H^+ and OH^- concentrations due to the differences in transport mechanism. These findings were compatible with literature data.
- Binary permselectivity values of lithium, hydrogen and hydroxyl ions were determined at constant concentration of the third species and were found to be in line with the other findings on membrane transport behaviour. Membrane's permselectivity for lithium ion against hydrogen ion, $P^{Li/H}$, was under unity in a large interval of concentration ratios since hydrogen ion's unique way of transport through membrane suppressed lithium's influence very strongly. As for $P^{Li/OH}$ values, permselectivity was generally very high in favour of lithium ion thanks to Donnan exclusion. Moreover, $P^{Li/OH}$ decreased with the increase of Li^+

concentration, actually with the suppression of H^+ transport. As for membrane's permselectivity for hydrogen ion against hydroxyl ion, $P^{H/OH}$ values were found to be generally much higher than unity suggesting a strong selectivity for hydrogen ion.

In the last stage of the study, the previous findings obtained with the usage of homogeneous Nafion® N-424 membrane was compared with another perfluorinated membrane (N-438) as well as a heterogeneous cation exchange membrane (MK-40) by carrying out similar regression analyses to model membrane transport. The main findings are as below:

- N-438 membrane showed similar performance as that of N-424 membrane. On the other hand, MK-40 exhibited a different and mostly a poorer performance. Moreover, concentration-transport number correlation was relatively lower. This was attributed mainly to the heterogeneous structure of MK-40, which possibly creates a more chaotic transport mechanism due to its complicated counter-ion pathway compared to the smooth pathway of homogeneous membranes and so makes it hard to put forward a regression model representing ion transport in terms of concentrations only.
- Comparison of the performances revealed that transport number of lithium was generally higher for perfluorinated homogenous N-424 and N-438 membranes than heterogeneous MK-40 membrane. Besides, hydrogen ion transport number did not change greatly according to the membrane used, which suggested that hydrogen ion's advantageous way of transport made it possible that hydrogen transport was not significantly restricted by membrane properties such as water content, fixed charge density and especially the distribution and ratio of hydrophilic domains through which ions and water are transported.
- On the other hand, the change of hydroxyl ion transport number according to the membrane type, especially according to the membrane structure (homogeneous/heterogeneous) was attributed to the differences in Donnan exclusion effect, which is a function of ion exchange capacity, solution concentration and the structure of the membrane (e.g. membrane heterogeneity). That's why heterogeneous MK-40 membrane exhibited higher hydroxyl ion transport values than the other homogeneous membranes despite its higher ion exchange capacity, which was in line with literature data.

With the help of the results of this study, lithium hydroxide concentration can be monitored and controlled during an electromembrane process, using catholyte conductivity data and the equation produced in this study. As for anolyte solution, ph/conductivity data and the regression equation produced can be helpful for the estimation of the order of anolyte concentration.

One of the most outstanding contributions of this study is that "acid-alkaline states of membranes" phenomena (Jörissen and Simmrock, 1991) was further examined with a detailed investigation of the interactions between ions and the results of this investigation was successfully expressed quantitatively with the help of regression equations.

Moreover, the mass balance relationships expressed for lithium sulphate membrane electrolysis, once coupled with the regression equations established as a result of experimental studies for the prediction of transport numbers, are able to model the whole electromembrane process. This is one of the most significant contributions of this study, i.e., one can predict the process outcomes (concentrations, efficiencies etc.) reached at any time "t" without the need of performing experiments.

ELEKTRO-MEMBRAN TUZ AYRIŞTIRMA PROSESİ İLE LİTYUM HİDROKSİT ÜRETİMİ

ÖZET

Elektrokimyasal tuz ayrıştırma, ileri teknoloji membranların geliştirilmesiyle ortaya çıkmış bir prosestir. Bu prosesin geliştirilmesinin arkasında yatan motivasyonun çoğunlukla çevresel kaygılar olduğundan, spesifik olarak ise klorsüz kostik soda üretimi ve ekonomik olarak uygulanabilir bir tuz geri kazanım prosesi arayışlarının öncü olduğundan bahsedilebilinir. Tuz ayrıştırma prosesinde bir tuz, asit ve/veya baz elde edilecek şekilde parçalanır. Bu prosesin ana reaksiyonları, hidrojen iyonu (H^+) oluşumunu sağlayan suyun anodik parçalanması ve hidroksil iyonu (OH-) oluşumunu sağlayan suyun katodik parçalanmasıdır. Anyon ve/veya katyonların iyon değiştirici membranlar vasıtasıyla seçici olarak taşınması ise prosesin temelini oluşturmaktadır.
Tuz ayrıştırma prosesi, sentez amaçlı da kullanılabilir. Lityum hidroksit (LiOH) de bu yolla, lityum sülfatın (Li_2SO_4) elektrokimyasal olarak parçalanması ile üretilebilecek bir kimyasaldır. Elektrokimyasal yöntemin, konvansiyonel reaksiyon/kristalizasyon yöntemine kıyasla;

- Kalsiyum karbonat gibi atık oluşumunun olmaması,
- Üretilen lityum hidroksitin göreceli olarak daha saf olması,

gibi nedenlerden ötürü daha üstün olduğu söylenebilir. Dolayısıyla, bu proses üzerine etki eden parametrelerin incelenmesi gerekmektedir. Özellikle, membran taşınım davranışının incelenmesi, bu elektromembran prosesin daha iyi anlaşılması açısından önem arz etmektedir.
Bu çalışmada, iki bölmeli membran elektroliz hücresinde lityum sülfatın elektrokimyasal olarak ayrıştırılması yoluyla lityum hidroksit eldesi prosesi detaylı olarak incelenmiştir. Bu doğrultuda, proses üzerine etki eden önemli parametreler tespit edilmiş ve elektroliz sırasında gerçekleşen membran taşınım davranışı izlenmiştir. Çalışmaların büyük bir bölümünde perflorine homojen Nafion® N-424 membranı kullanılmış, çalışmanın son kısmında ise iki farklı membran daha kullanılarak kıyaslamalar yapılmıştır.
Çalışmanın ilk aşamasında; pH ve iletkenlik verileri yardımıyla kimyasal analiz gerçekleştirmeden anlık olarak elektrolit konsantrasyonlarının tespit edilebilmesi amacıyla, konsantrasyon-iletkenlik regresyon denklemleri üretilmiştir. Elde edilen anolit denklemi vasıtasıyla, lityum sülfat ve sülfürik asit konsantrasyonları sırasıyla %6.0 ve %19.5 ortalama hata değerleri ile tespit edilebilmiştir. Burada lityum sülfat hatasının kabul edilebilir düşük seviyede, sülfürik asit hatasının ise biraz yüksek olduğu söylenebilir. Sülfürik asitteki bu hata, pH değerinin asit konsantrasyonu ile olan logaritmik ilişkisine bağlanmıştır. Lityum hidroksit konsantrasyonu ise katolit denklemi vasıtasıyla %4.6 gibi düşük bir hata değeri ile öngörülebilmiştir.
Çalışmanın sonraki aşamalarında ise membranlı elektroliz deneyleri gerçekleştirilmiştir. Öncelikle, iki bölmeli membran elektroliz hücresinde lityum sülfatın elektrokimyasal olarak ayrıştırılması yoluyla lityum hidroksit eldesi prosesi sırasındaki genel membran davranışı farklı parametreler altında (sıcaklık, akım

yoğunluğu, LiOH ürün konsantrasyonu) incelenmiştir. N-424 membranının kullanıldığı çalışma sonunda, akım verimi üzerine etki eden en önemli parametrenin LiOH konsantrasyonu olduğu tespit edilmiştir. LiOH konsantrasyonu artışı sonucu akım veriminin düşüşü, artan OH^- iyonu membran taşınım değerlerine bağlanmıştır. Çalışılan aralıkta akım yoğunluğu akım verimi üzerine ciddi bir etki yapmamıştır. Bu da büyük olasılıkla çalışılan aralığın "sınır akım" değerinin altında olmasından kaynaklanmaktadır. Sıcaklığın akım verimi üzerinde hafif artırıcı etkisi gözlemlenmiştir. Bu durum, sıcaklığın akışkanlık üzerindeki olumlu etkisi sonucu iyileşen taşınım özelliklerine bağlanmıştır. Artan akım yoğunluğu, beraberinde artan gerilim nedeniyle (Ohm yasası), birim elektroliz güç tüketim değerlerinde artışa neden olmaktadır. Tüketim miktarı ayrıca, akım veriminin düşmesine neden olan LiOH konsantrasyonu artışı ile artmakta, iletkenliğin artması ve gerilimin düşmesine neden olan sıcaklık artışı ile ise düşmektedir. Elde edilen veriler üzerinden bir maliyet öngörüm analizi gerçekleştirilmiş ve bu analizde %10 LiOH çözeltisi eldesi için gerekli elektroliz ve evaporasyon maliyetleri karşılaştırılmıştır. Analiz sonucunda; 60°C sıcaklık, %8 LiOH konsantrasyonu ve 4 A/dm^2 akım yoğunluğu değerlerinin, eldeki değerler arasında optimum çalışma parametrelerini oluşturduğu tespit edilmiştir. Bu durum yüksek sıcaklık ve düşük akım değerlerinin yukarıda bahsedildiği gibi elektroliz güç tüketim değerlerini düşürmesinden, yüksek LiOH konsantrasyonunun ise evaporasyon maliyetlerini düşürmesinden kaynaklanmaktadır.

Çalışmanın bir sonraki aşamasında ise, iyon konsantrasyonlarının (anolitte Li^+ ve H^+, katolitte OH^-) taşınım sayıları üzerine etkileri, iyonlar arasındaki etkileşimin tespit edilebilmesi ve membran taşınımını temsil edebilecek bir regresyon denkleminin ortaya konulabilmesi amacıyla daha detaylı bir biçimde incelenmiştir. N-424 membranı kullanılarak kesikli ve sürekli deneylerin gerçekleştirildiği bu çalışmada elde edilen ana bulgular şunlardır:

- İyonlar arasındaki etkileşim incelenmesi sonunda; belirli iyon konsantrasyon çarpım/bölüm değerlerinin, ilgili iyonun lityum taşınım değerleri (T_{Li}) üzerindeki etkisini belirlediği görülmüştür. Şöyle ki, lityum iyonunun T_{Li} üzerindeki etkisini "$Li^+.H^+$ ve Li^+/OH" çarpım çiftleri etkilemektedir. Bu değerlerin azalışı ile lityum iyon konsantrasyonunun etkisi azalmaktadır. Hidrojen ve hidroksil iyonları için ise bu çarpım çiftleri, sırasıyla, "H^+/Li^+ ve H^+/OH^-" ile"$OH^-.Li^+$ ve OH^-/H^+" değerleridir.
- Etkileşimler üzerine elde edilen bu bulgu üzerine, elde edilen çarpım çiftlerinin gerçek etkisini yansıtmak amacıyla, bu çarpım çiftleri; etkilerini değerleri azalınca azaltacak, artınca ise sabit bir değere getirecek şekilde eksponansiyel ifadelerle düzenlenmiştir. Bu eksponansiyel ifadelerle bir çoklu regresyon denklemi türetilmiştir. 0.953 R^2 değerine sahip olan bu denklem, lityum iyonu taşınım sayı değerlerini %8.9 gibi bir ortalama hata değeri ile öngörebilmektedir. Bu denklem üzerinden ayrıca, H^+ ve OH^- iyonları taşınım değerleri yaklaşık olarak tespit edilmiştir.
- Elde edilen bu denklemin R^2 değeri, sadece kesikli proses verisinin ele alınmasıyla 0.975 değerine kadar yükselebilmiştir. Bu durum, -her ne kadar sürekli proses sırasında konsantrasyonlar sabit tutulmaya çalışılmış olsa da, baş ve son konsantrasyonlar arasında hata getirebilecek muhtemel dalgalanmalara bağlanmıştır. Dolayısıyla sadece kesikli proses verilerinin işlenmesi durumunda gerçek durumunu daha iyi yansıtan bir denklem elde edilebilmiştir. Bununla birlikte, sürekli proses düşük asitlik koşullarını daha iyi yansıtabildiği için, bu

koşullar için daha uygundur. Dolayısıyla, çalışılan koşula (asitlik seviyesine) göre, iki denklemden biri tercih edilebilir.

- Su taşınım sayısı da, iyon ve su taşınımı arasında doğrudan bir korelasyon olması açısından, benzer bir regresyon analizine tabi tutulmuştur. Elde edilen denklem 0.912 R^2 değerine sahiptir.
- Regresyon denklemlerinde kullanılan deney verileri dışında, denklemleri test amaçlı iki deney daha gerçekleştirilmiştir. Bu deneyde elde edilen sonuçları üretilen denklemler; lityum için %7, su için ise %3 hata ile öngörebilmiştir.
- Hidrojen iyonunun kendine has taşınım mekanizmasının (tunneling) hem iyon hem de su taşınım sayılarına etki ettiği görülmektedir. Hidrojen konsantrasyonunun artışı ile birlikte lityum iyon taşınım değerlerinde ciddi bir düşüş yaşanmıştır. Hidroksil iyonlarına gelince, Donnan benzer iyon dışlama prensibi sayesinde daha az seviyede olmakla birlikte, lityum iyon taşınım sayısında hidroksil iyonu artışı ile birlikte de düşüş meydana gelmiştir. Membrandan su taşınım mekanizmasında, iyonların hidrat kabukları ile birlikte su taşınması mekanizmasının daha ağır bastığı görülmüştür. Bu yüzden, lityum taşınım katsayısının artışı ile birlikte su taşınımı artarken, membran geçişi sırasında beraberinde çok daha az su taşıyan hidrojen ve hidroksil iyonlarının artışı ile azalmaktadır. Bu bulgular literatür verisi ile uyumluluk arz etmektedir.
- İkili seçici geçirgenlik (perm-selektivite) değerleri üçüncü iyon konsantrasyonunun sabit olduğu durumlar için hesaplanmıştır. Hidrojen iyonuna karşı lityum iyonunun membran tarafından seçicilik değerleri, $P^{Li/H}$, geniş bir konsantrasyon aralığında 1'in altında olmaktadır. Bu da, taşınım sayısı sonuçlarında görüldüğü gibi, hidrojen iyonunun avantajlı membran geçiş mekanizmasının bir sonucu olarak lityum geçişini bastırması şeklinde yorumlanmaktadır. $P^{Li/OH}$ değerlerine gelince, Donnan benzer iyon dışlama prensibi sayesinde, lityumun seçiciliğinin yüksek olduğu görülmektedir. İlginç bir sonuç, sabit asit konsantrasyonunda, lityum konsantrasyonunun artışı ile birlikte $P^{Li/OH}$ değerlerinin azalmasıdır. Bu dolaylı bir etkidir, şöyle ki, lityum iyonunun artışı ile birlikte hidroksil iyon geçişine en büyük engel olan hidrojen etkisi bastırılmış olmaktadır. Hidrojenin bu bastırma etkisi yüksek $P^{H/OH}$ değerlerinden de anlaşılmaktadır.
- Genel olarak, membran taşınımında tüm iyonların etkili olduğu söylenebilirken, hidrojen iyon konsantrasyonunun daha kilit bir parametre olduğu iddia edilebilir. Dolayısıyla, bu proseste hidrojen iyon konsantrasyonunun, özellikle de Li/H oranının kontrol edilmesinin büyük önem arz ettiği söylenebilir. Bu durum da reaksiyon ile nötralizasyonun gerçekleştirildiği sürekli anolit beslemesi ile mümkündür.

Çalışmanın son bölümünde, homojen Nafion® N-424 membranı kullanılarak elde edilen sonuçlar, bir başka homojen membran (N-438) ile birlikte heterojen MK-40 membranı kullanılarak gerçekleştirilen çalışmalar ile kıyaslanmıştır. Genel bulgular şunlardır:

- N-438, genel olarak N-424 ile benzer performans sergilemiştir. Bununla birlikte, MK-40 membranının heterojen yapısı, daha farklı ve genellikle daha düşük bir performans göstermesine neden olmuştur.
- N-424için oluşturulmuş olan regresyon denklemleri diğer iki membran için de oluşturulmuş ve denklemlerin testi için model dışında tutulan ayrı test deneyleri gerçekleştirilmiştir. Tüm membranların denklem yapıları yaklaşık olarak aynıdır. N-438 membran denklemi; 0.974 R^2 değerine, model verileri için ortalama %6.4 test verisi için %12.0 lityum taşınım sayısı öngörme hatasına sahiptir. MK-40

membran denklemi ise; 0.859 R^2 değerine, model verileri için ortalama %16.7 test verisi için %23.2 lityum taşınım sayısı öngörme hatasına sahiptir. MK-40 denkleminin gösterdiği bu düşük öngörüm performansı, homojen ve heterojen membranlar arasında membran taşınım yolundaki farklılığa bağlanmıştır. Homojen membranlar, yüklü bölgeler üzerinde daha düzgün bir iyon geçiş yolu sağlarken, heterojen membranlar ise daha uzun ve kompleks bir iyon geçiş yolu sunarlar. Dolayısıyla, sadece konsantrasyonlar üzerinden membran geçiş sayılarını tanımlayabilmek heterojen MK-40 membranı için daha güç olmuştur.

- Membran performanslarının karşılaştırılması sonucunda; lityum iyonu taşınım sayısının, perflorine homojen N-424 ve N-438 membranları için, heterojen MK-40 membranına kıyasla genelde daha yüksek olduğu görülmüştür. Bunun yanısıra, hidrojen iyonu taşınım sayısı kullanılan membran türüne göre çok fazla değişiklik göstermemiştir. Ancak hidroksil iyonunun, özellikle heterojen membran kullanımıyla beraber yükseliş gösterdiği görülmüştür. Bu sonuçlar göstermektedir ki; hidrojen iyonu, sahip olduğu özel taşınım mekanizması sayesinde, taşınım sayılarının dağılımına o kadar etkilidir ki, membran yapısı (sabit yük miktarı, heterojenite, hidrofilik bölge oranı vb.) bu etkinin ortaya çıkışında sınırlayıcı bir etken olmamaktadır.
- Bununla birlikte, hidroksil iyonunun taşınım sayısında membran tipine göre oluşan farklılıklar, membranların Donnan benzer iyon dışlama performansındaki farklılıklardan kaynaklanmaktadır. Membran heterojenitesinin artması, çözelti ile dolu olan mikropor oranında artışa, bu da membran içerisinde daha fazla sayıda benzer iyon (hidroksil iyonu) bulunmasına neden olmaktadır. Bu yüzden, heterojen MK-40 membranı yüksek iyon değiştirme kapasitesine rağmen bu noktada daha düşük bir performans sergilemiştir.
- Membranların su taşıma sayıları ise, bu membranların iyon taşıma katsayıları ile yakından ilişkilidir. Bu yüzden, lityum iyon taşıma sayısı genelde daha düşük olan MK-40 membranı, diğer membranlara kıyasla daha düşük su taşıma sayılarına sahiptir. Özellikle, daha az su taşıyan hidroksil iyonunun MK-40 membranından daha yüksek oranda geçiyor olması, bu durumun başlıca nedenidir.

Bu çalışma sonucunda elde edilen veriler ışığında, elektromembran proses sırasında ürün lityum hidroksit konsantrasyonunun izlenme ve kontrolünün gerçekleştirilmesine olanak sağlayan bir denklem türetilmiştir. Anolit konsantrasyonun belirlenmesinde ise sayısal olarak yüksek hata bulunmasına rağmen, en azından konsantrasyon seviyesinin az çok belirlenebilmesi açısından anolit pH-iletkenlik verilerinin ölçülüp, elde edilen regresyon denkleminde kullanılmasının faydalı olacağı düşünülmektedir.

Çalışmanın öne çıkan sonuçlarından biri, literatürde "membranların asit/alkali durumları" (Jörissen and Simmrock, 1991) olarak adlandırılmış kavramın, iyon etkileşimlerinin daha detaylı bir biçimde incelenerek ele alınması ve elde edilen sonuçların sayısal bir ifadeye dökülmesidir.

Bunun yanısıra, çalışmada lityum sülfat membran elektroliz için ortaya konulan kütle enerji denkliklerinin, deneysel çalışmalar sonucunda elde edilen, taşınım sayılarını ifade etmekte kullanılan ampirik ifadelerle birleştirilmesi sonucu tüm prosesi tanımlayabilen matematik bir model ortaya çıkmaktadır. Bu çalışmanın getirdiği en önemli katkılardan biri budur. Şöyle ki; elektromembran proses boyunca, herhangi bir "t" anında bu model yardımıyla proses çıktıları (konsantrasyon, verim vs.), deneysel bir çalışmaya gerek kalmadan öngörülebilmektedir.

1. INTRODUCTION

Membranes, which are permselective transporters of species from one phase to another, have become widespread due to their growing number of industrial applications. Membrane processes can be broadly categorized according to the governing driving force (concentration difference, electric potential or pressure difference) which makes transport possible. Among these, electromembrane processes are of industrial significance, where the transport is controlled by the movement of charge carriers i.e. ions with the help of the driving force of electric potential difference (Strathmann, 2004).

Electromembrane processes can be classified in quite different groups based on their basic concept, practical application and technical relevance. However, in all these processes there is a common principle, which is that membranes carrying electrical charges are used to control the transport of ionic species under the influence of electric potential difference (Strathmann, 2004). These membranes are called "ion-exchange membranes" and they are the key components of an electromembrane process. The basic function of an ion exchange membrane is based on the Donnan membrane equilibrium principle, enabling the transport of counter ions while rejecting the transition of co-ions having the same sign of the fixed charges of the membrane (Koter and Warszawski, 2000; Nagarale et al, 2006).

A large variety of electromembrane processes have been developed so far for use in the production of sodium hydroxide via chlor-alkali process, the concentration of seawater for sodium chloride production by electrodialysis, desalination of seawater, desalination of cheese whey solutions, demineralization of sugar cane juice, etc. (Nagarale et al, 2006; Tanaka, 2007).

Salt splitting, an important electromembrane application, can be claimed to have come into prominence with the development of advanced membranes. The motivation in the development of electrochemical salt splitting process is mainly due to environmental concerns such as the demand for a chlorine-less caustic soda

production process and the search for an economically viable salt solution disposal process (Genders, 1995). In a salt splitting process, a salt is split to produce acid and/or alkali. The main reaction for this kind of process is water electrolysis at two electrodes. Anodic reaction;

$$H_2O \rightarrow 2H^+ + \frac{1}{2}O_2 + 2e^- \tag{1.1}$$

produces hydrogen ions and oxygen, while cathodic reaction;

$$2H_2O + 2e^- \rightarrow 2OH^- + H_2 \tag{1.2}$$

produces hydroxyl ions and hydrogen. The transport of the dissociated ions of the salt is controlled by the design of the membrane electrolysis cell. For a two-compartment cell with a cation-exchange membrane, X^+ ion of XY salt moves through the membrane to the catholyte solution, where XOH alkali of the salt is formed, while in the anolyte solution HY acid of the salt is formed (Figure 1.1a). However, in a three-compartment cell of two (anion and cation-exchange) membranes, both cation (X^+) and anion (Y^-) of the salt are transported in opposite directions through cation and anion-exchange membranes, respectively, and acid, alkali and salt are all in three different compartments (Figure 1.1.b). With the help of this electrochemical salt splitting process, hydroxides such as lithium hydroxide can be produced from their salts.

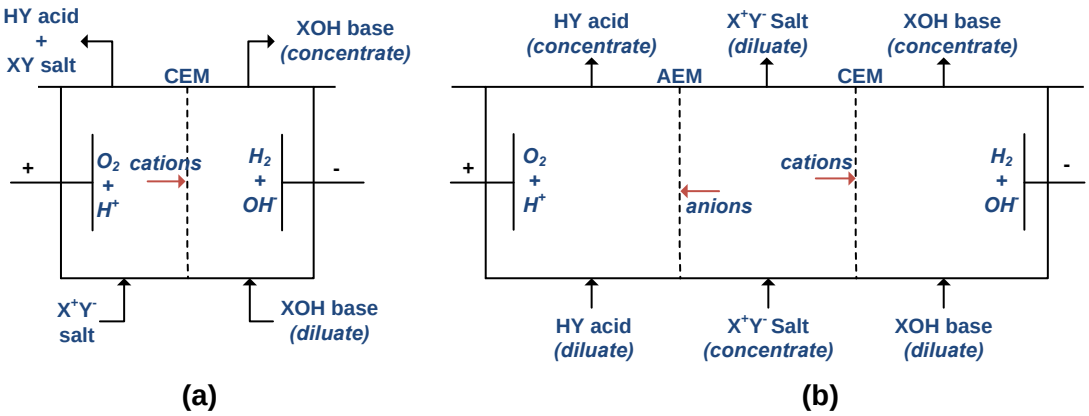

Figure 1.1 : Membrane electrolysis cell designs, (a) two-compartment (3) three-compartment.

Lithium hydroxide has several applications either as direct use or as a raw material for the production of other compounds in chemical industry. It can be used for the preparation of several lithium salts. The main use is the preparation of lithium stearate, which is utilized in lubricating greases. These greases have good viscosity

properties up to 200°C and are practically insoluble in water. Lithium hydroxide is also used in the production of dyes. Lithium hydroxide can be either in anhydrous or monohydrate form. In its anhydrous form, it can be used as an absorbent for carbon dioxide in confined spaces, especially in submarines and space vehicles. Anhydrous lithium hydroxide absorbs 450 mL CO_2 per gram, which means that nearly 750 g of lithium hydroxide can absorb the carbon dioxide generated by one person in one day (Kamienski et al, 2000).

Commercially lithium hydroxide is produced by the reaction between lithium carbonate and calcium hydroxide:

$$\mathrm{Li_2CO_3 + Ca(OH)_2 \rightarrow CaCO_3 + 2LiOH} \tag{1.3}$$

This yields quite dilute lithium hydroxide solutions (up to 3.5% lithium hydroxide). Working at higher concentration leads to the loss of lithium carbonate in the calcium carbonate residue due to the fact that lithium carbonate solubility is reduced by the presence of lithium hydroxide. Intensive agitation is required for the reaction to complete in many hours since the starting materials have quite low solubility. The practically insoluble calcium carbonate is removed and lithium hydroxide monohydrate is crystallized from the mother liquor by evaporation. During filtration process, lithium can also be lost in the residue together with calcium carbonate (Wietelmann and Steinbild, 2000).

Another way of producing lithium hydroxide is by membrane electrochemical process. The main advantages of this process over the conventional method described above are as follows:

- No solid residue (like calcium carbonate in the conventional method) is formed.
- The produced lithium hydroxide is expected to be purer since there is no source of impurity in the starting materials (like calcium hydroxide in the conventional method) and with the help of the permselective behaviour exhibited during membrane transport.

Thus, the determination of the parameters affecting this process has to be investigated. More precisely, the investigation of the membrane transport behaviour is vital to understand this electromembrane process. Moreover, optimization will give insight into the economy of the process.

1.1 Purpose of Thesis

The aim of this study is to investigate the electro-membrane salt splitting process to produce lithium hydroxide using lithium sulphate in a two-compartment membrane electrolysis cell by means of determining significant parameters affecting on the process and understanding the membrane transport behaviour during electrolysis. Specific objectives are:

- To establish a conductivity/pH vs. concentration regression equation in order to predict instantaneous concentration changes during membrane electrolysis to produce lithium hydroxide, which is very beneficial in process monitoring and control.
- To investigate the general membrane behaviour in the electrochemical production of lithium hydroxide in a two-compartment membrane electrolysis cell under different process parameters (temperature, current density, catholyte concentration), to compare its performance with similar previous studies and finally to recommend optimum membrane electrolysis parameters for this process based on a production cost estimation realized using the results of this study.
- To further investigate in detail the effect of ion concentrations (Li^+ and H^+ in anolyte, OH^- in catholyte) on transport numbers in order to examine the "acid/alkaline states of membranes" phenomenon as called by Jörissen and Simmrock (1991) and put forward a regression model equation, which will reflect the scientific reality observed in the membrane transport mechanism in a sensible manner.
- To compare the findings on Nafion® N-424 membrane with another perfluorinated membrane (N-438) as well as a heterogeneous cation exchange membrane (MK-40) by carrying out similar regression analyses to model membrane transport.

1.2 Literature Review

Electrochemical splitting studies of several salts such as sodium sulphate (Na_2SO_4), potassium sulphate (K_2SO_4) and Li_2SO_4 salts can be found in literature (Ryabtsev et

al, 2004; Rakib et al, 1999a, 1999b; Tzanetakis et al, 2003; Jörissen and Simmrock, 1991; Ata et al, 2008).

Jörissen and Simmrock (1991) investigated the mechanism of membrane transport in electrolysis and electrodialysis of sodium sulphate using Nafion® 390. They found that the current efficiency, which can also be defined as the transport number of sodium, is either a function of acid to salt ratio in the anolyte or a function of hydroxide concentration in the catholyte depending on the relative concentration values. At constant acid concentration, increasing concentration of alkaline has no effect on current efficiency until a threshold value. Likewise, at constant alkaline concentration, increasing concentration of acid has no effect on current efficiency until a threshold value. They defined this phenomenon as "acid/alkaline states of membranes".

Rakib et al. (1999a), in their to study sodium sulphate electrochemical salt splitting using Nafion® 350, reached similar findings as those of Jörissen and Simmrock (1991), i.e. the fact that membrane transport is controlled either by acid to salt ratio in anolyte or hydroxide concentration in catholyte. Moreover, they found that water transport numbers are close to hydration numbers of sodium and hydrogen ions, which suggests that water transport mechanism is mainly by ion hydration.In a similar study, they found that acid/salt ratio was dominant factor in the region they studied and they expressed sodium transport number in a 4th degree polynomial, where the only independent parameter was acid/salt ratio (Rakib et al, 1999b).

Tzanetakis et al. (2003) compared the performance of Nafion® 117 and Pall R1010membranes for the electrochemical splitting of sodium sulphate salt in a two-chamber membrane electrolysis cell. They found that different flow conditions in the membrane cell did not have a crucial influence on the current efficiency. The production rate was greater at higher current densities, however a slight decrease of the current efficiency was observed in the studied range. It was decided that salt concentration must be as high as possible, since higher concentration resulted in an increase of the sodium transport number. The influence of temperature did not have a significant effect on the system performance, in terms of current efficiencies and base concentrations. The use of the Pall R1010 as a CEM resulted in an enhancement of the current efficiency compared to Nafion® 117. In another study, Tzanetakis et al. (2005) carried out the same electrochemical process in two- and three-chamber cells

and compared the performance of the two. They found that the three-compartment cell gave a slightly lower performance, compared to the two-compartment cell, in terms of the maximum concentrations of base obtained. However, the three-compartment configuration produced high purity of acid and base at the expense of higher cell voltage and energy consumption (approximately 50%).

Ata et al. (2008) studied anion and cation exchange membranes for the salt partitioning of potassium sulphate. Membranes were Tokumaya Soda Co. production. A transport model was presented explaining experimental results and was based on properties of mono and multivalent anions. While multivalent anions can interact with membrane fixed charges, reducing membrane's ability to stop H^+ ion leakage through the anion exchange membrane; they can also combine with H^+ ions and then transport them in the desired direction into the anolyte. These opposing effects were determined to have influence on the overall permselectivity of anion exchange membranes.

Okada et. al, in a series of publications, studied ion and water membrane transport characteristics during electrodialysis (Okada, 1996, 1999a, 1999b; Okada et al, 1992, 1998a, 1998b, 2002, 2005; Xie and Okada, 1996; Saito et al, 2004, 2005). Their main findings were on the mechanisms of cation and water transport and on how the two interact.

Ryabtsev et al. (2004), in their study to produce lithium hydroxide, studied the performance of MK-40 membrane. They converted lithium carbonate to lithium sulphate, which is then alkalinized to remove impurities as hydroxide precipitates. In their study, they achieved to produce lithium hydroxide at over 50% current efficiencies.

Hamani et al. (2013) carried out a physical-chemistry study of modified Nafion® 117 membrane in order to establish a correlation between the transport number and current–voltage data of the membrane. They found that a modification on membrane surface changed the permselectivity characteristics of the membrane.

Davis (2006) studied an electrochemical cell process designed for the salt-splitting of sodium sulphate cake from a pulp mill into sodium hydroxide and sulphuric acid. He observed that current efficiency decreased as the sodium hydroxide catholyte concentration increased from 1 to 5 M, which was attributed to the increase of back-

transport of hydroxide ions from the cathode compartment to the centre compartment. The cell could produce 5 M sodium hydroxide solution using Nafion® 324 membrane at 48% current efficiency.

Carlberg (2015), in his study to investigate the electrochemical splitting of sodium sulphate, found that water transport through the membrane is highly affected by the cation concentration due to the transport of ions having hydrated shells.

Jajali et al. (2009) investigated the effects of various operating parameters on the cell voltage and current efficiency of a laboratory-scale chlor-alkali membrane cell operating at low caustic conditions. Taguchi and ANOVA techniques were employed for experimental design and data analysis, respectively. They found that current density (1-4 kA/m^2) and cell temperature (25-90°C) were the most striking parameters on the cell voltage. In case of current efficiency, the most significant parameter was brine concentration (20-30%) while cell temperature did not affect current efficiency significantly.

Geise et al. (2014) investigated membrane behaviour in ammonium bicarbonate solutions. They characterized the permselectivity of four commercial ion exchange membranes (Selemion CMV and PCCell PC-SK cation exchange membranes, Selemion AMV and PCCell PC-SA anion exchange membranes) in aqueous solutions of sodium chloride, ammonium chloride, sodium bicarbonate, and ammonium bicarbonate to understand how these specific ions affect ion transport in ion exchange membranes. They found that permselectivity was highest in sodium chloride and lowest in ammonium bicarbonate solutions, and the nature of both the counter- and co-ions appeared to influence measured permselectivity. They stated that the higher binding affinity between fixed charge sites and counter-ions within the membrane, the lower the effective membrane charge density, which led to a decrease in permselectivity.

Sata et al. (2002) reviewed the studies on selective permeation of some cations (Ca^{2+}, Mg^{2+}, Na^{+} etc.) through a cation exchange membrane in electrodialysis. It is stated in this study that the cation exchange groups, which have strong interaction with specific cations, cause decrease in the current efficiency and increase in voltage drop across the membrane. Since the number of possible cation exchange groups are limited (sulfonic acid, carboxylic acid and phosphonic acid groups, etc.), it is a

challenge to produce membranes having high selectivity for specific molecules and inorganic ions. Preparation of composite polymer membranes and using chelate forming agents were reported to possible solutions to overcome these problems.

Ersöz et al. (2001) investigated the sorption of NaCl and $CaCl_2$ and monovalent-divalent cation salt mixtures on the polysulfone cation exchange membranes (ICE-450 SA_3S and SA_3T). It was stated that the interaction between cations and the fixed anionic charge was reduced by hydration of the ions, which led to the conclusion that the extent of monovalent cation uptake regulated the absorption of mobile divalent cations.

Firdaous et al. (2007) carried out an experimental study in order to understand how divalent ion repulsion takes place in monovalent selective cation exchange membranes. They found that sodium ions, which remain sensitive to the concentration in solution, would profit from a weak repulsion energy at the solution-membrane interface and from a weak affinity towards the negative exchange sites, therefore of a great mobility from which a large diffusivity compensating the low number of available sites for their transfer, what would enable them to maintain a transfer flux higher than other divalent cations.

Kim (2010) studied electrodialysis process in order to improve the understanding of the properties of the boundary layer that limit the rate of the ionic separation in electrodialysis. The rate-limiting properties were found to be the thickness of the boundary layer, cationic partitioning and limiting current in the boundary layer.

Yazicigil (2007) investigated the regeneration of acid and base from different salt forms of potassium by electrodialysis in a two-compartment electromembrane cell. He found that the type of salt is effective on the transport potassium ions and the transport rate changed in the following order $-NO_3 > -Cl > -SO_4$.

Shibli and Noel (1993) investigated conductivity and transport properties of commercial membranes (Nafion® 315, 901 and 961) to be used in an electrochemical alkali concentrator. They found that the increase in current density caused a slight decrease in the Na^+ transport number. Moreover, they observed that the relative water transport decreased with increasing temperature due to the fact that the hydration number of Na^+ ions decrease with increasing temperature and water primarily passes through the membrane as water of hydration.

In a previous study by the author and his colleagues, electrochemical splitting of borax solution was studied to produce boric acid and sodium hydroxide using Nafion membranes (Turan et al, 2012a, 2012b; Elbeyli et al, 2015). Borax solution was fed to the anolyte chamber while sodium hydroxide solution was fed to the catholyte chamber. As sodium ions in borax solutions passed through the membrane under electrical field, boric acid formed in anolyte solution while sodium hydroxide was produced in catholyte with the reaction of transferred sodium ions with the cathodically generated hydroxyl ions. The results showed that current efficiency (sodium transport number) was a strong function of sodium hydroxide concentration, the increase of which caused a decrease in current efficiency. On the other hand, boric acid having higher purity than the one produced in conventional method (colemanite-sulphuric acid reaction) was successfully obtained upon crystallisation of anolyte solution.

In addition to the studies mentioned above, there are a number of other studies on electromembrane processes in literature (Ceynowa et al, 1981; Zabolotsky and Nikonenko, 1993; Chapotot et al, 1994; Choi et al, 2001; Kaveh et al, 2008; Volkov et al, 2011; Kim et al, 2012; Calatayud et al, 2014). These studies mainly cover investigation of membrane transport characteristics. However, as far as is known, a detailed study does not exist in literature investigating ion concentrations and the interactions between them comprehensively in order to put forward a regression model, which explains permselective behaviour of the membrane and which can predict transport numbers successfully.

1.3 Scope of Thesis

This study involves both theoretical knowledge and experimental data on an electro-membrane salt splitting process. In Chapter 2, the theoretical background on both electrochemistry and electromembrane processes is explained in detail with a special emphasis on transport phenomena in ion exchange membranes. In Chapter 3, electrochemical splitting of lithium sulphate via membrane electrolysis process is modelled by mass balances in anolyte and catholyte chambers. The balance equations required for both batch and continuous processes are produced. The produced equations are used in the calculation of experimental study results.

Chapter 4 includes all of the experimental study carried out and mainly consists of the following sub-studies: In Section 4.4, membrane characterization is performed in terms of water content and ion exchange capacity. Section 4.5 explains the preparation and purification study of anolyte (Li_2SO_4) solutions, which is performed by acidic reaction and ion exchange resin treatment processes. Section 4.6 involves the studies to establish a conductivity/pH vs. concentration regression equation in order to predict instantaneous concentration changes during membrane electrolysis to produce lithium hydroxide. In Section 4.7, general behaviour of homogeneous perfluorinated Nafion® N-424 membrane in the electrochemical production of lithium hydroxide in a two-compartment membrane electrolysis cell under different process parameters (temperature, current density, catholyte concentration) is investigated. Within this section, the performance of Nafion® N-424 is compared similar previous studies and optimum membrane electrolysis parameters for this process is recommended based on a production cost estimation. In Section 4.8, based on the findings in the previous section (Section 4.7), the effect of ion concentrations (Li^+ in anolyte, H^+ in anolyte and OH^- in catholyte) on transport numbers is further investigated and a regression model equation is put forward reflecting the scientific reality observed in the membrane transport mechanism. Also, in this section, continuous feed experiments are done in addition to batch experiments in order to both supply near zero acidity condition and to simulate a constant concentration process, which is required to reflect industrial process conditions. In Section 4.9, the findings on N-424 are compared with another perfluorinated membrane (N-438) as well as a heterogeneous cation exchange membrane (MK-40). Similarly, regression analyses are carried out for N-438 and MK-40 membranes to model membrane transport.

2. THEORETICAL BACKGROUND

Electromembrane processes are based on several scientific phenomena. First of all, it should be noted that the main driving force in this process is “electric field”. With an input of electrical power, both electrode reactions and transport of species can be realized. So, the issues related with electrochemistry such as the nature of electrode reactions, the behaviour of electrolytes under electric field, the change of conductivity etc. has to be handled to be able to investigate electromembrane processes.

On the other hand, in an electromembrane process, ion-exchange membrane is the vital element governing the transport of species. That’s why; the scientific ground about ion-exchange membranes has to be explained. The issues related with ion-exchange membranes mainly focus on the selectivity in mass transport. In this sense, the important concepts are Donnan exclusion phenomena, perm-selectivity of membrane, transport number of a certain species through membrane etc.

All these phenomena about electrochemistry and ion-exchange membranes will be further explained in this chapter in order to be able to understand the actual mechanism operating at the background.

2.1 Electrochemistry Fundamentals

2.1.1 Electrochemical reactions

Redox reactions, in other words, reduction-oxidation reactions, cause electron transfer to/from a molecule or ion changing its oxidation state. To define clearly, a simple example is given;

$$2.\mathrm{Mg} + \mathrm{O_2} \rightarrow 2.\mathrm{Mg^{2+}O^{2-}} \tag{2.1}$$

In the example above, magnesium reacts with oxygen to give magnesium dioxide. However, this overall reaction is actually composed of two half reactions. In one of

these, neutral O_2 (state = 0) is reduced to O^{2-} level (state = -2), while in the other, neutral Mg is oxidised to Mg^{2+} level. These half reactions are;

$$O_2 + 4e^- \rightarrow 2.O^{2-} \tag{2.2}$$

$$2.Mg \rightarrow 2.Mg^{2+} + 4e^- \tag{2.3}$$

Electrochemical reactions are a kind of redox reactions which take place in a solution at the interface of an electron conductor (electrode) and an ionic conductor (electrolyte), and which involve electron transfer between the electrode and the electrolyte or species in solution. From a reaction chemistry point of view, electrochemical reactions are heterogeneous electrolyte-electrode reactions. Electrochemical reactions can occur in several ways. Some of the common electrochemical reactions, as shown in Fig. 2.1 are (Pletcher and Walsh, 1990);

- Electron transfer reaction: e.g. Fe^{3+} in solution is reduced to Fe^{2+} by receiving an electron at the electrode.
- Metal deposition: e.g. Cu^{2+} in solution is reduced to metallic copper (Cu^0) and deposited on the electrode. This is a very common electro-winning process to produce metallic copper.
- Gas evolution: e.g. Cl^{2-} in solution is oxidised to Cl_2 gas at the electrode. This reaction occurs in chlor-alkali process.
- Surface film transformation: e.g. PbO_2 surface reacts with H^+ and $SO4^{2-}$ transforming into $PbSO_4$ while Pb^{4+} is reduced to Pb^{2+} in an electrochemical reaction.

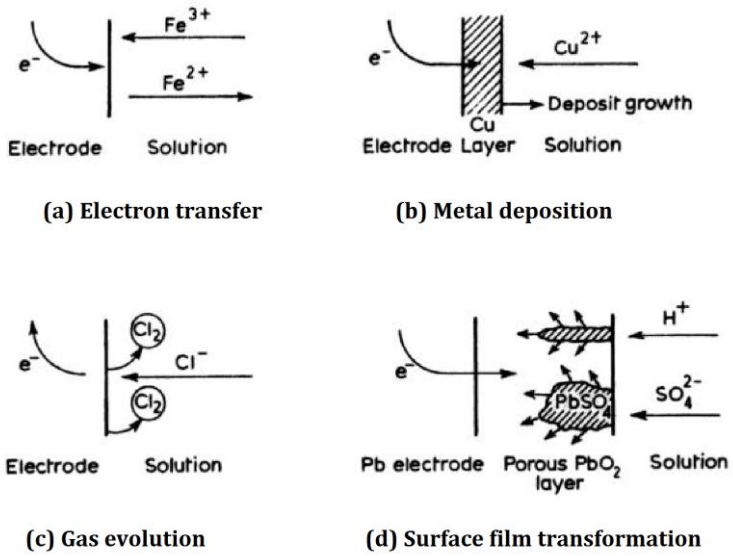

Figure 2.1 : Common electrochemical reaction types (Pletcher and Walsh, 1990).

Electrochemical reactions can only occur when the cell contains both an anode and a cathode and, in order not to experience the accumulation of net positive or net negative charge somewhere in the cell, the extent of reduction at the cathode and oxidation at the anode must be the same. This principle is called **electro-neutrality**, which makes it essential to meet the following requirements (Pletcher and Walsh, 1990):

- Electrons must pass from anode to the cathode through an external electrical circuit which connects the two electrodes for electrolysis to occur.
- Within the cell, the structure must be appropriate for charge transfer between the electrodes.

2.1.2 Electrochemistry thermodynamics

An electrochemical reaction can either go spontaneously or non-spontaneously. If the Gibbs free energy of a reaction is smaller than zero ($\Delta G < 0$), then the reaction is spontaneous, which makes it possible to produce energy with the flow of electrons as in a fuel cell circuit. For the second case, where the Gibbs free energy of a reaction is greater than zero ($\Delta G > 0$), then the reaction is non-spontaneous, which means that input of electrical energy is required to realize the reaction (Wendt and Kreysa, 1999).

Electrical work is equal to the product of the total charge needed to drive one mole of electrons and the voltage through which the charge is driven (O'Brien et al, 2005;

Zoski, 2007). The charge required to drive a mole of electrons is 96485 C, which is a Faraday, shown as F. When the equilibrium cell voltage, E_{eq}, drives n moles of electrons; the electrical work, which is also the decrease in the free energy of reaction, is equal to (Newman and Thomas-Alyea, 2004);

$$\Delta G = n.F.E_{eq} \tag{2.4}$$

The Gibbs free energy is a function of temperature, pressure and the chemical potential of the species involved in the reaction and the general expression of the Gibbs free energy is;

$$dG = -S.dT + V.dP + \sum \mu_i . dn_i \tag{2.5}$$

where μ_i is the chemical potential and n_i is the number of moles of a certain species. Electrochemical processes are generally carried at isothermal and isobaric states. At constant temperature and pressure (2.5) becomes;

$$dG = \sum \mu_i . dn_i \tag{2.6}$$

which, upon integration, is;

$$G_{T,P,n} = \sum \mu_i . n_i \tag{2.7}$$

Differentiation of (2.7) leads to;

$$(dG)_{T,P} = \sum(n_i d\mu_i + \mu_i dn_i) \tag{2.8}$$

Combining (2.6) and (2.8) gives;

$$\sum n_i d\mu_i = 0 \tag{2.9}$$

Gibbs free energy expression can be arranged to represent the change of free energy in a reaction;

$$\Delta G = \sum_{products}(v_i . \mu_i) - \sum_{reactants}(v_i . \mu_i) \tag{2.10}$$

where v is the stoichiometric coefficient of a certain species in a reaction. In case of a electrochemical reaction shown as;

$$v_{ox}.[Ox] + n.e^- \rightarrow v_{rd}.[Rd] \tag{2.11}$$

where Rd and Ox are reduced and oxidised species, respectively. At equilibrium, the relationship is;

$$v_{rd}.\mu_{rd} - v_{ox}.\mu_{ox} - n.\mu_e = 0 \tag{2.12}$$

where μ_e is defined as;

$$\mu_e = -F.E_{eq} \tag{2.13}$$

Generally, the value of chemical potential can be defined as;

$$\mu = \mu_0 + R.T.\ln a_i \tag{2.14}$$

where μ_0 is called the standard Gibbs free energy of formation at standard conditions (298 K and 1 bar pressure) and unit activity, a. R is the gas constant (8.3145 J.mol^{-1}.K^{-1}) and T is the temperature (K).

Substitution of (2.14) and (2.13) into (2.12), one obtains Nernst equation;

$$E_{eq} = E^0 + \frac{R.T}{n.F}.\ln\frac{(a_{ox})^{\nu ox}}{(a_{rd})^{\nu rd}} \tag{2.15}$$

where E^0 is the standard cell potential of the electrochemical reaction(O'Brien et al, 2005). Standard cell potential is the potential difference formed between the anode and cathode poles of the cells. For an electrolysis circuit, where the reaction is realized with an input of power (non-spontaneously), the standard cell potential is;

$$E^0 = E_c^0 - E_a^0 \tag{2.16}$$

where E_a^0 and E_c^0 are standard reduction potentials of anode and cathode, respectively. It should be noted that the value of a standard potential is not an absolute value but a value which is compared to a reference. Saturated calomel electrode, Ag/AgCl electrode and hydrogen electrode are possible reference electrodes. Standard reduction potentials measured versus SHE (standard hydrogen electrode) is given in Table 2.1 (Petrucci et al, 2011).

In Table 2.1, standard reduction potential of H^+ is zero since it is the reference point for all potential measurements. The reactions that are highlighted in red boxes are anodic water splitting reaction in acidic medium and cathodic water splitting reaction in alkaline medium. These reactions are of primary importance since they realize in most of the industrial electrochemical process. Moreover, in this study, the main electrode reactions that occur are these water electrolysis reactions.

Table 2.1 : Standard electrode (reduction) potentials of some reactions (Petrucci et al, 2011).

Reduction Half-Reaction	E^0, V
Acidic solution	
$F_2(g) + 2e^- \longrightarrow 2F^-(aq)$	+2.866
$O_3(g) + 2H^+(aq) + 2e^- \longrightarrow O_2(g) + H_2O(l)$	+2.075
$S_2O_8^{2-}(aq) + 2e^- \longrightarrow 2SO_4^{2-}(aq)$	+2.01
$H_2O_2(aq) + 2H^+(aq) + 2e^- \longrightarrow 2H_2O(l)$	+1.763
$MnO_4^-(aq) + 8H^+(aq) + 5e^- \longrightarrow Mn^{2+}(aq) + 4H_2O(l)$	+1.51
$PbO_2(s) + 4H^+(aq) + 2e^- \longrightarrow Pb^{2+}(aq) + 2H_2O(l)$	+1.455
$Cl_2(g) + 2e^- \longrightarrow 2Cl^-(aq)$	+1.358
$Cr_2O_7^{2-}(aq) + 14H^+(aq) + 6e^- \longrightarrow 2Cr^{3+}(aq) + 7H_2O(l)$	+1.33
$MnO_2(s) + 4H^+(aq) + 2e^- \longrightarrow Mn^{2+}(aq) + 2H_2O(l)$	+1.23
$O_2(g) + 4H^+(aq) + 4e^- \longrightarrow 2H_2O(l)$	+1.229
$2IO_3^-(aq) + 12H^+(aq) + 10e^- \longrightarrow I_2(s) + 6H_2O(l)$	+1.20
$Br_2(l) + 2e^- \longrightarrow 2Br^-(aq)$	+1.065
$NO_3^-(aq) + 4H^+(aq) + 3e^- \longrightarrow NO(g) + 2H_2O(l)$	+0.956
$Ag^+(aq) + e^- \longrightarrow Ag(s)$	+0.800
$Fe^{3+}(aq) + e^- \longrightarrow Fe^{2+}(aq)$	+0.771
$O_2(g) + 2H^+(aq) + 2e^- \longrightarrow H_2O_2(aq)$	+0.695
$I_2(s) + 2e^- \longrightarrow 2I^-(aq)$	+0.535
$Cu^{2+}(aq) + 2e^- \longrightarrow Cu(s)$	+0.340
$SO_4^{2-}(aq) + 4H^+(aq) + 2e^- \longrightarrow 2H_2O(l) + SO_2(g)$	+0.17
$Sn^{4+}(aq) + 2e^- \longrightarrow Sn^{2+}(aq)$	+0.154
$S(s) + 2H^+(aq) + 2e^- \longrightarrow H_2S(g)$	+0.14
$2H^+(aq) + 2e^- \longrightarrow H_2(g)$	0
$Pb^{2+}(aq) + 2e^- \longrightarrow Pb(s)$	−0.125
$Sn^{2+}(aq) + 2e^- \longrightarrow Sn(s)$	−0.137
$Fe^{2+}(aq) + 2e^- \longrightarrow Fe(s)$	−0.440
$Zn^{2+}(aq) + 2e^- \longrightarrow Zn(s)$	−0.763
$Al^{3+}(aq) + 3e^- \longrightarrow Al(s)$	−1.676
$Mg^{2+}(aq) + 2e^- \longrightarrow Mg(s)$	−2.356
$Na^+(aq) + e^- \longrightarrow Na(s)$	−2.713
$Ca^{2+}(aq) + 2e^- \longrightarrow Ca(s)$	−2.84
$K^+(aq) + e^- \longrightarrow K(s)$	−2.924
$Li^+(aq) + e^- \longrightarrow Li(s)$	−3.040
Basic solution	
$O_3(g) + H_2O(l) + 2e^- \longrightarrow O_2(g) + 2OH^-(aq)$	+1.246
$OCl^-(aq) + H_2O(l) + 2e^- \longrightarrow Cl^-(aq) + 2OH^-(aq)$	+0.890
$O_2(g) + 2H_2O(l) + 4e^- \longrightarrow 4OH^-(aq)$	+0.401
$2H_2O(l) + 2e^- \longrightarrow H_2(g) + 2OH^-(aq)$	−0.828

2.1.3 Electrochemistry kinetics

Thermodynamics analysis of electrochemical reactions leads to the conclusion that the overall reaction will occur and current will flow whenever the two electrodes of the cell are connected by an external electrical current and either;

- the cell has a negative free energy, or
- the cell reaction has a positive energy but a voltage larger than the equilibrium cell potential is applied across the two electrodes to drive the chemical change (Pletcher and Walsh, 1990).

However, in order to be able to determine how and at what speed electrochemical reactions take place, issues related to kinetics has to be handled together with thermodynamics analysis.

In a cell, for an electrochemical reaction like (2.16) to take place, the following steps are required:

- Mass transport of Ox from bulk solution to electrode surface
- Electrode reaction as electron transfer to transform Ox into Rd.
- Mass transport of Rd from electrode surface to bulk solution.

Of these, the slowest will determine the rate of the overall reaction. In case of fast mass transport, which can be enabled by perfect mixing or fast flowrates, mass transfer limitations can be ignored and one can assume that electrode reaction is the rate-limiting step.

Moreover, it should be noted that, in practice, the potential required for an electrochemical process to be carried out is much higher than the theoretical value due to inefficiencies such as polarization at interfaces (electrode, membrane etc.) and ohmic resistance within the electrolyte.

Current density (kA/m^2), which is the amount of current fed on electrode surface, is one of the most important parameters in the electrochemistry kinetics. The rate of an electrochemical reaction depends on the electrode reactions. Some electrode reactions are quite fast and give very high current densities close to the equilibrium potential. However, some are very slow and require additional potential in order to obtain the desired current density (Pletcher and Walsh, 1990). This additional

potential beyond the equilibrium potential required for a non-spontaneous cell reaction to occur is called **overpotential** (η);

$$\eta = E - E_{eq} \tag{2.17}$$

The Butler–Volmer equation can be used to predict the current that results from overpotential when mass-transfer limitations are ignored. Eq. **(2.11)** can be considered as a reversible reaction, where forward reduction and back oxidation electrode reactions can take place with heterogeneous rate constants of k_f and k_b (cm.s^{-1}) for forward and backward reactions, respectively (Zoski, 2007). The overall current in an electrochemical process, *I*, (Amps) can be viewed as the difference between cathodic (I_c) and anodic (I_a) currents:

$$I = I_c - I_a \tag{2.18}$$

These currents are proportional to their corresponding heterogeneous rate constants:

$$I_c = F.A.k_f.C_{Ox}(0,t) \tag{2.19}$$

$$I_a = F.A.k_b.C_{Rd}(0,t) \tag{2.20}$$

where *A* is electrode area (m^2), $C_i(x,t)$ (mol.cm^{-3}) is the concentration of species *i* at the distance *x* (cm) from the electrode at time *t* (s). In this case, the reaction occurs at electrode surface, which means that x=0. Reaction rate constants can be re-written as a function of k^0, standard heterogeneous rate constant:

$$k_f = k^0.\exp\left[-\alpha.f.\left(E - E_{eq}\right)\right] \tag{2.21}$$

$$k_b = k^0.\exp\left[(1-\alpha).f.\left(E - E_{eq}\right)\right] \tag{2.22}$$

where $f=F/(RT)$ and the transfer coefficient,α, is a dimensionless parameter, which is between 0-1 and is generally accepted to be 0.5.combining the equations above;

$$I = F.A.k^0.\left\{C_{Ox}(0,t).\exp\left[-\alpha.f.\left(E - E_{eq}\right)\right] - C_{Rd}(0,t).\exp\left[(1-\alpha).f.\left(E - E_{eq}\right)\right]\right\} \tag{2.23}$$

When an electrochemical cell is at equilibrium, the net current equals to zero since cathodic current is balanced by anodic current at the same rate. This net current at equilibrium is called **exchange current density**, I_0;

$$I_0 = I_c = I_a \tag{2.24}$$

Ion-exchange density relation can be derived from the equations above as;

$$I_0 = F.A.k^0.C_{Ox}^{*(1-\alpha)}.C_{Rd}^{*\alpha} \quad (2.25)$$

where* indicates the bulk concentration of the species. Combining equations above and inserting overpotential term, one gets current vs. overpotential equation;

$$I = I_0.\left[\frac{C_{Ox}(0,t)}{C_{Ox}^*}.\exp(-\alpha.f.\eta) - \frac{C_{Rd}(0,t)}{C_{Rd}^*}.\exp[(1-\alpha).f.\eta]\right] \quad (2.26)$$

When mass transfer limitations are ignored, concentration at electrode surface can be assumed to be equal to bulk concentration, which helps (2.26) reduce to Butler-Volmer equation:

$$I = I_0.\left[\exp(-\alpha.f.\eta) - \exp[(1-\alpha).f.\eta]\right] \quad (2.27)$$

The Tafel equation represents a relation between the applied overpotential and the current that passes through the cell, which is shown as;

$$\eta = \frac{R.T}{\alpha.f} ln I_0 - \frac{R.T}{\alpha.f} log I \quad (2.28)$$

From this equation, exchange current density can be calculated at η=0 point. (2.28) can be simplified to the following form, the graphic representation of which is known as Tafel plot (Zoski, 2007);

$$\eta = a - b.\log I \quad (2.29)$$

2.1.4 Faraday's law and reaction rate

Faraday's law links the number of electrons to the number of reactants in an electrochemical reaction. That is to say, the number of reactant molecules involved in an electrode reaction is related stoichiometrically to the number of electrons flowing in the circuit. This is the basic argument of the laws formulated by Michael Faraday in 1832–1833 (Bagotsky, 2006).

First law of Faraday reveals the following truth: In electrolysis, the quantities of substances involved in the chemical change are proportional to the quantity of electricity, which passes through the electrolyte. As for the second law: The masses of different substances set free or dissolved by a given amount of electricity are proportional to their chemical equivalents (Bagotsky, 2006).

The amount of electrons, which corresponds to the conversion of one chemical equivalent of substance, is named as Faraday constant, *F*. The amount of charge

required to convert 1 mole of substance j is nF/z_j. When the amount of charge consumed at an electrode is Q, the following relation gives the number of moles Δn_j of substance $_j$ that have formed or reacted;

$$\Delta n_j = \frac{z_j.Q}{n.F} \tag{2.30}$$

where z_i is the valence of substance j (Bagotsky, 2006; Goodridge and Scott, 1995). The total amount of substance being converted is proportional to the amount of electrons. That's why the **specific reaction rate,** r_j, which is the amount of substance j converted in unit time per unit surface area of the electrode, is proportional to current density i;

$$r_j = \frac{1}{A}.\frac{dn_j}{dt} = z_j.\frac{i}{n.F} \tag{2.31}$$

Faraday's laws are valid in most electrochemical cases, especially for steady currents and can be used in many applications, such as electrogravimetry (to find the amount of substance deposited at an electrode) and coulometry (to find the total amount of electricity required for complete electrolysis of a compound); it can also be used for finding the number of electrons utilized in an electrolytic process. However, deviations from Faraday's laws can be observed in case of transient currents, when charges accumulate in some parts of the cell, near interfaces. Such transient currents are called nonfaradaic currents (Bagotsky, 2006).

An electrode process actually involves some sub-steps that govern the reaction rate and current at electrodes as shown in Figure 2.2 (Zoski, 2007): (i) mass transfer from the bulk solution to the electrode surface, (ii) adsorption on the surface, (iii) electrode reaction (kinetics of electron transfer), (iii) desorption from the surface (iv) mass transfer from the surface to the bulk solution. Of these, the slowest process will be the rate determining step. For an electrochemical reaction to proceed, first reactant O_x (as in (2.11)) is required to move from the bulk solution near the electrode surface. This step is related to mass transfer and is governed by equations such as Fick's laws of diffusion and Nernst–Planck. In case of a mass transfer limitation, this step could limit the rate of the reaction. When all of the other steps leading to the electrode reaction are fast, this leaves the electron transfer reaction as the limiting factor.

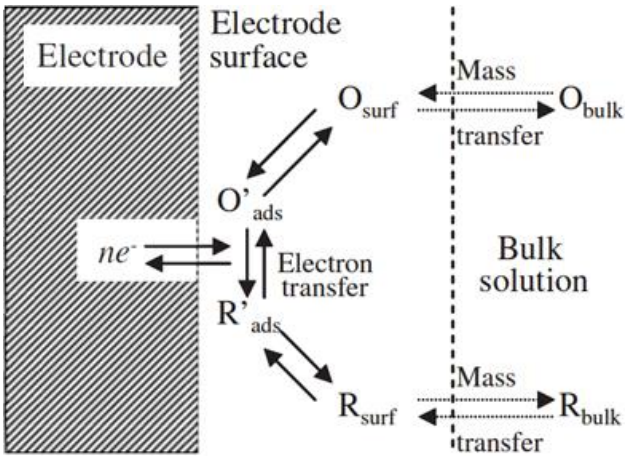

Figure 2.2 : Process sub-steps of electrode reactions (Zoski, 2007).

2.1.5 Ionic conductivity and mobility

During an electrolysis process, the transport of electric charges is achieved in two ways (Kortüm, 1957):

- The transport of electrons through solid materials (electrodes)
- The transport of ions through solutions (electrolytes)

The conductivity of electrodes is generally 3-5 times higher than the conductivity of electrolyte solutions. Furthermore, the conductivity of metals is decreasing with increasing temperature while the conductivity of electrolyte solutions is increasing with temperature. So, in case of an isothermal operation and fixed electrode structure, the overall conductivity of the process is expected to change by the changes in ionic conductivity (Strathmann, 2004).

In electrochemical processes, one of the most important qualities that a medium must possess is its ability to let current flow easily. Electrochemical reactions always produce or consume ions at electrodes, and the electrolyte provides the pathway for ions to flow between and among electrodes in the cell to maintain charge balance. In other words, electrolyte is a part of the electrical circuit in an electrochemical process. The ability of an electrolyte to support current flow with the help of ions within it when an electric field is applied is called **specific conductivity**, generally shown as κ ($S.cm^{-1}=ohm^{-1}.cm^{-1}$);

$$\kappa = \frac{1}{R}.\frac{L}{A} \tag{2.32}$$

where R is resistance (ohm) of an electrolyte with a uniform cross section of area A (cm^2) and length L (cm). So, conductivity is the inverse of resistivity or specific

resistance, generally abbreviated as ρ (*ohm.cm*). Representative values of ionic conductivity for some commonly used solvent-electrolyte combinations in electrochemistry are given in Table 2.2 (Zoski, 2007).

Table 2.2 : Ionic conductivity values for some common solvent-electrolyte combinations (Zoski, 2007).

Solvent	Electrolyte	Electrolyte concentration (M)	Temperature (°C)	Conductivity (ohm^{-1} cm^{-1})
Water	HCl	6.0	25	0.84
Water	HCl	1.0	25	0.33
Water	HCl	0.1	25	0.039
Water	H_2SO_4	0.53	25	0.21
Water	H_2SO_4	0.10	25	0.048
Water	KCl	1.05	25	0.11
Water	KCl	0.1	25	0.013
Water	$LiClO_4$	0.1	25	0.0089
Acetonitrile	$TEAClO_4$	1.0	25	0.050
Acetonitrile	$TEAClO_4$	1.0	22	0.026
Acetonitrile	$TEAClO_4$	0.1	22	0.0084
Acetonitrile	$TEABF_4$	1.0	25	0.056
Acetonitrile	$TEAPF_6$	1.0	25	0.055
Acetonitrile	$TEACF_3SO_3$	1.0	25	0.042
Acetonitrile	$TBAClO_4$	1.0	22	0.023
Acetonitrile	$TBAPF_6$	1.0	25	0.031
Acetonitrile	$LiPF_6$	1.0	25	0.050
Acetonitrile	$LiCF_3SO_3$	1.0	25	0.0097

Ionic conductivity in electrolytes depends on two main factors: (i) concentration of ions, which can also be called as free charge carriers (ii) ion mobility in an electric field. Generally, ion concentration is high when the concentration of dissolved salt (electrolyte) is high and in general more concentrated salt solutions are expected to exhibit higher conductivities. This generalization is valid for low to medium salt concentrations. However, at very high salt concentrations near the solubility limit, conductivity tends to decrease. This is due to the limited availability of solvent, which decreases ionic solvation. Another factor is that the ion mobility decreases due to the high viscosity of highly concentrated salt solutions (Zoski, 2007).

Electrolytes (generally acids, bases, and salts) dissociate into ions when dissolved in solvent, where dissociation can be complete or partial. The fraction of the original molecules that dissociates is known as the degree of dissociation, α. Substances that exhibit a low degree of dissociation in solution are called weak electrolytes, whereas when the value of α comes close to unity, the electrolyte in question is called a strong one (Bagotsky, 2006). The dissociation equation can be shown as;

$$M_{v_+}A_{v_-} \rightleftharpoons v_+.M^{z+} + v_-.A^{z-} \tag{2.33}$$

In this dissociation;

$$z_+.v_+ = z_-.v_- = z_k \tag{2.34}$$

relation is valid, where z_k is the electrolyte's charge number, namely the number of elementary charges of each sign appearing on dissociation of one molecule of the electrolyte. In order to define the concentration of the dissociated species, one can assume C_t to be the concentration of *MA* compound before dissociation. So, the other concentrations can be defined as;

$$C_+ = \alpha.v_+.C_t \tag{2.35}$$

$$C_- = \alpha.v_-.C_t \tag{2.36}$$

$$C_n = (1-\alpha).C_t \tag{2.37}$$

$$C_\theta = [1 + \alpha.(v_+ + v_- - 1)].C_t \tag{2.38}$$

where C_+, C_-, C_n and C_θ are concentrations of cation, anion, undissociated molecules and total dissolved ions, respectively. A substance such as $ZnSO_4$, where $z_+ = z_-$ is called a symmetrical or z:z electrolyte; a particular case of the z:zelectrolytes are the 1:1 electrolytes, of which KCl is an example (Bagotsky, 2006).

The flow of electric current in electrolyte solutions is the directed motion of ions under the influence of an applied electric field, i.e. conductivity in electrolytes is coupled with ionic motion. Ions are in a state of continuous kinetic molecular motion in solutions. This motion is random and chaotic when an electric field is not present i.e., the ions do not prefer to move in any particular direction. The mean distance travelled by the ions as a whole is zero because while some are displaced in one direction, an equal number are displaced in the opposite direction. Therefore, the random walk of ions can be ignored because it does not lead to any net transport of matter (as long as there is no concentration gradient leading to a diffusive flux) [169]. So, the net result is as if the ions were at rest. However, when an electric field, ϵ *(V.cm^{-1})*, is applied, each ion having z_j valence finds itself under the influence of an electrical driving force, f_{dr};

$$f_{dr} = z_j.F.\epsilon \tag{2.39}$$

Under the influence of the electric field, ions move in a certain direction according to the direction of the electric field, which is called the **migration of ions**. The comparison of ions at rest and ions under the influence of electric field is shown in Fig 2.3.

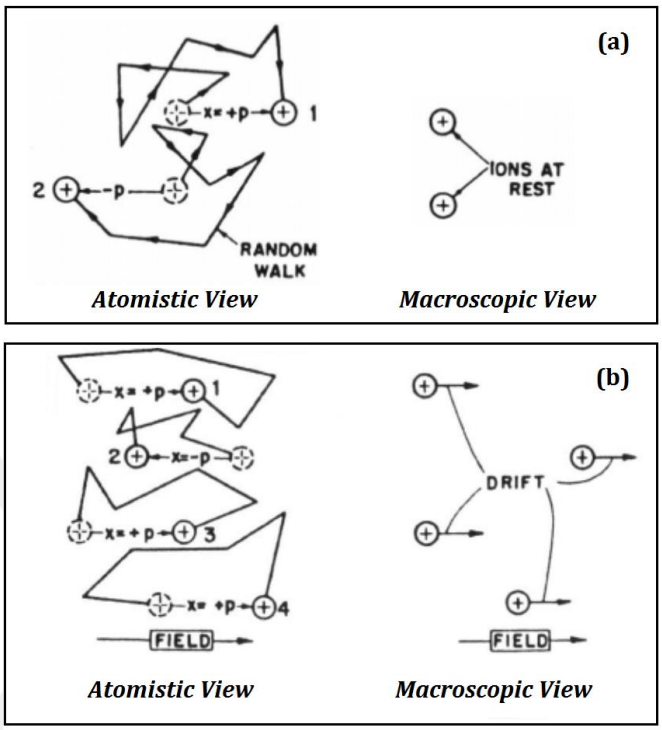

Figure 2.3 : Ions at rest (a), under electric field (b) (Bockris and Reddy, 2002).

The flux of migrating ions, which is defined as the number of moles crossing a unit area in unit time, is;

$$J_j = C_j . \upsilon_j \tag{2.40}$$

whereυ_j is the linear velocity of ion *j* (Bagotsky, 2006).

The total flux of ions is constant along the entire path while the system is in steady state. This flux continuity condition is due to mass balance; i.e. ions do not accumulate or vanish in certain locations. However, around locations where ions are produced or consumed by chemical reactions, this condition of continuity is disturbed. Therefore, it is necessary to preserve the balance that any excess of ions supplied correspond to the amount of ions reacting, and that any excess of ions eliminated correspond to the amount of ions formed in the reaction (Bagotsky, 2006).

External driving force and viscosity of the medium are the factors affecting the magnitude of the mean velocity of migration, υ_j. The retarding force defined by the

viscosity is proportional to the velocity. The velocity increases under the influence of the external and reaches the value of υ_j, where the retarding force becomes equal to the external driving force;

$$\upsilon_j = \frac{1}{\theta}.f_{dr} = \frac{1}{\theta}.z_j.F.\epsilon \tag{2.41}$$

$$J_j = C_j.\upsilon_j = C_j.\frac{1}{\theta}.f_{dr} = C_j.\frac{1}{\theta}.z_j.F.\epsilon \tag{2.42}$$

where θ is the drag coefficient, and so $\upsilon_j.\theta$ becomes the retarding force.

The ratio of the velocity of migration to the electric field is called the **mobility** of the ions (Bagotsky, 2006), u_j $(m^2.s^{-1}.V^{-1})$;

$$u_j = \frac{\upsilon_j}{\epsilon} = \frac{1}{\theta}.z_j.F \tag{2.43}$$

So, migration flux expression becomes;

$$J_j = C_j.u_j.\epsilon \tag{2.44}$$

The partial current density, which is the number of charges that in unit time cross the unit cross-sectional area due to the migration of ions *j*, can be inserted into the flux expression to obtain;

$$i_j = z_j.F.J_j = z_j.F.C_j.u_j.\epsilon \tag{2.45}$$

In ionic solutions, cations and anions move in opposite directions when an electric field is applied. Thus, the effect of the motion of cations is the same as that of the motion of anions, and the total current density is the sum of the partial currents due to the transport of each type of ion:

$$i = \sum i_j = F.\epsilon.\sum z_j.C_j.u_j \tag{2.46}$$

The fraction of current transported by a certain ion type is called the **transport number**, t_j, of a certain ion;

$$t_j = \frac{i_j}{i} = \frac{z_j.C_j.u_j}{\sum z_j.C_j.u_j} \tag{2.47}$$

$$\sum t_j = 1 \tag{2.48}$$

Transport number of a certain ion is between 0-1. In case of a single type of ion, the transport number of these ions is unity. As for electrolytes having different types of

ions, the individual transport number of a given ion depends on the concentrations and mobilities of all ions (Bagotsky, 2006);

$$\kappa = F.\sum z_j.C_j.u_j \tag{2.49}$$

Combination of (2.33) and (2.48) for the conductivity of a binary electrolyte gives;

$$\kappa = \alpha.z_k.C_t.F.(u_+ + u_-) \tag{2.50}$$

With the help of (2.46), one can calculate the transport number for a binary electrolyte;

$$t_j = \frac{u_j}{u_+ + u_-} \tag{2.51}$$

Ion mobility is concentration dependent, which is highest in dilute solutions (the limiting mobility, u_j^0) and decrease gradually with the increase of concentration. So, in dilute binary solutions of strong electrolytes (α=1), the conductivity is proportional to the total concentration C_k. The increase of concentration causes an increase in conductivity, yet at a degressive rate, since mobility decreases with the increase of concentration. In case of weak electrolytes, this degressive rate is even more pronounced since the degree of dissociation decreases in addition to the mobilities (Bagotsky, 2006).

In the case of metallic conductors, once the specific conductivity is defined, the macroscopic description of the conductor is complete. However, in the case of electrolytic conductors, further characterization is required because not only can the concentration of charge carriers vary but also the charge per charge carrier. So, even though two electrolytes have the same geometry, they do not necessarily have to have the same specific conductivity. The number of charge carriers in that normalized geometry may be different, in which case their fluxes under an applied electric field will be different. The normalization of the geometry defines the specific conductivity; however, since the specific conductivity of an electrolytic solution varies as the concentration, an additional normalization in terms of concentration is vital for fair comparison. Hence, a new quantity, the molar conductivity of the electrolyte, $\Lambda_m$has been put forward;

$$\Lambda_m = \frac{\kappa}{C_t} \tag{2.52}$$

The molar conductivity is the sum of the contributions of its individual ions. This is referred to as the law of independent migration of ions (Strathmann, 2010). Thus;

$$\Lambda_m = \alpha.(v_+\lambda_+ + v_-\lambda_-) \tag{2.53}$$

whereλ_+ and λ_- refer to the ion conductivity of cation and anion, respectively. The ion conductivity is a function of the ion mobility, which is given by;

$$\lambda_j = |z_j|.F.u_j \tag{2.54}$$

The molar conductivities of two electrolytic solutions can be readily compared only if the charges borne by the charge carriers in the two solutions are the same. If there are singly charged ions in one electrolyte (e.g., NaCl) and doubly charged ions in the other (e.g., $CuSO_4$), then the two solutions will contain different amounts of charge even though the same quantity of the two electrolytes is dissolved. In such a case, the specific conductivities of the two solutions can be compared only if they contain equivalent amounts of charge. Hence, one more new quantity, the equivalent conductivity of the electrolyte, $\Lambda_m$has been put forward;

$$\Lambda_{eq} = \frac{\kappa}{C_{eq}} = \frac{\kappa}{C_t.z} \tag{2.55}$$

Though normalized with geometry and ion charges, the equivalent conductivity varies significantly with the concentration of ions, that is to say it increases as the ionic concentration decreases. That's why, there is necessity to define some reference value forthe equivalent conductivity. Experimental experience show that as the electrolytic solution gets more dilute, the equivalent conductivity approaches a limiting value. This limiting value forms an excellent basis for comparing the conductivity of different electrolytes due to the fact that it is the only value in which the effects of ionic concentration are removed. This limiting value is called the equivalent conductivity at infinite dilution and is represented by the symbol, Λ^0 (Strathmann, 2010).

Conductivity is a very crucial parameter in electrochemical processes. It directly affects the power consumption due to the following relations;

$$P = E_{app} \times I \tag{2.56}$$

$$E = I \times R_{tot} \tag{2.57}$$

Where P is power (*Watt*), E_{app} is the applied voltage (*Volt*), I is the total current (*Amps*) and R_{tot} is the total resistance (*Ohm*). An adaptation of Ohm's law with the insertion of electric field and current density terms reveals the effect of conductivity more apparently;

$$\epsilon = \frac{i}{\kappa} \tag{2.58}$$

In electrochemical processes, since metal conductivity is already much higher than electrolyte conductivity, ionic conductivity is the critical parameter in the determination of overall conductivity.

2.2 Electromembrane Process Fundamentals

The term electromembrane process is used to describe an entire family of processes that can be quite different in their basic concept and their application. However, they are all based on the coupling of a mass transport with an electrical current through an ion permselective membrane (Strathmann, 2010). Electromembrane processes are used today mainly in three areas:

- The deionization of salt solutions (eg. electrodialysis)
- The electrochemical synthesis of inorganic and organic compounds (e.g. chlor-alkali process)
- The conversion of chemical energy into electrical energy (e.g. fuel cells)

2.2.1 Properties of ion-exchange membranes

2.2.1.1 General features

The key elements in electromembrane processes are ion-exchange membranes, in which charged groups are attached to the polymer backbone of the membrane material. These fixed charge groups partially or completely exclude ions of the same charge from the membrane (Baker, 2001). Ion-exchange membranes can be classified as "cation-exchange and anion-exchange membranes" in terms of their charge type. Another classification is based on the structure of the membrane, which leads to "heterogeneous and homogeneous membranes".

Ion exchange membranes are very similar to ion exchange resins in terms of chemical structure. However, there is a significant difference in that membranes have

excellent mechanical properties compared to resins due to the requirement of an electromembrane process (Inamuddin and Luqman, 2012).

There are three different types of ion-exchange membranes based on their function;

(1) cation-exchange membranes, which contain negatively charged groups fixed to the polymer matrix,

(2) anion-exchange membranes, which contain positively charged groups fixed to the polymer matrix,

(3) bipolar membranes, which are composed of an anion- and a cation-exchange layer laminated together.

In a cation-exchange membrane, the fixed negative charges are in electrical equilibrium with mobile cations within its porous structure. Likewise, in an anion-exchange membrane, the fixed positive charges are in electrical equilibrium with mobile anions. In either case, the mobile ions with the opposite charge of the fixed structure are called counterions while the ones, which carry the same electrical charge as the membrane, are referred to as coions. Due to the exclusion of the coions away from the membrane, a cation-exchange membrane is more or less impermeable to anions while an anion-exchange membrane is preferentially permeable to anions and more or less impermeable to cations. The extent of this exclusion depends on the membrane as well as on the solution properties. Bipolar membranes promotes the dissociation of water molecules into H^+ and OH^- ions and are used in combination with monopolar anion- and cation-exchange membranes to convert salts into their corresponding acids and bases (Strathmann, 2010; Wilhelm, 2001).

The following parameters affect the properties of ion-exchange membranes;

- the density of the polymer network,
- the hydrophobic/hydrophilic character of the matrix polymer,
- the type and concentration of the charges in the polymer,
- the morphology of the membrane itself.

With the optimization of these parameters, the following properties are aimed to obtain:

- high permselectivity;

- low electrical resistance
- good mechanical, chemical and thermal stability.

Broadly speaking, the properties of ion-exchange membranes are determined by two parameters, i.e., the basic material they are made from and the type and concentration of the functional group in the fixed structure. The basic material determines to a large extent the mechanical, chemical, and thermal stability of a membrane. The type and the concentration of the fixed ionic charges determine its permselectivity and electrical resistance, but they also have a significant effect on the mechanical properties of the membrane. For example, the degree of swelling is affected by the type and concentration of the fixed charges. The following functional groups are used as fixed charges in ion-exchange membranes;

- for CEM: $-SO_3^-$, $-COO^-$, $-PO_3^{2-}$, $-PHO_2^-$, $-AsO_3^{2-}$, $-SeO_3^-$
- for AEM: $-N^+H_2R$, $-N^+HR_2$, $-N^+R_3$, $-P^+R_3$, $-S^+R_2$

The functional group is very significant in terms of being decisive in the dissociation pH range. The sulfonic acid group is completely dissociated over almost the entire pH range, while the carboxylic acid group is hardly dissociated in the pH range <3. The quaternary ammonium group again is completely dissociated over the entire pH range, while the secondary ammonium group is only weakly dissociated. With this information, ion-exchange membranes are referred to as being weakly or strongly acidic or alkaline in character (Strathmann, 2010).

2.2.1.2 Preparation of ion-exchange membranes

For the preparation of membranes, several technologies can be applied according to the structure of the membrane. The variation in the preparation method of ion-exchange membranes and the resulting structure brings forward another classification: homogeneous and heterogeneous membranes. In homogeneous ion-exchange membranes, the fixed charged groups are attached to the polymer and evenly distributed over the entire membrane matrix. Heterogeneous ion-exchange membranes are made of dispersed ion exchange particles and they have distinct macroscopic domains of these ion exchange resins in the matrix of a polymer (Scott and Hughes, 1996). The structure of both can be seen in Fig. 2.4 (Strathmann, 2010).

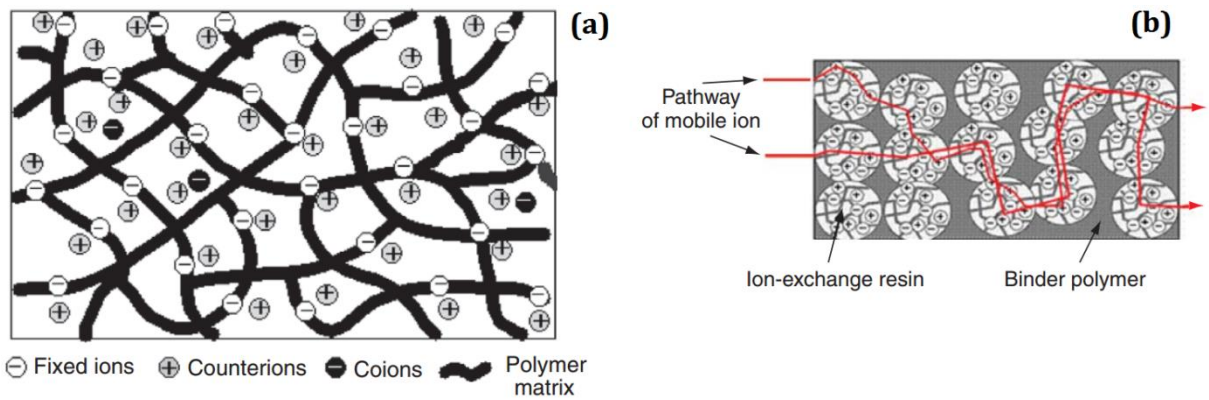

Figure 2.4 : The structure of a (a) homogeneous (b) heterogeneous cation-exchange membrane (Strathmann, 2010).

Homogeneous membranes

The structure of a homogeneous membrane can be seen in Fig. 2.4.a, which represents a cation-exchange membrane with negative charges fixed to the polymer matrix that are balanced by mobile cations and a few anions in the porous structure of the polymer backbone. The ion-exchange capacities of homogeneous ion-exchange membranes are in the range of 1-3 equivalent per kilogram dry membrane. Their water sorption ratio in solution, which is a function of the ion exchange capacity, the membrane polymer matrix and the electrolyte concentration is between 10 and 30 % (Strathmann, 2010).

Early homogeneous membranes were made by simple condensation reactions, such as phenol-formaldehyde condensation. The mechanical stability and ion exchange capacity of these membranes were comparatively low. Later, a more sensible approach emerged, that is to prepare a suitable cross-linked base membrane and convert it to a charged form in the following reactions. A typical homogeneous cross-linked membrane preparation procedure is;

- A mixture of 60% styrene and 40% divinyl benzene is cast onto a fabric web, squeezed between two plates and heated in an oven to form the membrane matrix. The membrane is then sulphonated with 98% sulphuric acid or a concentrated sulphur trioxide solution. The degree of swelling and the crosslinking density in the final membrane is controlled by varying the divinyl benzene concentration in the initial mix. The degree of sulphonation can also be varied.

The synthesis of cross-linked homogeneous membrane is given in Fig. 2.5 (Baker, 2001);

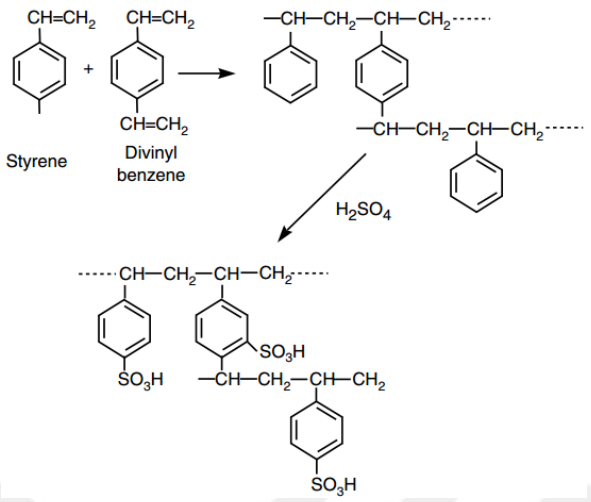

Figure 2.5 : The synthesis of a cross-linked homogeneous cation-exchange membrane (Baker, 2001).

Anion exchange membranes can be made from the same cross-linked polystyrene membrane base by post-treatment with monochloromethyl ether and aluminium chloride to introduce chloromethyl groups into the benzene ring, followed by formation of quaternary amines with trimethyl amine(Baker, 2001).

Another worth-mentioning type of membranes due to commercial significance is the perfluorinated membranes mostly produced under the trade mark of Nafion®. Perfluorinated polymers enhance chemical stability, while ionic conductivity results from using monomers with side chains with terminal acid groups. In these membranes the hydrophobic perfluoro-polymer domains provide a non-swelling matrix, ensuring the integrity of the membrane while the ionic hydrophilic domains absorb water and form small clusters distributed throughout the matrix as seen in Fig 2.6 (Baker, 2001; Pletcher and Walsh, 1990).

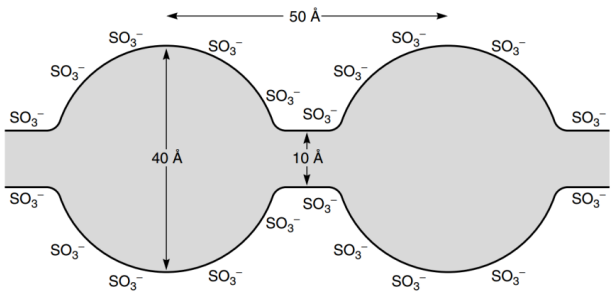

Figure 2.6 : The cluster model used to describe the distribution of functional groups in perfluorocarbon-type cation exchange membranes (Baker, 2001).

Perfluorinated membranes can be prepared by copolymerization of tetrafluoroethylene with perfluorovinylether having a carboxylic or sulphonic acid group at the end of a side chain. The synthesis of perfluorocarbon membranes is rather complex and requires a multistep process. There are several variations of a general basic structure commercially available today (Strathmann, 2010).

Two basic types of perfluorinated membranes were developed, based on strong acid and weak acid functions. Strong acid membranes are superior over weak acid membranes in terms of better chemical stability and higher electrical conductivity. However, at very highly alkaline medium, strong acid membranes offer lower current efficiencies due to increased anion back-transport. This increase in back-transport rate is due to the higher water content of strong acid membranes. That's why weak acid membranes allow the direct production of highly alkaline solutions without a significant loss in current efficiency. However, these membranes result quite high resistances especially when they are in contact with an acidic solution. Therefore, bilayer membranes were developed especially for chlor-alkali process, where sodium hydroxide and chlorine are produced together. In this membrane structure a strong acid membrane is coated on another membrane of weak acid type. With this combination, favourable properties of both membranes are joined in one membrane. The chemical structure of strong and weak acid perfluorinated membranes are shown in Fig. 2.7 (Pletcher and Walsh, 1990).

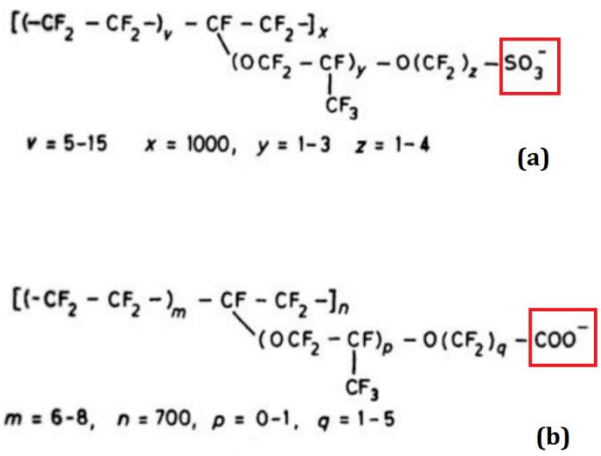

Figure 2.7 : The chemical structure of strong (a) and weak (b) acid perfluorinated membranes (Pletcher and Walsh, 1990).

There are various types of Nafion membranes, developed for special purposes. Nafion® 900 and 2000 series membranes are designed for optimum performance in the production of chlorine and caustic soda. As mentioned above, they are reinforced

composite membranes, having sulfonate and carboxylate polymer layers. Nafion® 300, 400 and 500 series membranes are reinforced, all sulfonate polymer, membranes designed for dilute caustic and caustic potash production (DuPont Co., 2006).

Heterogeneous membranes

The structure of a heterogeneous membrane can be seen in Fig. 2.4.b, which represents a cation-exchange membrane made of fine cation-exchange particles placed in an inert binder polymer. The discontinuous phase of the ion-exchange material is the key element describing heterogeneous ion-exchange membranes. Ion transport through the membrane is realized either via a contact between the ion-exchange particles or an ion-conducting solution between the particles. Therefore, heterogeneous membranes have generally a higher electric resistance and a lower permselectivity compared to homogeneous membranes (Strathmann, 2010).

In the simplest form of heterogeneous membranes, there exists very finely powdered cation or anion exchange particles uniformly dispersed in polypropylene. A film of the material is then extruded to form the membrane. The mechanical properties of these membranes are often poor because of swelling of the large ion exchange particles. A much finer heterogeneous dispersion of ion exchange particles, and consequently a more stable membrane, can be made with a poly(vinyl chloride) (PVC) plastisol. A plastisol of approximately equal parts PVC, styrene monomer and crosslinking agent in a dioctyl phthalate plasticizing solvent is prepared. The mixture is then cast and polymerized as a film. The PVC and polystyrene polymers form an interconnected domain structure. The styrene groups are then sulfonated by treatment with concentrated sulphuric acid or sulphur trioxide to form a very finely dispersed but heterogeneous structure of sulfonated polystyrene in a PVC matrix, which provides toughness and strength (Baker, 2001).

2.2.1.3 Ion-exchange equilibrium

As mentioned earlier, in an electrolyte solution or in an electron conducting phase like ion-exchange membranes, electro-neutrality is the required phenomena on a macroscopic scale, i.e. every charge has to be counter-balanced by an opposite charge. The fixed negative charges of a cation-exchange membrane are balanced by positively charged cations, the so-called counterions as mentioned earlier. Therefore,

if an ion-exchange membrane is in equilibrium with an adjacent electrolyte solution, counterions will be drawn into the membrane and coions will be removed from the membrane by the strong Coulomb forces of the fixed ions(Strathmann, 2004).

The electrostatic force of the fixed membrane charges affects certain counterions with certain preference due to distances and charge number of the ions. Besides, van der Waals forces can also be different for different counterions, which cause membrane favour certain counterions in taking into its structure. The distribution of counterions between a membrane and an adjacent electrolyte solution is determined by the counterion exchange equilibrium. Considering an electrolyte of two counterions, X and Y, the following equilibrium is valid between a cation-exchange membrane and the adjacent electrolyte solution;

$$X_m^+ + Y_s^+ \rightleftharpoons X_s^+ + Y_m^+ \tag{2.59}$$

where *m* and *s* refer to membrane and solution, respectively. This equilibrium can be defined by the equilibrium constant, $K_{Y,X}$;

$$K_{Y,X} = \frac{C_{Y_m^+}.C_{X_s^+}}{C_{Y_s^+}.C_{X_m^+}} \tag{2.60}$$

When it is assumed that the concentration in solution is much lower than the fixed ion concentration in the membrane, coions can be accepted to be partially or completely excluded and the counterion concentration is almost equal to the fixed ion concentration of the membrane. This can be expressed as;

$$C_{fix_m} = C_{X_m^+} + C_{Y_m^+} \tag{2.61}$$

2.2.1.4 Electrochemical equilibrium and Donnan potential

From a thermodynamics point of view, an ion-exchange membrane and an adjacent solution will be in equilibrium if the electrochemical potentials, η, of all ions in the two phases are equal, which can be expressed as;

$$\eta_i^m = \eta_i^s = \mu_i^m + z_i.F.\varphi^m = \mu_i^s + z_i.F.\varphi^s \tag{2.62}$$

Here, μ_i and η_i are the chemical and electrochemical potential of the component *i*, φ is the electrical potential and *F* is Faraday constant. Chemical potential difference between membrane and solution phases can be expressed as;

$$\Delta\mu_i = \mu_i^m - \mu_i^s = \overline{V}_i.(P^m - P^s) + R.T.\ln\frac{a_i^m}{a_i^s} \tag{2.63}$$

where a is the ion activity, $\bar{V}_i$is the partial molar volume, P is pressure, R is the ideal gas constant and T is temperature. Combination of (2.62) and (2.63) gives the electrical potential difference between membrane and solution phases, which is known as **Donnan potential**, φ_{Don};

$$\varphi_{\mathrm{Don}} = \varphi^{\mathrm{m}} - \varphi^{\mathrm{s}} = \frac{1}{z_i.F}.\left[R.T.\ln\frac{a_i^s}{a_i^m} + \bar{V}_i.(P^s - P^m)\right] \tag{2.64}$$

Donnan potential (DP) between an electrolyte solution and an ion-exchange membrane cannot be measured directly, yet can be calculated (Donnan, 1932). The pressure difference between solution and membrane is called swelling pressure and be expressed in terms of osmotic pressure, $\Delta\pi$;

$$\Delta\pi = P^m - P^s = \frac{R.T}{\bar{V}_w}.\ln\frac{a_w^m}{a_w^s} \tag{2.65}$$

where w subscript indicates water. Combination of (2.63) and (2.64) gives;

$$\varphi_{\mathrm{Don}} = \frac{1}{z_i.F}.\left[R.T.\ln\frac{a_i^s}{a_i^m} - \bar{V}_i.\frac{R.T}{\bar{V}_w}.\ln\frac{a_w^m}{a_w^s}\right] = \frac{1}{z_i.F}.\left[R.T.\ln\frac{a_i^s}{a_i^m} - \bar{V}_i.\Delta\pi\right] \tag{2.66}$$

When ion exchange membranes are in contact with an electrolyte solution, a distribution in ion concentration and DP emerges between membranes and solution, as seen in Fig. 2.8 (Strathmann, 2004). The first remarkable thing in Fig.2.8 is that the ion concentration in membranes is significantly higher than in solution. The reason that counterion concentration in membranes is slightly higher than fixed ion concentration is due to the existence of small amount of coions that are not excluded from the membrane.

The most important issue with Fig 2.8 is that at the interface where membrane and solution are in contact, there is a sharp change in the ion concentration. In the direction from membrane towards solution, coion concentration increases while counterion concentration decreases. From a thermodynamics point of view, this concentration gradient is expected to cause an ion flow in the opposite direction. However, due to the chemistry of the membrane, coions have to be excluded, i.e. they cannot flow into membrane despite the existence of a concentration gradient. This means that the concentration gradient driving force has to be counter-balanced by another driving force acting in the opposite direction. This driving force is the DP as shown in Fig. 2.8.c (Strathmann, 2004).

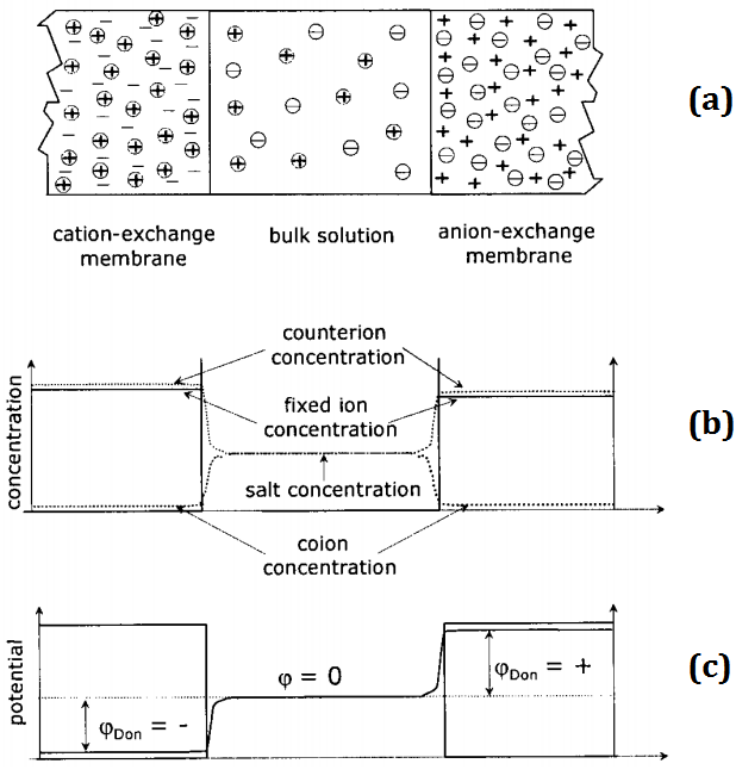

Figure 2.8 : (a) The distribution of ions between membranes and solution, (b) Concentration change of ions between membranes and solution, (c) Donnan potential change between membranes and the adjacent solution (Strathmann, 2004).

Donnan relation given in (2.66) can also be expressed in terms of cation or anion activities;

$$\varphi_{Don} = \frac{1}{z_c.F}.\left[R.T.\ln\frac{a_c^s}{a_c^m} - \overline{V}_c.\Delta\pi\right] = \frac{1}{z_a.F}.\left[R.T.\ln\frac{a_a^s}{a_a^m} - \overline{V}_a.\Delta\pi\right] \qquad (2.67)$$

where subscripts *c* and *a* indicates cation and anion, respectively. In case of a completely dissociating electrolyte, molar volume of the electrolyte will be equal to the sum of the partial molar volumes of the ions;

$$\overline{V}_s = v_a.\overline{V}_a + v_c.\overline{V}_c \qquad (2.68)$$

Combination of (2.34), (2.67) and (2.68) gives;

$$\left(\frac{a_a^s}{a_a^m}\right)^{\frac{1}{z_a}}.\left(\frac{a_c^m}{a_c^s}\right)^{\frac{1}{z_c}} = \exp\left(-\frac{\overline{V}_s.\Delta\pi}{R.T.z_c.v_c}\right) \qquad (2.69)$$

Coion concentration in the membrane is very crucial for the membrane permselectivity. In order to be able to supply a fully permselective membrane, the coions should have been completely excluded from the membrane. This phenomenon is called **Donnan exclusion**.

As mentioned before, electro-neutrality is one of the most important conditions that strictly has to be met in any ionic medium. The expression of electro-neutrality for membrane-solution system gives the following relations;

$$|z_{cou}|.C_{cou}^{m} = C_{fix}^{m} + |z_{co}|.C_{co}^{m} \tag{2.70}$$

$$z_{cou}.C_{cou}^{s} = -z_{co}.C_{co}^{s} \tag{2.71}$$

where*co*, *cou* and *fix* subscripts indicate coion, counterion and fixed ion while *m* and *s* superscripts refer to membrane and solution, respectively (Liberti and Hellferich, 1983).

Ion activity terms in Eq. (2.69) can also be expressed in concentration terms via $a_i = C_i.\gamma_i$ relation, where γ_i is the activity coefficient of ion *i*. The introduction of concentration terms gives;

$$\left(\frac{C_{co}^{s}}{C_{co}^{m}}\right)^{\frac{1}{z_{co}}}.\left(\frac{C_{fix}+z_{co}.C_{co}^{m}}{z_{cou}.C_{cou}^{s}}\right)^{\frac{1}{z_{cou}}} = \left(\frac{\gamma_{co}^{m}}{\gamma_{co}^{s}}\right)^{\frac{1}{z_{co}}}.\left(\frac{\gamma_{cou}^{s}}{\gamma_{cou}^{m}}\right)^{\frac{1}{z_{cou}}}.\exp\left(-\frac{\bar{V}_s.\Delta\pi}{R.T.z_c.v_c}\right) \tag{2.72}$$

which describes the distribution of the coions between membrane and solution as a function of the concentration of all types of ions (co-, counter- and fixed). This equation can be simplified with certain assumptions to be able to utilize it readily, such as;

1) The osmotic pressure term is small compared to the energy term, i.e. $\Delta\pi.\bar{V}_s \ll R.T$, which makes it possible to cancel exponential term according to $\exp\left(-\frac{\bar{V}_s.\Delta\pi}{R.T.z_c.v_c}\right) \approx 1$assumption.

2) For a monovalent electrolyte; salt, coion and counterion have the same concentrations and the activity coefficients can be expressed by $\gamma_{\pm}^{m}$ and $\gamma_{\pm}^{s}$, which are average activity coefficients for the ions in membrane and solution, respectively.

With these assumptions (2.72) can be simplified as;

$$\left(\frac{C_s^s}{C_{co}^m}\right).\left(\frac{C_s^s}{C_{fix}-C_{co}^m}\right) = \left(\frac{\gamma_{\pm}^{s}}{\gamma_{\pm}^{m}}\right)^2 \tag{2.73}$$

This equation can be further simplified by assuming that $C_{co}^{m} \ll C_{fix}$, which is valid especially for dilute solutions. So the simplest form of Eq. (2.72) is;

$$C_{co}^{m} = \frac{(C_s^s)^2}{C_{fix}} . \left(\frac{\gamma_{\pm}^{s}}{\gamma_{\pm}^{m}}\right)^2 \tag{2.74}$$

This equation tells that while working at high solution concentrations (C_s^s), the membrane has to have high fixed ion concentration (C_{fix}) in order to be able to exclude enough coions from the membrane for the good of permselectivity (Strathmann, 2004).

2.2.2 Transport in ion-exchange membranes

2.2.2.1 Definition of the flux term

The Nernst-Planck flux equation is a widely used expression defining how the transport is performed through membranes. This equation consists of all transport mechanisms possible for a membrane (Sata, 2004; Krol, 1997).

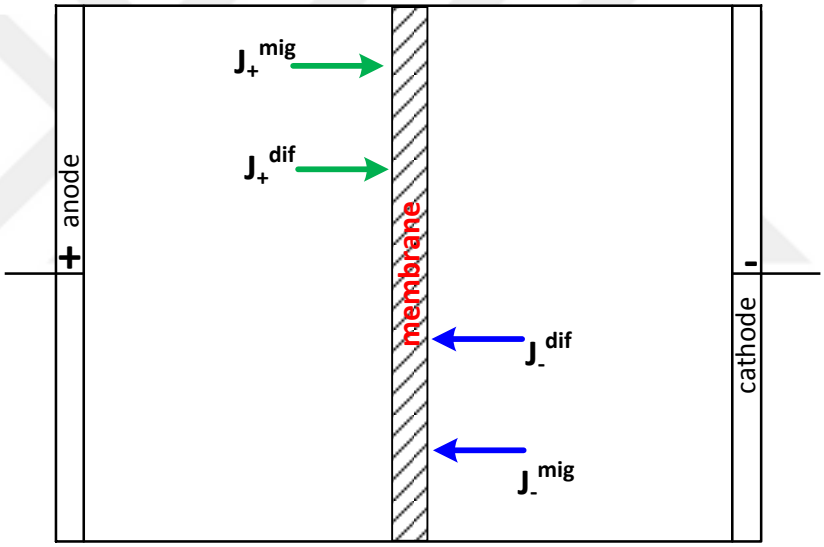

Figure 2.9 : Mechanisms of ion transport through membrane.

First, thinking of an ion diffusing in the direction perpendicular to membrane as seen in Fig. 2.9, the diffusive flux can be expressed in terms of chemical potential and activity gradients;

$$J_i^{dif} = \frac{D_i}{R.T} . C_i . \left(-\frac{d\mu_i}{dx}\right) \tag{2.75}$$

$$J_i^{dif} = -D_i . C_i . \frac{da_i}{dx} \tag{2.76}$$

where $J_i^{dif}$is the diffusive flux term of ion *i*, D_i is the diffusion coefficient of ion *i*, a_i is the activity of*i*, *x* is the direction perpendicular to membrane. Introducing

concentration, C, and activity coefficient, γ, terms instead of activities gives the following relation;

$$J_i^{dif} = -D_i . C_i . \left(\frac{d\ln C_i}{dx} + \frac{d\ln \gamma_i}{dx}\right) \tag{2.77}$$

$$J_i^{dif} = -D_i . \left(\frac{dC_i}{dx} + C_i . \frac{d\ln \gamma_i}{dx}\right) \tag{2.78}$$

When there exists an electric potential gradient within a solution, a migration flux,J_i^{mig}, occurs proportional to electric potential driving force,$\frac{d\varphi}{dx}$ and mobility,u_i;

$$J_i^{mig} = -u_i . z_i . C_i . \frac{d\varphi}{dx} \tag{2.79}$$

Here, another expression of mobility can be introduced, referred as Nernst-Einstein equation;

$$u_i = D_i . \frac{F}{RT} \tag{2.80}$$

Combination of two gives;

$$J_i^{mig} = -D_i . \frac{F}{R.T} . z_i . C_i . \frac{d\varphi}{dx} \tag{2.81}$$

A third possible flux is the convectional flux, which is defined by;

$$J_i^{con} = C_i . \vartheta_x \tag{2.82}$$

whereϑ_x is the convective flow of *i* ion in *x* direction.

So, the total flux of *i* ion through the membrane is expressed as;

$$J_i = J_i^{dif} + J_i^{mig} + J_i^{con} \tag{2.83}$$

$$J_i = -D_i . \left(\frac{dC_i}{dx} + C_i . \frac{d\ln \gamma_i}{dx}\right) + -D_i . \frac{F}{R.T} . z_i . C_i . \frac{d\varphi}{dx} + C_i . \vartheta_x \tag{2.84}$$

This relation can be simplified with the help of the following assumptions; the solution is ideal and convection is negligible compared to other fluxes;

$$J_i = -D_i . \left(\frac{dC_i}{dx} + \frac{F}{R.T} . z_i . C_i . \frac{d\varphi}{dx}\right) \tag{2.85}$$

One further assumption can be assuming that there is no significant concentration change due to position, or in other words considering the fact that migration is the dominant phenomena in mass transfer, which results in removing diffusion term;

$$J_i = -D_i . \frac{F}{R.T} . z_i . C_i . \frac{d\varphi}{dx} \tag{2.86}$$

2.2.2.2 Transport number and membrane permselectivity

The concept of transport number in aqueous solutions has been mentioned above in "Ionic conductivity and mobility" section and transport has been defined as a function of mobility and concentration. In solutions, the current is carried almost equally by cations and anions. However, in ion exchange membranes most of the current is carried by counterions due to the Donnan exclusion phenomena mentioned above. The transport number of a counterion in membrane, T_i, can be expressed as;

$$T_i = \frac{z_i \cdot J_i}{\sum z_i \cdot J_i} \tag{2.87}$$

In an ideal cation exchange membrane, where all co-ions are excluded, the transport number of counterion is 1. However in practice, in an ion-exchange membrane, the transport number of counterions can be only claimed to be much higher than coions. Besides, the transport rate of different counterions can be quite different. The transport rates of ions in a solution or through a membrane are proportional to their permeabilities in the solution and in the membrane (Strathmann, 2010).

The permeability of an ion is a function of its concentration and mobility. During transport of ion through membrane, the concentration of the counterions is always close to the concentration of the fixed charges of the membrane while their mobility mainly depends on the radius of the hydrated ions and the membrane structure (Strathmann, 2004).

In an aqueous solution, mobilities of different ions do not differ significantly from each other. Generally, smaller hydration shells and higher charge numbers lead to higher mobility values. However, this generalization fails at H^+ and OH^- ions, which exhibit extraordinary high mobilities (Kortüm, 1957).

High mobility value of H^+ ion is due to the advantageous transport mechanism of hydrogen ions. Protonation of water in aqueous solutions produce hyronium ions as seen in Fig. 2.10.a. The uniqueness in hydronium ion is that the three hydrogen ions are not distinguishable, i.e. they are equal in terms of carrying the positive charge. Ions other than hydronium move with their hydrate shell through the solution. However, hydrogen ion (proton), is mostly carried via a **tunneling (or hopping) mechanism**, where proton moves from one hydronium ion to the other over a water bridge (Fig. 2.10.b). Similar phenomenon is valid for hydroxyl ions, too (Tuckerman

et al, 2002, 2005). That's why these two ions can exhibit more than expected mobilities. Another effect of this is that the water transport number of these ions is lower than common ions since they are transported through membrane via hydration shells only at small extents (Strathmann, 2004; Saito et al, 2005).

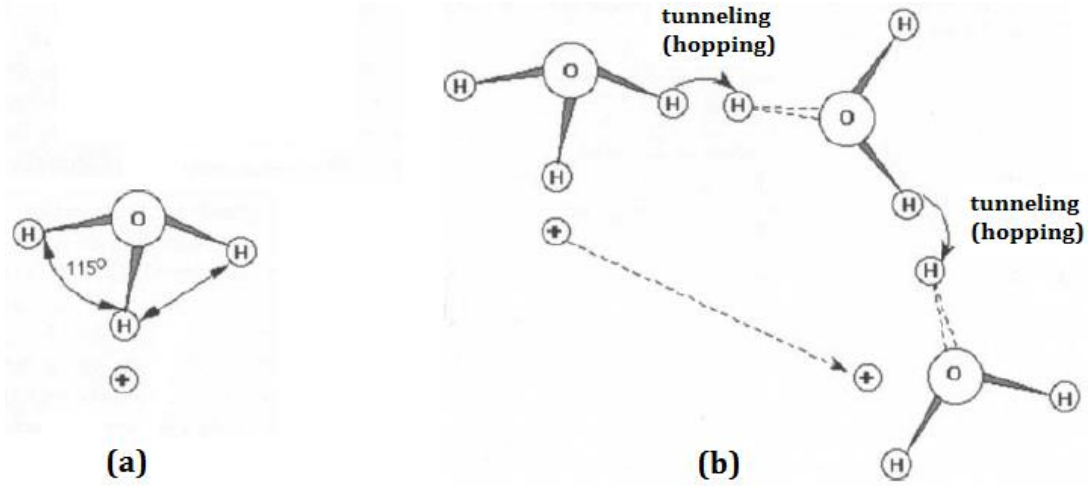

Figure 2.10 : (a) Hydronium ion (b) Mechanism of proton transport through membrane (Strathmann, 2004).

Another important definition in ion exchange processes is "the membrane permselectivity", which determines the performance of membrane. It describes the degree to which a membrane selectively passes an ion while excluding the one with the opposite charge. The permselectivity of a CEM, Ψ^{cm}, can be expressed as;

$$\Psi^{cm} = \frac{T_c - t_c}{t_a} \tag{2.88}$$

where, T_c and t_c are transport numbers of cation in membrane and in solution, respectively while t_a is the transport number of anion in solution. As permselectivity goes to "0", it means that the membrane does not selectively pass cations, which indicates that membrane does not work. As the ratio of $\frac{concentration\ of\ fixed\ charges}{concentration\ of\ solution}$ increases, the permselectivity of a cation-exchange membrane, Ψ^{cm} increases. On the other hand, very high increase of fixed charges increases the interaction of the membrane with water, i.e. swelling pressure, which decreases the mechanical properties of the membrane and even can lead to the dissolution of the membrane.

Another important definition of permselectivity coefficient is the ratio of the flux of a specific species to that of another species having the same concentration. Thus permselectivity coefficient of ion A against B, $P^{A/B}$, is defined as follows;

$$P^{A/B} = \frac{\left(\frac{z_A \cdot J_A}{z_B \cdot J_B}\right)}{\left(\frac{z_A \cdot C_A}{z_B \cdot C_B}\right)} \tag{2.89}$$

where C is concentration. The insertion of transport numbers into this equation gives;

$$P^{A/B} = \frac{\left(\frac{T_A}{T_B}\right)}{\left(\frac{z_A \cdot C_A}{z_B \cdot C_B}\right)} \tag{2.90}$$

The obtained PA/B coefficient gives an idea about how strong species A is selected in membrane transport compared to species B.

2.2.2.3 Water transport through membrane

Along with ions, water also passes through the membrane. The transport of water can occur through different mechanisms such as; electroosmotic flux, flux due to hydration shell, osmotic flux.

The flux of water through membrane as coupling of water with electric current due to the potential difference driving force is called **electroosmotic flux**. Electroosmotic flow is the motion of liquid induced by an applied potential across a porous or capillary structure, which in this case is ion exchange membrane. When a potential difference is applied across a membrane, the ions tend to move along the membrane dragging a certain amount of water. Linear flow velocity in electroosmosis is expressed as;

$$u = \frac{\varepsilon . \Delta\varphi . \zeta}{4 . \pi . \eta . l} \tag{2.91}$$

Here, u is the linear flow velocity, ε is the dielectric constant of the solution, $\Delta\varphi$ is the potential difference applied over membrane (capillary), η is the dynamic viscosity of the solution, l is the length of the membrane (capillary) and ζ is zeta potential.

The flux of water through membrane as coupling of water with the transporting ions is called **flux due to hydration shell**. Ions do not move independently in solution, but together with n amount of water molecules that surround the ion. Likewise, as they move through membrane, the water in their hydration shell also is also transported along.

In an ion hydration controlled mechanism, transport of water is directly related with the type of the transported species since different cations have different ion hydration

numbers. Determination of the number of water molecules associated with a certain ion is not easy to obtain and the results vary according to the method used. For lithium, ion hydration number can be reported to be between 2 and 22, which is a quite large interval. However, relative comparisons can be easily made since tendency of the ions according to their chemical structure is a widely agreed issue. So, it can be claimed that hydration numbers fall with increasing ionic size (e.g. $Li^+ > Na^+ > K^+ > Rb^+ > Cs^+$). Small ions have a greater charge density on their surface than do larger ones, which helps them form more links with water molecules resulting in a larger hydration shell. Hydration numbers also increase with the increase of ion charge (e.g. $Al^{3+} > Mg^{2+} > Na^+$) (Aidley and Stanfield, 1996).

The differences of ions in ion hydration numbers leads to a difference in the velocity at which they will move through a solution in an electric field, i.e. ion mobility. The greater the ion hydration number, the less is its mobility since ions carrying more water will have to move more slowly (e.g. Li+ < Na+ < K+) (Aidley and Stanfield, 1996).

The flux of water through membrane due to a chemical potential gradient in the membrane is called **osmotic flux**. In most practical applications, osmotic flux can be neglected since it is generally very low compared to the other two. So, electroosmotic flux and flux due to hydration shell can be claimed to be the dominating factors in water transport through membrane.

The water transport number refers to the number of water molecules transferred by one ion through a given membrane. It is expressed as;

$$T_w = \frac{J_w}{\sum J_i} \tag{2.92}$$

where T_w is the water transport number and J_w is the water flux through membrane while the summation in the denominator refers to the total ion flux through membrane. It is a function of the properties of the membrane and electrolyte (e.g. ion size, valence, concentration). In most commercial electromembrane processes with aqueous salt solutions, T_w is between 4-8 (Strathmann, 2004).

2.2.2.4 Effect of membrane heterogeneity in transport

The structure of the membrane, especially membrane heterogeneity, is very important in the characteristics of membrane transport. The structure of a membrane

may be considered to be consisting of two or more phases. There are several proposals to define this structure of phases in literature (Elmidaoui et al, 1998; Bouma et al, 1997; Choi et al, 2001). Timashev (1991) claimed that membrane can be defined in a two-phase model with a hydrophobic backbone and a hydrophilic ion-exchange group, including sorbed water. On the other hand, Zabolotsky and Nikonenko (1993) proposed a membrane structure of a conducting phase and a non-conducting phase. The conducting phase (f_{gel}), also called as the gel fraction, is composed of ionic groups, hydrophilic parts of the matrix polymer chains, and electroneutral solution as a filler. The non-conducting phase (f_{inert}), called as the inert fraction, involves the hydrophobic parts of the polymer matrix or the inert binder (Pabby et al, 2009).

Homogeneous membranes have a higher conducting fraction (f_{gel}) than heterogeneous membranes. That's why homogeneous membranes can be called as coherent ion-exchanger gels and heterogeneous membranes can be called as structures having colloidal ion exchanger particles embedded in an inert binder. This structure difference greatly affects the transport mechanism.

In homogeneous membranes, the primary ion transport mechanism is realized by the leaping of a cation from one charged site to the next within the membrane (Fig. 2.11.a). As for heterogeneous membranes, high inert phase ratio causes resistance to ion transport in the following ways (Pabby et al, 2009);

- tortuosity or the path length of ion transfer through the membrane is increased as illustrated in Fig. 2.11.b,
- the inert phase without ionic groups is always less conducive to transport of ions.

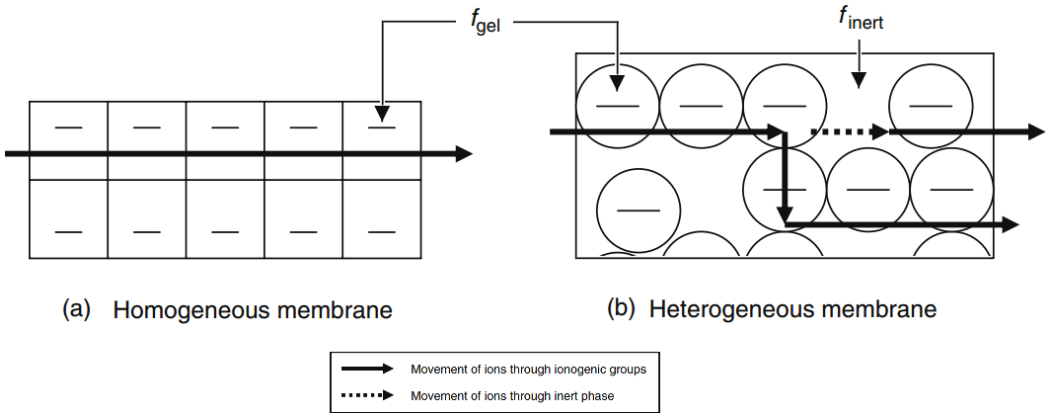

Figure 2.11 : Transport mechanisms of ions in (a) homogeneous (b) heterogeneous membranes (Pabby et al, 2009).

2.3 Electromembrane Process Applications

There is a large number of electromembrane processes that utilize ion-exchange membranes as key components and applied at commercial scale. All these processes are based on the separation of some species with the help of membrane and electrical field. However, the targets of these separation processes are different and can be roughly categorized into three groups;

- Processes where the main target is to separate; e.g. electrodialysis (ED), electrodeionization (EDI) (Porter, 1990; Noble and Stern, 1995).
- Processes where the main target is chemical synthesis; e.g. chlor–alkali process or hydrogen production (Numes and Peinemann, 2001).
- Processes where the main target is to generate power; fuel cells or batteries.

The processes, like ED or chlor-alkali, have one thing in common, i.e. in both processes a salt is split in order to facilitate the processes. That's why these kinds of processes can also often be referred as **electrochemical splitting** or **electromembrane splitting** processes.

In this section, some of the electromembrane processes applications of industrial significance will be dealt with.

2.3.1 Electrodialysis

ED is a combination of electrolysis and ion selective permeation. In case a potential is applied across a ionic solution, ions are transported across the solution and their transport is realized selectively with the help of ion exchange membranes (Judd, 2003).

First industrial applications of ion exchange membranes were in the field of electrodialysis. Moreover, it can be claimed that the emergence of electrodialysis boosted the development of fundamental ion exchange process theory (Tanaka, 2007).

A simple ED process is illustrated in Fig. 2.12. The solution to be desalted is fed to the electrodialysis cell, where cation and anion exchange membranes are placed alternately. Under the influence of electrical field, anions move towards anode, while cations move towards cathode. When the ions move through the membrane to the

next chamber, they cannot move further since they are rejected by the next membrane, which has the same fixed charge as the ion. So, one chamber gets rich in ions (concentrate chamber) while the adjacent chamber gets deionized (diluate chamber).

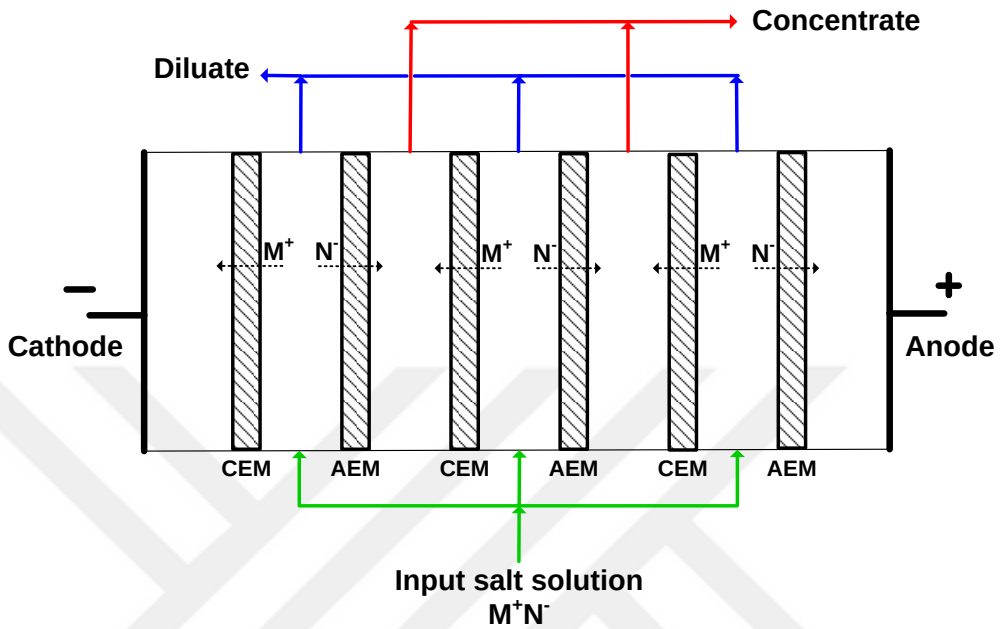

Figure 2.12 : Electrodialysis process.

Initial applications of ED, mainly in Japan, were to produce sodium chloride from seawater. Later, it spread to desalination and a number of recovery applications.

Water desalination by ED attained commercial level during 1960's, which was before the introduction of reverse osmosis. Today, the most important large-scale application of ED is the production of portable water from brackish water. This technology competes with reverse osmosis and multistage flash evaporation. For solutions having low salt concentration comparatively (<5000 ppm), ED seems to be the most economical option. An important advantage of ED is that the concentrate stream can be highly concentrated (around up to 20%).

There are several applications of ED other than desalination such as; demineralization of molasses in order to increase the sugar recovery (Elmidaoui et al, 2004), acid removal from fruit juice (Serre et al, 2016), separation of amino acids and minerals in amino acid production process (Eliseeva et al, 2009), regeneration of sorbents (Liu et al, 2010), acid regeneration/production (Koter and Kultys, 2008; Ahmed, 2002;Korngold et al, 2006), treatment of industrial wastewater for both

pollution reduction and valuable mineral recovery purposes (Scoma et al, 2016; Marder et al, 2016; Guo et al, 2015; Rácz and Ilea, 2013).

Another important application of this process is called reverse electrodialysis (RED). As the name suggests, RED is the reverse of electrodialysis by means of input/output relations. In RED, salinity gradient between different solutions are utilized to generate electricity. This technology emerged in 1950's and has been further developed (Güler, 2014).

2.3.2 Electrosynthesis

All electrochemical processes where a synthesis occurs can be evaluated under this title, while the most typical example is chlor-alkali process. In chlor-alkali process, with the electrolysis of sodium chloride, sodium hydroxide is produced along with chlorine and hydrogen gases.

The basic cell reaction in chlor-alkali process is illustrated in Fig. 2.13. Concentrated NaCl solution is fed to the anode chamber of the cell while water (more commonly dilute sodium hydroxide) is fed to the cathode chamber. In anode chamber chloride ion is oxidised to chloride gas and sodium ions pass through the membrane to the cathode cell. In cathode chamber, water is split at cathode to give hydroxyl ions and hydrogen gas. These hydroxyl ions combine with the sodium ions transported from the anode chamber to give sodium hydroxide.

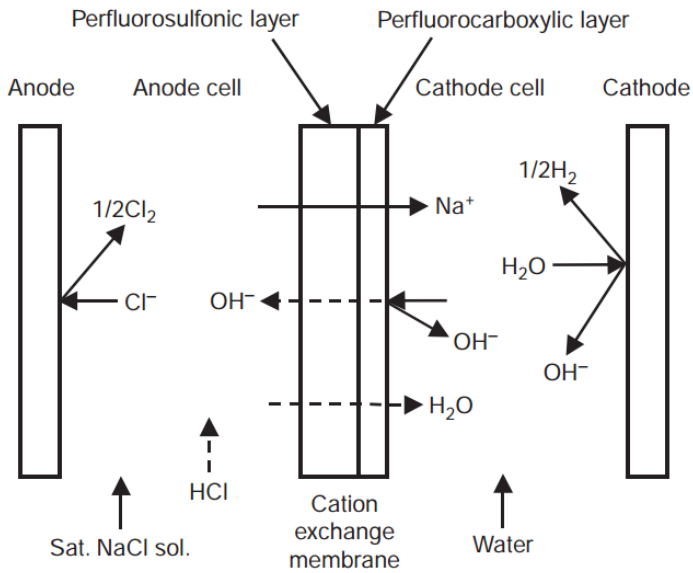

Figure 2.13 : Chlor-alkali process(Tanaka, 2007).

The development of chemically and thermally stable perfluorinated ion exchange membranes has led to the growth of the chlor-alkali industry. Perfluorinated carboxylic acid group membranes make high current efficiencies possible in caustic soda production while surface treatment of the membrane that helps release bubbles from the membrane surface reduces the cell voltage, therefore power consumption, significantly (Tanaka, 2007).

Before the introduction of membrane chlor-alkali process, caustic soda production was dependent on mercury and diaphragm technologies. The shift to membrane process has brought along the following benefits: reduction in power costs, attainment of higher purity level and elimination of environmental hazards associated with mercury and asbestos (Chandran and Chin, 1986).

Ion exchange membrane can also be used for the electrolysis of water to produce hydrogen gas for energy purposes. In this case, perfluorocarbon cation-exchange membranes and inorganic ion exchange membranes can be utilized (Jensen et al, 2008; An et al, 2014; Manabe et al, 2013; Tuomi et al, 2013).

2.3.3 Fuel cells

Fuel cell is an electrochemical energy conversion device, which that converts the chemical energy from a fuel into electricity through a chemical reaction of positively charged hydrogen ions with oxygen (Fig. 2.14). Proton exchange membrane (PEM) has recently gained popularity for fuel cells. The usage of perfluorosulphonic acid membranes for hydrogen-oxygen fuel cell as an electrolyte is well known.

In a hydrogen-oxygen fuel cell, hydrogen is fed into the anode chamber of the fuel cell, where it is activated by a catalyst to split into protons and electrons. The proton passes through the electrolyte, which is a cation exchange membrane, while electrons pass through a circuit to generate electricity. The protons that pass through the membrane combine with oxygen in the cathode compartment to produce water (Lee et al, 2006).

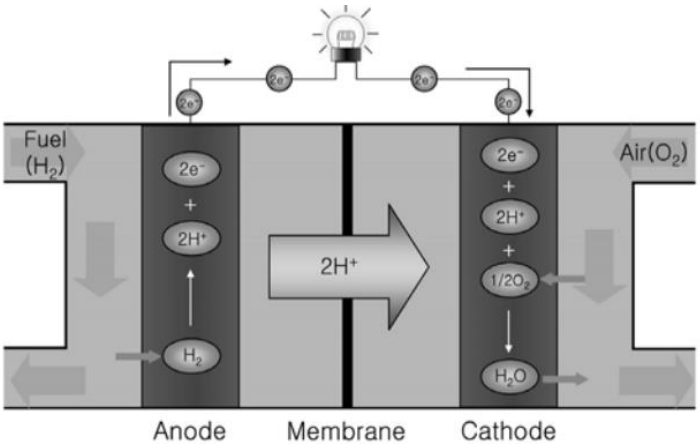

Figure 2.14 : Fuel cell (Tanaka, 2007).

3. ELECTROMEMBRANE PROCESS for LIOH PRODUCTION

In this chapter, lithium sulphate membrane electrolysis process is modelled as both a batch and continuous process. In this modelling, basic faradaic equations, which define the production of hydrogen/oxygen gases as well as the transport of species through membrane are utilized.

In the macroscopic modelling of membrane electrolysis process, concentration gradients due to location in the cell or the reactors are ignored ($\nabla C \cong 0$). Thus, perfect mixing is assumed and formation of concentration boundary layers at any interface is not taken into consideration. The only components leaving the system are assumed to be oxygen and hydrogen gases produced by anodic and cathodic reactions. Mass loss due to evaporation is ignored. Modelling is performed with the help of faradaic equations, yet it can be reinforced with the help of empirical relationships obtained in experimental studies (Chapter 4). First, mass change of the anolyte and catholyte solutions are calculated, after which mass balance of the whole system is evaluated. Two types of process alternatives are considered in this section:

1) Batch process
2) Continuous process

3.1 Batch Process

In the modelling of batch process, only the initial amount of electrolyte solutions are taken into consideration without any further feeding to the system. The anolyte and catholyte solutions are circulated from their reactors to their respective compartments continuously at a constant flow rate and temperature. First, anolyte and catholyte mass balances are solved. Then, the change of mass in the whole system is calculated. The schematical expression of mass balance of anolyte and catholyte solutions is shown in Figure 3.1.

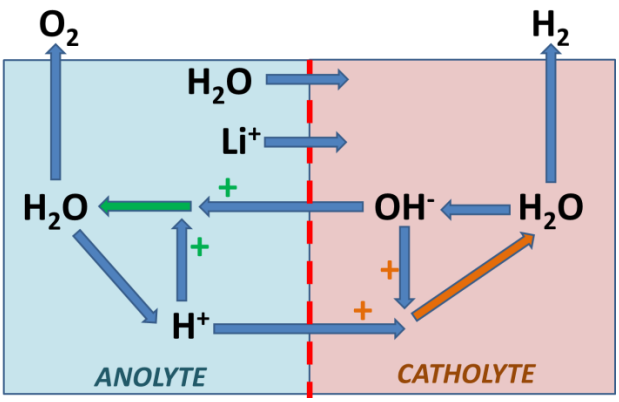

Figure 3.1 : Mass balance of anolyte and catholyte solutions in batch process.

3.1.1 Anolyte mass balance

For anolyte, mass balances of the following components are taken into consideration:

- Lithium ion (Li^+), sulphate ion (SO_4^{2-}), hydrogen ion (H^+), oxygen gas (O_2), water (H_2O)

The production, consumption and transport of components in anolyte are clearly seen in Figure 3.1. Sulphate amount is assumed to be constant since theoretically it neither passes through membrane nor decomposes.

In the anode chamber, oxygen is produced as a result of anodic water splitting reaction, which is defined by the first term (*i*) on the right side of the equation;

$$\Delta N_{O_2}^{a} = \underbrace{\frac{I.t}{4.F}}_{i} - \underbrace{Q_{out_{O_2}}^{a}}_{ii} \tag{3.1}$$

In this equation and in the equations following, Δ indicates the change of a quantity while N is number of moles, F is Faraday constant (96485C.mol^{1-}), t is time in seconds (s). The superscript of N term shows whether the change term belongs to the anolyte (a) or catholyte (c), while its subscript indicates the related component. So, $\Delta N_{O_2}^{a}$ term indicates "the change of number of moles of oxygen in the anolyte solution". The change of oxygen due to anodic reaction is positive, however, since the produced oxygen leaves the chamber ($Q_{out_{O_2}}^{a}$), total change of oxygen is zero.

The change of the amount of hydrogen ions in anolyte occurred in three ways: *i*) production as a result of anodic water splitting reaction, *ii*) consumption as a result of reaction with the hydroxyl ions transported from catholyte chamber to anolyte

chamber through membrane, *iii*) transport of hydrogen ions from anolyte chamber to catholyte chamber through membrane. These equations can be expressed as;

$$\Delta N_H^a = \underbrace{\frac{I.t}{F}}_{i} - \underbrace{\frac{I.t}{F}.T_{OH}}_{ii} - \underbrace{\frac{I.t}{F}.T_H}_{iii} \tag{3.2}$$

As for water, the change occurred in three ways: *i*) consumption as a result of anodic water splitting reaction, *ii*) production of water due to reaction of produced hydrogen ions with hydroxyl ions which are transported from catholyte chamber to anolyte chamber through membrane *iii*) transport of water from anolyte chamber to catholyte chamber through membrane due to different water transport mechanism such as shell hydration, electroosmotic transfer and pumping effects. These equations can be expressed as;

$$\Delta N_{H_2O}^a = -\underbrace{\frac{I.t}{2.F}}_{i} + \underbrace{\frac{I.t}{F}.T_{OH}}_{ii} - \underbrace{\frac{I.t}{F}.T_{H_2O}}_{iii} \tag{3.3}$$

Lithium is not produced or consumed in any reaction in anolyte. So, the only lithium change is via transport through membrane, which is defined by the following equation;

$$\Delta N_{Li}^a = -\frac{I.t}{F}.T_{Li} \tag{3.4}$$

T_{Li}, T_{OH} , T_H and T_{H_2O} are transport numbers for Li^+, OH^-, H^+ and H_2O, respectively.

The equations above are re-arranged adding their initial amounts in the equations and considering the transport relation (2.47) in order to define their instantaneous amount at any time "t" during membrane electrolysis process. The amounts of Li^+, H^+, H_2O and SO_4^{2-} at any time "t" are given in the following equations, respectively;

$$M_{Li}^a = \left(N_{(Li)_0}^a - \frac{I.t}{F}.T_{Li}\right).w_{Li} \tag{3.5}$$

$$M_H^a = \left(N_{(H)_0}^a + \frac{I.t}{F}.T_{Li}\right).w_H \tag{3.6}$$

$$M_{H_2O}^a = \left[N_{(H_2O)_0}^a + \frac{I.t}{F}.\left(T_{OH} - T_{H_2O} - \frac{1}{2}\right)\right].w_{H_2O} \tag{3.7}$$

$$M_{SO_4}^a = N_{(SO_4)_0}^a.w_{SO_4} \tag{3.8}$$

In these equations, M refers to the weight of a component (g), while w is the molecular weight of a component (g/mole) and N_0 values are the initial values. The initial total weight of anolyte is;

$$M^a_{T_0} = N^a_{(Li)_0}.w_{Li} + N^a_{(H)_0}.w_H + N^a_{(H_2O)_0}.w_{H_2O} + N^a_{(SO_4)_0}.w_{SO_4} \quad (3.9)$$

Summation of the individual amounts of change gives the total mass change of anolyte, which is;

$$\Delta M^a_T = \frac{I.t}{F}.\left[-T_{Li}.w_{Li} + T_{Li}.w_H + \left(T_{OH} - T_{H_2O} - \frac{1}{2}\right).w_{H_2O}\right] \quad (3.10)$$

So, the total weight of anolyte at time "t" is,

$$M^a_T = M^a_{T_0} + \Delta M^a_T \quad (3.11)$$

Percentage concentration is a very useful parameter letting the easy track of the changes in electrolytes. Percentage concentrations are;

$$X^a_{Li} = \frac{M^a_{Li}}{M^a_T}.100 \quad (3.12)$$

$$X^a_H = \frac{M^a_H}{M^a_T}.100 \quad (3.13)$$

$$X^a_{H_2O} = \frac{M^a_{H_2O}}{M^a_T}.100 \quad (3.14)$$

$$X^a_{SO_4} = \frac{M^a_{SO_4}}{M^a_T}.100 \quad (3.15)$$

respectively for (% w/w)Li^+, H^+, H_2O and SO_4^{2-} components. X is weight percentage concentration (% w/w).

3.1.2 Catholyte mass balance

In catholyte mass balance, the following components are taken into consideration:

- Lithium ion (Li^+), hydroxyl ion (OH^-), hydrogen gas (H_2), water (H_2O)

The production, consumption and transport of components in catholyte can be seen in Figure 3.1.

In the cathode chamber, hydrogen gas is produced as a result of cathodic water splitting reaction, which is defined by the first term on the right side of the equation (*i*);

$$\Delta N^{c}_{H_2} = \underbrace{\frac{I.t}{2.F}}_{i} - \underbrace{Q^{c}_{out_{H2}}}_{ii} \tag{3.16}$$

The change of hydrogen due to cathodic reaction is positive, however, since the produced hydrogen leaves the chamber ($Q^{c}_{out_{H_2}}$), total change of oxygen is zero.

The change of the amount of hydroxyl ions in catholyte occurred in three ways: i) production as a result of cathodic water splitting reaction, ii) consumption as a result of reaction with the hydrogen ions transported from anolyte chamber to catholyte chamber through membrane, iii) transport of hydroxyl ions from catholyte chamber to anolyte chamber through membrane. These equations can be expressed as;

$$\Delta N^{c}_{OH} = \underbrace{\frac{I.t}{F}}_{i} - \underbrace{\frac{I.t}{F}.T_H}_{ii} - \underbrace{\frac{I.t}{F}.T_{OH}}_{iii} \tag{3.17}$$

As for water, the change occurred in three ways: i) consumption as a result of cathodic water splitting reaction, ii) production of water due to reaction of produced hydroxyl ions with the hydrogen ions which are transported from anolyte chamber to catholyte chamber through membrane iii) transport of water from anolyte chamber to catholyte chamber through membrane due to different water transport mechanism such as shell hydration, electroosmotic transfer and pumping effects. These equations can be expressed as;

$$\Delta N^{c}_{H_2O} = \underbrace{-\frac{I.t}{F}}_{i} + \underbrace{\frac{I.t}{F}.T_H}_{ii} + \underbrace{\frac{I.t}{F}.T_{H_2O}}_{iii} \tag{3.18}$$

Lithium is not produced or consumed in any reaction in catholyte. So, the only lithium change is via transport through membrane from anolyte chamber, which is defined by the following equation;

$$\Delta N^{c}_{Li} = \frac{I.t}{F}.T_{Li} \tag{3.19}$$

T_{Li}, T_{OH} , T_H and T_{H_2O} are transport numbers for Li^+, OH^-, H^+ and H_2O, respectively.

The equations above are re-arranged adding their initial amounts in the equations and considering the transport relation (2.48) in order to define their instantaneous amount at any time "t" during membrane electrolysis process. The amounts of Li^+, $OH^-$and H_2O in catholyte at any time "t" are given in the following equations, respectively;

$$M_{Li}^{c} = \left(N_{(Li)_0}^{c} + \frac{I.t}{F}.T_{Li}\right).w_{Li} \tag{3.20}$$

$$M_{OH}^{c} = \left(N_{(OH)_0}^{c} + \frac{I.t}{F}.T_{Li}\right).w_{OH} \tag{3.21}$$

$$M_{H_2O}^{c} = \left[N_{(H_2O)_0}^{c} + \frac{I.t}{F}.\left(T_H + T_{H_2O} - 1\right)\right].w_{H_2O} \tag{3.22}$$

In these equations, M refers to the weight of a component (g), while w is the molecular weight of a component (g/mole) and N_0 values are the initial values. The initial total weight of catholyte is;

$$M_{T_0}^{c} = N_{(Li)_0}^{c}.w_{Li} + N_{(OH)_0}^{c}.w_{OH} + N_{(H_2O)_0}^{c}.w_{H_2O} \tag{3.23}$$

Summation of the individual amounts of change gives the total mass change of catholyte, which is;

$$\Delta M_{T}^{c} = \frac{I.t}{F}.\left[T_{Li}.w_{Li} + T_{Li}.w_{OH} + \left(T_H + T_{H_2O} - 1\right).w_{H_2O}\right] \tag{3.24}$$

So, the total weight of anolyte at time "t" is,

$$M_{T}^{c} = M_{T_0}^{c} + \Delta M_{T}^{c} \tag{3.25}$$

Percentage concentration is a very useful parameter letting the easy track of the changes in electrolytes. Percentage concentrations are;

$$X_{Li}^{c} = \frac{M_{Li}^{c}}{M_{T}^{c}}.100 \tag{3.26}$$

$$X_{OH}^{c} = \frac{M_{OH}^{c}}{M_{T}^{c}}.100 \tag{3.27}$$

$$X_{H_2O}^{c} = \frac{M_{H_2O}^{c}}{M_{T}^{c}}.100 \tag{3.28}$$

respectively for (% w/w) Li^+, OH^- and H_2O and SO_4^{2-} components. X is weight percentage concentration (% w/w).

3.2 Continuous Process

For the macroscopic modelling of continuous process, the conditions and assumptions for batch process are valid. Additionally, feed terms are inserted into the continuous process model for both electrolytes. The schematical expression of mass balance of anolyte and catholyte solutions is shown in Figure 3.2.

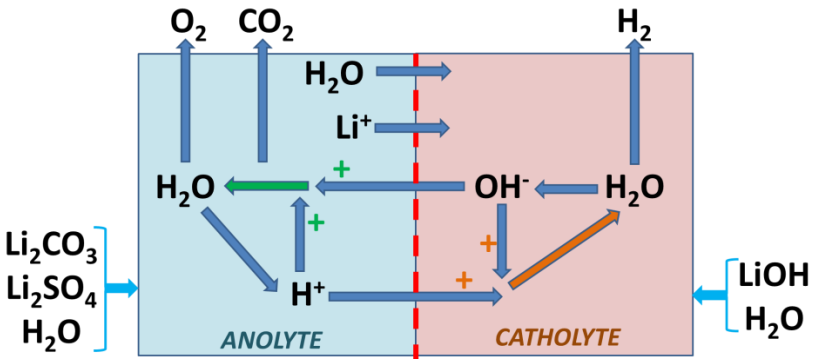

Figure 3.2 : Mass balance of electrolyte solutions in continuous process.

As seen in Figure 3.2, anolyte feed can be either of the following;

- Solid Li_2CO_3
- Li_2SO_4 solution

while catholyte feed is either,

- H_2O or
- LiOH solution

Mass balance for continuous process will be set up according to the general mass conservation relation;

$$Input - Output + Reaction = Accumulation$$

Applying this relation to membrane electrolysis case gives the following possible transformation/transport processes:

- Input:
  - Li_2CO_3/Li_2SO_4 feed to anolyte solution
  - LiOH feed to catholyte solution
  - Transport of species from the other side of the membrane
- Output:
  - Output of the overflowing solutions from both sides
  - Transport of species to the other side of the membrane
  - Gases leaving from system in both chambers
- Reaction:

- Generation/consumption of species due to electrodic water splitting reaction for both electrolytes
- Generation/consumption of species due to the reaction of the fed Li_2CO_3 in anolyte solution

3.2.1 Anolyte mass balance

In the calculation of anolyte mass balance for continuous operation, the two options for anolyte feed will be evaluated in one term, Q_{in}^{a} (kg/s), which is the total feed rate of all possible species to be fed into anolyte reactor.$C_{in_\alpha}^{a}$, $C_{in_\beta}^{a}$ and $C_{in_\gamma}^{a}$are weight concentrations (moles/kg) for Li_2CO_3, Li_2SO_4 and H_2O species present in the feed, respectively. Thus, in case of solid 100% pure Li_2CO_3 feed only, $C_{in_\beta}^{a}$ and $C_{in_\gamma}^{a}$ will be equal to 0 while $C_{in_\alpha}^{a}$ will be equal to the inverse of the molecular weight of Li_2CO_3.

For continuous operation, some amount of the solution has to overflow from both electrolytes in order to maintain constant mass steady state operation in each reactors. For anolyte side, Q_{out}^{a} (kg/s) is the term representing the total amount of the solution overflowing from anolyte reactor.

Mass balances of the following components in anolyte are taken into consideration for continuous process;

- Lithium ion (Li^+), sulphate ion (SO_4^{2-}), hydrogen ion (H^+), oxygen gas (O_2), water (H_2O), carbon dioxide gas (CO_2), solid lithium carbonate (Li_2CO_3)

Li_2CO_3 has negligible solubility in water. So, it is assumed that Li_2CO_3 has one phase as solid and does not dissolve in the electrolyte solution. That's why it is handled as a separate component and is not included in the lithium ion mass balance.

Lithium carbonate which is fed to the anolyte reactor reacts with sulphuric acid that is produced by anodic reaction according to reaction. This reaction consumes Li_2CO_3 and H_2SO_4, while producing carbon dioxide and increasing the amount of water;

$$\mathrm{Li_2CO_3 + H_2SO_4 \rightarrow Li_2SO_4 + CO_2 + H_2O} \tag{3.29}$$

In this modelling, it is assumed that Li_2CO_3 feed rate is not higher than the stoichiometric equivalence of H_2SO_4 since solid unreacted/undissolved lithium carbonate may cause a serious problem in the process (clogging the membrane,

sticking on the electrode surface etc.) So, it is assumed that lithium carbonate will be the limiting reactant in all cases, which means that Li_2CO_3 is consumed completely and does not accumulate in the system.

The general mass conservation relation for anolyte solution is expressed in the following equation;

$$\dot{F}_x^{a_in} - \dot{F}_x^{a_out} - r_x^a = \frac{d(C_x^a.M_T^a)}{dt} \tag{3.30}$$

where F indicates the flowrate (moles/s) while its subscript indicates the component in question and its superscript indicates whether the flowrate is into or out of the anolyte solution. Inward flow can be either due to the anolyte feed or due to the transport of species from catholyte side of the membrane while outward flow can be due to the following: overflowing from anolyte solution, transport of species to the catholyte side of the membrane, oxygen gas leaving from anode chamber. $r$isthe reaction rate (moles/s), that is generation and/or consumption of the component. The right hand side of the equation is the accumulation term while C is the molar concentration (moles/s).M_T^a (kg) is the total amount of solution in anolyte reactor. The subscript,a, which is present in all terms above, shows that the related term belongs to anolyte solution.

To begin with lithium carbonate mass balance, it can be said that the rate of Li_2CO_3 feed (i) is equal to the rate of its consumption (ii) since it is the limiting reactant in its reaction with sulphuric acid. These changes can be expressed as;

$$\underbrace{Q_{in}^a.C_{in_\alpha}^a}_{i} - \underbrace{Q_{in}^a.C_{in_\alpha}^a}_{ii} = 0 \tag{3.31}$$

Carbon dioxide is generated as a reaction of the fed lithium carbonate with sulphuric acid to produce lithium sulphate (ii), yet the generated gas does not accumulate and leaves the anode chamber (i) ;

$$-\underbrace{Q_{in}^a.C_{in_\alpha}^a}_{i} + \underbrace{Q_{in}^a.C_{in_\alpha}^a}_{ii} = 0 \tag{3.32}$$

Oxygen has no input flow. It is produced as a result of anodic water splitting reaction (ii) and the produced oxygen does not accumulate but leaves the chamber (i). So, the expression becomes;

$$\underbrace{-Q^{a}_{out_{O_2}}}_{i} + \underbrace{\frac{I}{4.F}}_{ii} = 0 \tag{3.33}$$

There is not input of hydrogen ions into anode chamber. The change of the amount of hydrogen ions in anolyte occurred in the following ways: *i*) outward flow of overflowing hydrogen ions *ii*) outward flow of hydrogen ions from anolyte chamber to catholyte chamber through membrane, *iii*) generation as a result of anodic water splitting reaction, *iv*) consumption as a result of reaction with the hydroxyl ions transported from catholyte chamber to anolyte chamber through membrane, *v*) consumption due to the reaction with the fed lithium carbonate. These changes can be expressed as;

$$\underbrace{-Q^{a}_{out}.C^{a}_{H}}_{i} \underbrace{-\frac{I}{F}.T_{H}}_{ii} \underbrace{+\frac{I}{F}}_{iii} \underbrace{-\frac{I}{F}.T_{OH}}_{iv} \underbrace{-2.Q^{a}_{in}.C^{a}_{in_{\alpha}}}_{v} = \frac{d(C^{a}_{H}.M^{a}_{T})}{dt} \tag{3.34}$$

As for water, the change occurred in the following ways: *i*) inward flow of water within lithium sulphate solution feed, *ii*)outward flow of overflowing water *iii*) outward flow of water from anolyte chamber to catholyte chamber through membrane due to different water transport mechanism such as shell hydration, electroosmotic transfer and pumping effects, *iv*) generation of water due to the reaction of produced hydrogen ions with hydroxyl ions which are transported from catholyte chamber to anolyte chamber through membrane, *v*) generation of water as a result of the reaction of sulphuric acid with the fed lithium carbonate, *vi*) consumption as a result of anodic water splitting reaction. These changes can be expressed as;

$$\underbrace{Q^{a}_{in}.C^{a}_{in_{\gamma}}}_{i} \underbrace{-Q^{a}_{out}.C^{a}_{H_2O}}_{ii} \underbrace{-\frac{I}{F}.T_{H_2O}}_{iii} \underbrace{+\frac{I}{F}.T_{OH}}_{iv} \underbrace{+Q^{a}_{in}.C^{a}_{in_{\alpha}}}_{v} \underbrace{-\frac{I}{2.F}}_{vi} = \frac{d\left(C^{a}_{H_2O}.M^{a}_{T}\right)}{dt} \tag{3.35}$$

Lithium ion is directly fed to the anolyte solution within lithium sulphate feed (*i*) and/or generated as a reaction of the fed lithium carbonate with sulphuric acid to produce lithium sulphate (*iv*). The outward flow of lithium ions occurred via overflowing water (*ii*) and migration through membrane under electric field (*iii*). These changes are summarized in the following equation;

$$\underbrace{2.Q_{in}^{a}.C_{in_\beta}^{a}}_{i} - \underbrace{Q_{out}^{a}.C_{Li}^{a}}_{ii} - \underbrace{\frac{I.t}{F}.T_{Li}}_{iii} + \underbrace{2.Q_{in}^{a}.C_{in_\alpha}^{a}}_{iv} = \frac{d(C_{Li}^{a}.M_{T}^{a})}{dt} \tag{3.36}$$

Sulphate is not produced or consumed in any reaction in anolyte. So, the only sulphate input is via lithium sulphate solution feed (*i*) while the only output occurred with overflowing sulphate ions (*ii*);

$$\underbrace{Q_{in}^{a}.C_{in_\beta}^{a}}_{i} - \underbrace{Q_{out}^{a}.C_{SO_4}^{a}}_{ii} = \frac{d\left(C_{SO_4}^{a}.M_{T}^{a}\right)}{dt} \tag{3.37}$$

The general mass conservation relation (4.29) can be adopted to find the instantaneous total amount of mass in anolyte solution, M_T^a, as expressed in the following equation;

$$\sum(\dot{F}_{x}^{a_{in}} - \dot{F}_{x}^{a_{out}} - r_{x}^{a}).w_{x} = \frac{d(M_{T}^{a})}{dt} \tag{3.38}$$

where F indicates the flowrate (moles/s) while its subscript indicates the component in question and its superscript indicates whether the flowrate is into or out of the anolyte solution. w is the molecular weight of each component. So, the left hand side of (3.37) gives the total amount of mass change in anolyte solution, which is calculated by the summation of individual amount of mass changes as shown in equations (3.31)-(3.37);

$$\frac{d(M_{T}^{a})}{dt} = \left(-Q_{out}^{a}.C_{H}^{a} - \frac{I}{F}.T_{H} + \frac{I}{F} - \frac{I}{F}.T_{OH} - 2.Q_{in}^{a}.C_{in_\alpha}^{a}\right).w_{H} + \left(Q_{in}^{a}.C_{in_\beta}^{a} - Q_{out}^{a}.C_{SO_4}^{a}\right).w_{SO_4} + \left(2.Q_{in}^{a}.C_{in_\beta}^{a} - Q_{out}^{a}.C_{Li}^{a} - \frac{I.t}{F}.T_{Li} + 2.Q_{in}^{a}.C_{in_\alpha}^{a}\right).w_{Li} + \left(Q_{in}^{a}.C_{in_\gamma}^{a} - Q_{out}^{a}.C_{H_2O}^{a} - \frac{I}{F}.T_{H_2O} + \frac{I}{F}.T_{OH} + Q_{in}^{a}.C_{in_\alpha}^{a} - \frac{I}{2.F}\right).w_{H_2O} \tag{3.39}$$

The right hand side of (3.38) is simplified as $\Delta\dot{M}_T^a$, which is the total amount of mass change in anolyte solution, and the differential equation was integrated over time t to find;

$$M_{T}^{a} = M_{T0}^{a} + \Delta\dot{M}_{T}^{a}.t \tag{3.40}$$

where which M_T^a is the instantaneous amount of total mass in anolyte solution while M_{T0}^a is the initial amount of total mass in anolyte solution.

3.2.2 Catholyte mass balance

In the calculation of catholyte mass balance for continuous operation, catholyte feed is expressed in one term, Q_{in}^{c}(kg/s), which is the total feed rate into catholyte reactor.$C_{in_\theta}^{c}$ and $C_{in_\gamma}^{c}$ are weight concentrations (mol/kg) for LiOH and H_2O species present in the feed, respectively. Thus, in case of 100% H_2O feed only, $C_{in_\theta}^{c}$will be equal to 0 while and $C_{in_\gamma}^{c}$will be equal to the inverse of the molecular weight of H_2O.

For continuous operation, some amount of the solution has to overflow from catholyte solution in order to maintain constant mass steady state operation in catholyte reactor. Q_{out}^{c} (kg/s) is the term representing the total amount of the solution overflowing from catholyte reactor.

Mass balances of the following components in catholyte are taken into consideration for continuous process;

- Lithium ion (Li^+), hydroxyl ion (OH^-), hydrogen gas (H_2), water (H_2O)

In continuous operation, the general mass conservation relation for catholyte solution is expressed in the following equation;

$$\dot{F}_x^{c_in} - \dot{F}_x^{c_out} - r_x^c = \frac{d(C_x^c \cdot M_T^c)}{dt} \tag{3.41}$$

where F indicates the flowrate (moles/s) while its subscript indicates the component in question and its superscript indicates whether the flowrate is into or out of the catholyte solution. Inward flow can be either due to the anolyte feed or due to the transport of species from anolyte side of the membrane while outward flow can be due to the following: overflowing from catholyte solution, transport of species to the anolyte side of the membrane, hydrogen gas leaving from anode chamber. r is the reaction rate (moles/s), that is generation and/or consumption of the component. The right hand side of the equation is the accumulation term while C is the molar concentration (moles/s). M_T^c (kg) is the total amount of solution in catholyte reactor. The subscript,c, which is present in all terms above, shows that the related term belongs to catholyte solution.

In the cathode chamber, hydrogen gas is produced as a result of cathodic water splitting reaction (*ii*) and the produced hydrogen gas does not accumulate but leaves the chamber (*i*). So, the expression becomes;

$$\underbrace{-Q^{c}_{out_{H_2}}}_{i} + \underbrace{\frac{I}{2.F}}_{ii} = 0 \tag{3.42}$$

The change of the amount of hydroxyl ions in catholyte occurred in the following ways: *i*) inward flow of hydroxyl ions within lithium hydroxide solution feed, *ii*)outward flow of overflowing catholyte solution, *iii*) outward flow of hydroxyl ions to anolyte chamber through membrane, *iv*) production as a result of cathodic water splitting reaction, *v*) consumption as a result of reaction with the hydrogen ions transported from anolyte chamber to catholyte chamber through membrane. These equations can be expressed as;

$$\underbrace{Q^{c}_{in}.C^{c}_{in_\theta}}_{i} - \underbrace{Q^{c}_{out}.C^{c}_{OH}}_{ii} - \underbrace{\frac{I}{F}.T_{OH}}_{iii} + \underbrace{\frac{I}{F}}_{iv} - \underbrace{\frac{I}{F}.T_{H}}_{v} = \frac{d(C^{c}_{OH}.M^{c}_{T})}{dt} \tag{3.43}$$

For water, the change occurred in five ways: *i*) inward flow of water within catholyte feed, *ii*) inward flow of water from anolyte chamber through membrane due to different water transport mechanisms (shell hydration, electroosmotic transfer etc.), *iii*) outward flow of overflowing water, *iv*) production of water due to reaction of produced hydroxyl ions with the hydrogen ions which are transported from anolyte chamber to catholyte chamber through membrane, *v*) consumption as a result of cathodic water splitting reaction,. These equations can be expressed as;

$$\underbrace{Q^{c}_{in}.C^{c}_{in_\gamma}}_{i} + \underbrace{\frac{I}{F}.T_{H_2O}}_{ii} - \underbrace{Q^{c}_{out}.C^{c}_{H_2O}}_{iii} + \underbrace{\frac{I}{F}.T_{H}}_{iv} - \underbrace{\frac{I}{F}}_{v} = \frac{d\left(C^{c}_{H_2O}.M^{c}_{T}\right)}{dt} \tag{3.44}$$

Lithium is not produced or consumed in any reaction in catholyte. However, the following changes occur: *i*) inward flow of lithium within lithium hydroxide feed, *ii*) inward flow of lithium from anolyte chamber through membrane under electric field, *iii*) outward flow of overflowing lithium.

$$\underbrace{Q^{c}_{in}.C^{c}_{in_\theta}}_{i} + \underbrace{\frac{I}{F}.T_{Li}}_{ii} - \underbrace{Q^{c}_{out}.C^{c}_{Li}}_{iii} = \frac{d(C^{c}_{Li}.M^{c}_{T})}{dt} \tag{3.45}$$

The general mass conservation relation (3.30) can be adopted to find the instantaneous total amount of mass in catholyte solution, M^{c}_{T}, as expressed in the following equation;

$$\sum(\dot{F}_x^{c_{in}} - \dot{F}_x^{c_{out}} - r_x^c).w_x = \frac{d(M_T^c)}{dt} \tag{3.46}$$

where F indicates the flowrate (moles/s) while its subscript indicates the component in question and its superscript indicates whether the flowrate is into or out of the anolyte solution. w is the molecular weight of each component. So, the left hand side of (3.44) gives the total amount of mass change in catholyte solution, which is calculated by the summation of individual amount of mass changes as shown in equations (3.41)-(3.43);

$$\frac{d(M_T^c)}{dt} = \left(Q_{in}^c.C_{in_\theta}^c + \frac{I}{F}.T_{Li} - Q_{out}^c.C_{Li}^c\right).w_{Li} + \left(Q_{in}^c.C_{in_\theta}^c - Q_{out}^c.C_{OH}^c - \frac{I}{F}.T_{OH} + \frac{I}{F} - \frac{I}{F}.T_H\right).w_{OH} + \left(Q_{in}^c.C_{in_\gamma}^c + \frac{I}{F}.T_{H_2O} - Q_{out}^c.C_{H_2O}^c + \frac{I}{F}.T_H - \frac{I}{F}\right).w_{H_2O} \tag{3.47}$$

The right hand side of (3.45) is simplified as $\Delta\dot{M}_T^c$, which is the total amount of mass change in catholyte solution, and the differential equation was integrated over time t to find;

$$M_T^c = M_{T0}^c + \Delta\dot{M}_T^c.t \tag{3.48}$$

where which M_T^c is the instantaneous amount of total mass in catholyte solution while M_{T0}^c is the initial amount of total mass in catholyte solution.

4. EXPERIMENTAL STUDIES

4.1 Overview of Experimental Studies

The main aim of the experimental studies was to investigate the electro-membrane salt splitting process to produce lithium hydroxide using lithium sulphate in a two-compartment membrane electrolysis cell by means of determining significant parameters affecting on the process and understanding the membrane transport behaviour during the electro-membrane process. Most of the experimental study was realized with perfluorinated homogeneous Nafion®N-424 membrane. Further experiments were realized with perfluorinated homogeneous Nafion®N-438 and heterogeneous MK-40 membranes in order to be able to compare the findings for Nafion®N-424 membrane with other commercial membranes of the same/different type.

First, membrane characterization was performed in terms of water content and ion exchange capacity. Then anolyte solution was prepared and purified by means of acidic reaction and ion exchange resin treatment processes. Next, experimental studies to establish a conductivity/pH vs. concentration regression equation in order to predict instantaneous concentration changes during membrane electrolysis was performed. After that, membrane electrolysis experiments were carried out, which can be classified in three sections:

- In Section 4.6, general behaviour of Nafion® N-424 membrane in the electrochemical production of lithium hydroxide in a two-compartment membrane electrolysis cell under different process parameters (temperature, current density, catholyte concentration) was investigated. Within this section, the performance of Nafion® N-424 was compared similar previous studies and optimum membrane electrolysis parameters for this process is recommended based on a production cost estimation.

- In Section 4.7, based on the findings in the previous section (Section 4.6), the effect of ion concentrations (Li^+ in anolyte, H^+ in anolyte and OH^- in catholyte) on transport numbers was further investigated and a regression model equation was put forward reflecting the scientific reality observed in the membrane transport mechanism. Also, in this section, continuous feed experiments were done in addition to batch experiments in order to both supply near zero acidity condition and to simulate a constant concentration process, which was required to reflect industrial process conditions.

- In Section 4.8, the findings on N-424 were compared with another perfluorinated membrane (N-438) as well as a heterogeneous cation exchange membrane (MK-40). Similarly, regression analyses were carried out for N-438 and MK-40 membranes to model membrane transport.

4.2 Materials and Equipment

Catholyte solution was prepared from technical grade lithium hydroxide (min. 99%, Sorel Co.) and used without further purification steps. Anolyte solution, lithium sulphate, was prepared from technical grade lithium carbonate (min. 99%, Sorel Co.) and analytical grade sulphuric acid (Merck) and was purified as described below. Distilled water was used when necessary. Technical grade lithium carbonate was declared to contain max. 40 mg/kg Ca and max.10 mg/kg Mg by the supplier.

Conductivity and pH measurements were done with WTW pH/cond 340i multimeter. To keep the solutions at constant temperature during measurements, a water bath (Julabo SW22) was used.

Amberlite® IRC 748 resin, which was used in anolyte purification process for the removal of hardness was supplied by Dow Co.

In membrane electrolysis experiments, the required current was fed by Aim TTI QPX1200SP DC power supply (60V-50A max.) to the electromembrane cell (EC Electro MP-Cell), which was supplied by Electrocell Co. The cell was composed of a hydrogen evolving cathode (SS), an oxygen evolving platinized titanium build up anode (DSA) and an ion exchange membrane allowing the transport of cations but reducing the back-transport of cathodically-formed hydroxyl ions. Properties of the cell are given in Table 4.1 (Electrocell Co., n.d.).

Table 4.1 : Properties of the electromembrane cell (EC Electro MP-Cell).

Cell module dimensions	Height: 306 mm Width: 182 mm
Projected electrode area (min)	0.01 m^2
Current density (max)	4 kA/m^2
Electrode-membrane gap	3 mm
Anode	DSA® platinized Ti build
Cathode	Stainless steel
Injection-moulded frames and other plastic components	PVDF
Gaskets (O-rings)	EPDM

4.3 Chemical Analysis Methods

In electrolysis experiments, anolyte and catholyte solutions were analysed to determine certain ion concentrations. In the study explained in Section 4.7, only lithium analysis was performed to determine lithium transport number. However, in the studies explained in Section 4.8 and Section 4.9, along with lithium ion, hydrogen and hydroxyl ions were determined as well. Since it was preferred to weigh samples instead of measuring their volumes, all analysis results are reported as mg/kg.

Anolyte solutions were analysed for their Li^+ and H^+ content, while catholyte solutions were analysed for their Li^+ and OH^- content. Lithium analysis was performed with ICP-OES (Thermo Scientific iCAP 6500). Samples were weighed and diluted to the calibration interval (10-50 ppm Li) prior to analysis.

Hydrogen ion analysis was performed titrimetically with 0.5 N NaOH. Known amount of sample was diluted to around 50 mL with water in a beaker. A pH-meter was inserted into the beaker to control the end-point of titration, which is around 7. Prior to sample analysis, a known amount of sulphuric acid solution was titrated in order to make sure accurate results are obtained at the end-point.

Titrimetric method was also applied for hydroxyl ion analysis. Known amount of sample was diluted to around 50 mL with water in a beaker. 2-3 drops of phenolphthalein solution was added. Titration was performed with 1 N HCl, where the end-point was determined with the disappearance of the pink colour.

4.4 Membrane Characterization

Most of the experimental study was realized with Nafion®N-424 membrane. Further experiments were realized with Nafion®N-438 and MK-40 membranes in order to be able to compare the findings for Nafion®N-424 membrane with other commercial membranes.

Nafion® membranes (Nafion®N-424 and Nafion®N-438), products of Dupont, were supplied by Ion Power Co., USA, while MK-40 cation exchange membrane was supplied by Shchekinoazot Co., Russia.

Nafion® N-424 and N-438 are perfluorosulfonic acid cation exchange membranes with polytetrafluoroethylene (PTFE) fiber reinforcement. They may be used in chlor-alkali process as well as in other electrolysis processes. N-438 -as stated by the producer- has a new PTFE monofilament reinforcement with high strength but flatter profile than N-424 (Dupont Co., 2010; Ion Power Co., n.d.). Detailed information about perfluorinated membranes can be found in Section 2.2.1.2. Both membranes were supplied in dry H^+ form.

MK-40 is a heterogeneous cation exchange membrane (Section 2.2.1.2), which is a high-molecular-weight polymer (polystyrene, divinylbenzene) containing SO_3H functional groups. During the production polyethylene inert binder is used while the polymeric structure is reinforced with polyamide (Novikova et al, 2005; (Azotom Co., n.d.). MK-40 is supplied Na^+ form. Pictures of all membranes are shown in Fig. 4.1.

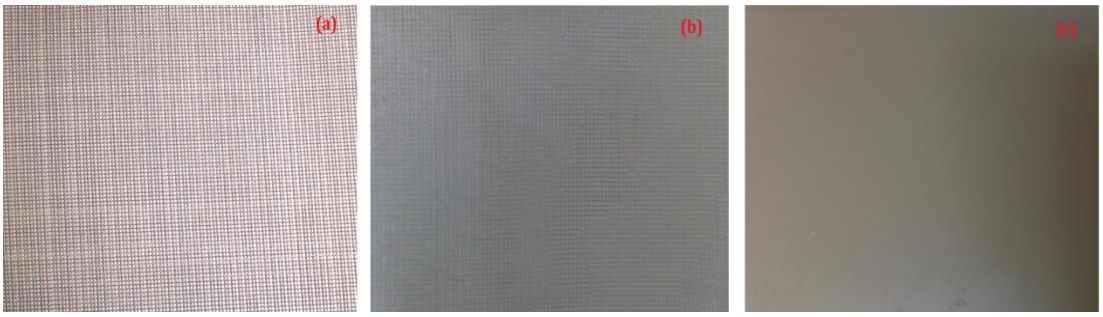

Figure 4.1 : Membranes used in the experimental studies (a) N-424, (b) N-438, (c) MK-40.

4.4.1 Experimental

4.4.1.1 Pre-treatment of membranes

The membranes that were supplied in H^+ and Na^+ forms were transformed into Li^+ form prior to use in the electrolysis experiments. Membranes were soaked into 1% LiOH solution. Membranes stayed in this solution for 3 days and every day the solution was refreshed. Moreover, the first experiment of each membrane was for pre-treatment purpose to guarantee the removal of any unwanted cations from the membrane.

4.4.1.2 Determination of water content

Water content is the amount of water adsorbed in the matrix of the membrane. Prior to the determination of water content of membranes, all membranes were converted to H^+ form. Approximately 1 g sample of membranes were cut and soaked in 9% HCl solution, where they stayed for 24 hours with a couple of refreshment of the solutions. After that, membranes were washed with ultra-pure water to remove excess HCl and were soaked in demi water for another 24 hours. After 24 hours, membranes were drawn out, the excess water on their surface was removed by wiping the surface gently and they were weighed (w_{wet}). Wet membranes were dried at 60°C for 24 hours and weighed again (w_{dry}). Water content of the membrane, W_{mem} (%), was calculated as (Hwang et al, 1999; Savari et al, 2008);

$$W_{mem} = 100.\frac{w_{wet} - w_{dry}}{w_{dry}} \tag{4.1}$$

4.4.1.3 Determination of ion exchange capacity

Ion exchange capacity is the equivalent number of fixed charges per unit weight of dry membrane. To determine ion exchange capacity, first membranes were converted to H^+ form. Approximately 1 g sample of membranes were soaked in 9% HCl solution, where they stayed for 24 hours with a couple of refreshment of the solutions. After that, membranes were washed to remove excess HCl and were soaked in ultra-pure water for another 24 hours. After 24 hours, membranes were drawn out and the excess water on their surface was removed by wiping the surface gently. Next, membranes were soaked in 0.5 N 50 mL NaOH solution in a closed container for 24 hours. Then a sample was taken from NaOH solution and ion

exchange capacity was determined from the reduction in alkalinity by back titration with 1 N HCl. Ion exchange capacity (IEC, meq/g) was calculated as;

$$\mathrm{IEC} = \frac{V_N.N_N - \frac{V_1}{V_2}.V_H.N_H}{w_{dry}} \tag{4.2}$$

where, V_N and N_N are the initial volume and molarity of NaOH solution, V_H and N_H are the volume and molarity of HCl solution used in titration, V_1 is the final volume of NaOH solution, V_2 is the volume of the sample taken from final NaOH solution for titration and w_{dry} is the dry weight of the membrane used in analysis (Hwang et al, 1999; Savari et al, 2008).

4.4.2 Results

Water content and ion exchange capacity results are given in Table 4.2. The most remarkable thing is the comparatively high water content and ion exchange capacity of MK-40 membrane. One significant factor for this is the comparatively very thick structure of MK-40, which is unique to heterogeneous membranes. For a fair comparison, the thickness of the membranes were measured and found to be 290µm, 320 µm and 520 µm for dry N-424, N-438 and MK-40 membranes, respectively. When the differences between wet and dry thicknesses of the membranes are compared, it is seen than MK-40 swells greatly (Table 4.2) while the thickness of N-424 or N-438 does not change dramatically. So, when ion exchange capacities are normalized to the volume of the membranes, it can be claimed that the difference in ion exchange capacities will decrease though MK-40 membrane is still expected to have a higher ion exchange capacity per volume. This is in line with the fact that water content increases with the increase of the concentration of ion exchange groups (Saito et al, 2005).

Table 4.2 : Membrane characterization results.

Membrane	Water content (%)	Ion exchange capacity (meq/dry membrane)	Wet thickness (µm)	Dry thickness (µm)
N-424	18.8	1.01	290	270
N-438	19.6	1.00	340	320
MK-40	63.4	3.08	610	520

4.5 Anolyte preparation and purification

4.5.1 Purpose

Anolyte solutions were synthesized by lithium carbonate - sulphuric acid reaction and exposed to a pre-treatment procedure. This is because, in membrane electrolysis technology, the performance and life of the membrane is related to the purity of the electrolyte solution. Previous studies show that, especially multivalent cations in anolyte solution cause precipitation in the inner pores and outer walls of the membrane which causes an increase in cell potential along with a decrease in the service life of membrane (Molnar, 1977; Ogata et al, 1989).

Therefore, anolyte solutions were pre-treated by ion exchange resin to decrease their total hardness (calcium, magnesium) content prior to membrane electrolysis.

4.5.2 Experimental

Anolyte solution was prepared according to the reaction **(3.29)** and the preparation and purification procedure is given in Figure 4.2.

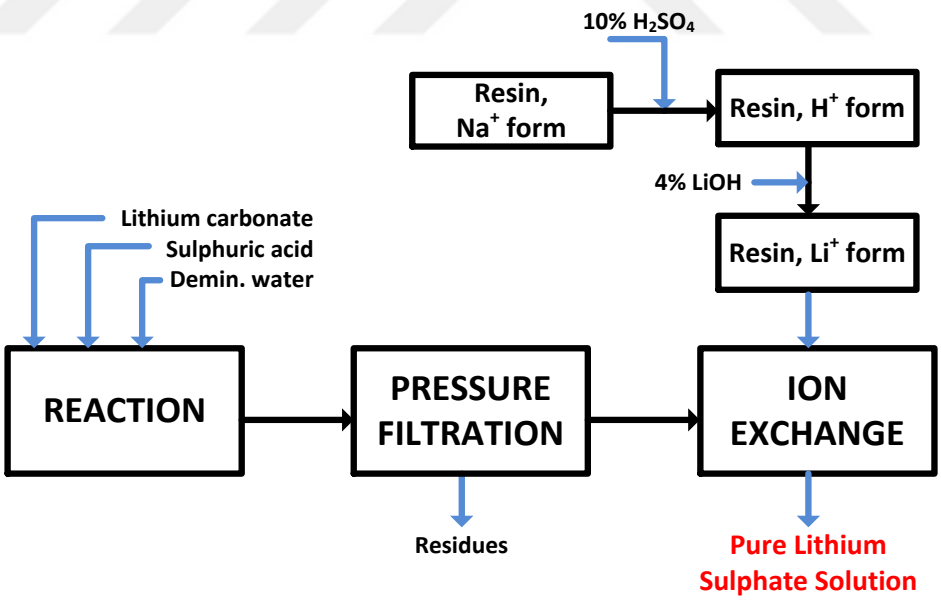

Figure 4.2 : Anolyte preparation and pre-treatment procedure.

First, a sulphuric acid solution was prepared in a 50 L HDPE tank slowly enough to prevent high temperatures. The tank was stirred with an overhead stirrer. Temperature and pH of the tank was monitored during the whole process. Then, lithium carbonate was added gradually in order not to cause overflowing due to the

carbon dioxide evolution. Excess lithium carbonate was added to ensure the complete consumption of sulphuric acid. After addition, the slurry product was further stirred and stayed overnight to complete the reaction. When pH value increased to ca. 8.25-8.50, the stirrer was stopped. The slurry stayed still a couple of hours so that non-dissolved solids could settle. Then the solution was filtrated with a pressure filter to remove impurities and non-reacted solids. The filtrate was then subjected to an ion exchange resin process to decrease calcium, magnesium and iron content for the good of electro-membrane process.

For the ion exchange process, Amberlite IRC 748 resin was used. This resin was originally in sodium form. A regeneration process was applied to convert it to lithium form so that the resulting solution would not contain any sodium impurity. The regeneration procedure recommended by the supplier was adopted for lithium-form regeneration (Rohm and Haas Co., 2006). For this purpose, 350 ml resin was placed in a column and regeneration solutions were passed through the column in the following order: (i) Initial washing with water, (ii) transformation into H^+ form with 10% H_2SO_4 solution, (iii) transformation into Li^+ form with 4% LiOH solution, (iv) final washing to remove excess regenerant solution. After regeneration, the anolyte solution to be purified was fed from the top of the column at 10 BV/h (bed volume/h) speed.

Calcium and magnesium amounts of anolyte solutions were analysed with ICP-OES prior to and after ion exchange process to determine the efficiency of the removal process.

4.5.3 Results

The effectiveness of the hardness (Ca-Mg) removal by ion exchange process was evaluated with the help of the analysis of anolyte before and after the ion exchange process with ICP-OES. The results are given in Table 4.3. In this table it is seen that calcium and magnesium removal rates are acceptable while lithium loss was negligible with as low as 1% removal percentage.

Table 4.3 : Results of anolyte ion exchange purification process.

	Li, %	**Ca, ppm**	**Mg, ppm**
Beginning of the I.Ex. process	2.63	10.16	6.46
End of the I.Ex. process	2.61	1.68	2.84
Removal, %	0.8	83.5	56.0

4.6 Conductivity/pH v.s. Concentration Relation of Electrolytes

4.6.1 Purpose

Conductivity is a very crucial parameter in electrolysis experiments. It directly affects the power consumption due to the basic relationships mentioned in the theoretical section (Eq. 2.56-2.58).

The determination of the conductivity-concentration correlation is beneficial for membrane electrolysis experiments in two ways:

- It is required to determine the maximum conductivity level of the solution.
- It is the easiest way to predict the instantaneous concentration change without analysing the solution.

Moreover, since pH is a very important parameter revealing the H^+ and OH^- concentration of electrolytes, the correlation of pH and concentration becomes a useful tool to monitor the electrochemical processes.

Due to these reasons, conductivity-pH vs. concentration correlation was determined for anolyte (Li_2SO_4-H_2SO_4) and catholyte (LiOH) solutions at certain concentrations and temperatures.

4.6.2 Experimental

Conductivity-concentration regression analyses were performed for anolyte (Li_2SO_4) and catholyte (LiOH) solutions at certain concentrations and temperatures as given in Table 4.4. Solutions that were prepared at certain concentrations were poured into 150 ml erlenmeyer flasks and placed into a pre-set shaking water bath. As the set temperature was reached, conductivity measurements were performed.

Table 4.4 : Preliminary conductivity measurements.

Factors:	**Li_2SO_4 %**	**LiOH %**	**Temperature °C**
Levels:	5	1	30
	10	3	45
	15	5	60
	20	7	
	23		

These "preliminary conductivity measurements" were done to determine the optimum lithium sulphate concentration for anolyte. This helped to decide the optimum initial anolyte concentration for a batch process. However, during electrolysis, lithium sulphate concentration decreases while sulphuric acid concentration increases. Thus, it is vital to determine conductivity-concentration regression equation for lithium sulphate-sulphuric acid mixtures in order to be able to predict the instantaneous anolyte concentration. That's why, concentration change of anolyte during electrolysis was simulated with the help of lithium sulphate-sulphuric acid mixtures having varying concentrations prepared regarding the determined optimum initial lithium sulphate concentration and according to theoretical anodic reaction. At these concentration levels, "secondary conductivity measurements" were performed, as described in the following "Results" section. In these measurements, pH was also measured since two different regression equations (for conductivity and pH) are required in order to be able to predict two different concentrations (lithium sulphate and sulphuric acid).

On the other hand, "preliminary conductivity measurements" is sufficient for regression analysis of catholyte since catholyte is a solution of lithium hydroxide only.

The accuracy of the established concentration-conductivity regression equations were tested in a separate experiment.

Moreover, in order to be able to observe the changes in a larger matrix, conductivity/pH values of anolyte solutions in a larger concentration range were measured and a separate regression analysis was carried out for this case.

4.6.3 Results

The results of “preliminary conductivity measurements” for catholyte solutions are shown in Figure 4.3. In Fig. 4.3, conductivity increases with the increase of concentration and temperature. However, a peak point, that is to say an optimum lithium concentration level in terms of conductivity, was not observed in the range studied. A polynomial was fitted to express the conductivity-concentration regression equation as seen in Figure 4.3.

The results of “preliminary conductivity measurements” for anolyte solutions are shown in Figure 4.4. In Fig. 4.4, it can be seen that anolyte conductivity increases with the increase of Li_2SO_4 concentration till a concentration level between 15 and 20% Li_2SO_4. Above this concentration level, conductivity tends to decrease. This is due to the solvent deficiency phenomena aforementioned in Chapter 2 (Theoretical Background). To determine the peak concentration point from local maxima, a third degree polynomial was fitted to each curve. It was found that maximum conductivity could be achieved at Li_2SO_4 concentration of 17, 16.5 and 17.3% for temperatures of 30, 45 and 60°C, respectively. So, the average peak concentration for 30-60°C temperature range is ca. 17% Li_2SO_4.

Since the electrolysis experiments in this section would be conducted batch-wise, the decrease in the anolyte concentration should be considered for selecting the appropriate initial anolyte concentration. Since ca. 5% decrease in Li_2SO_4 concentration during the experiments was predicted, the initial anolyte concentration was selected to be around 20%, which could compensate the decrease of the anolyte concentration as being higher than the peak point of 17%.

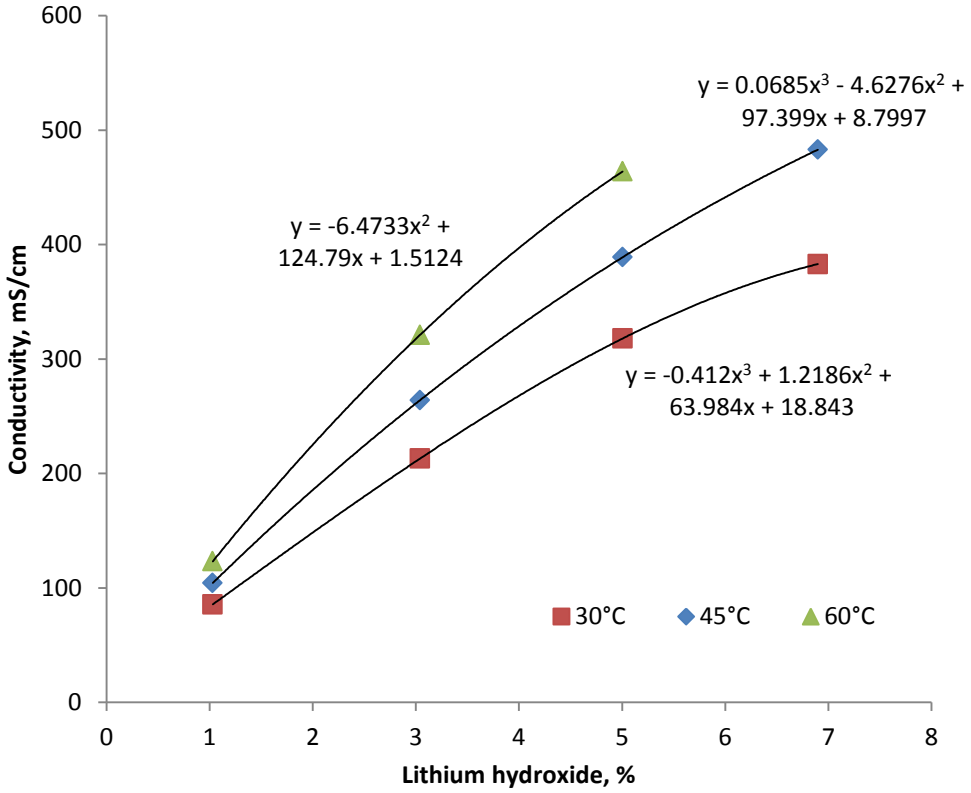

Figure 4.3 : Conductivity-concentration regression for catholyte (LiOH) solution.

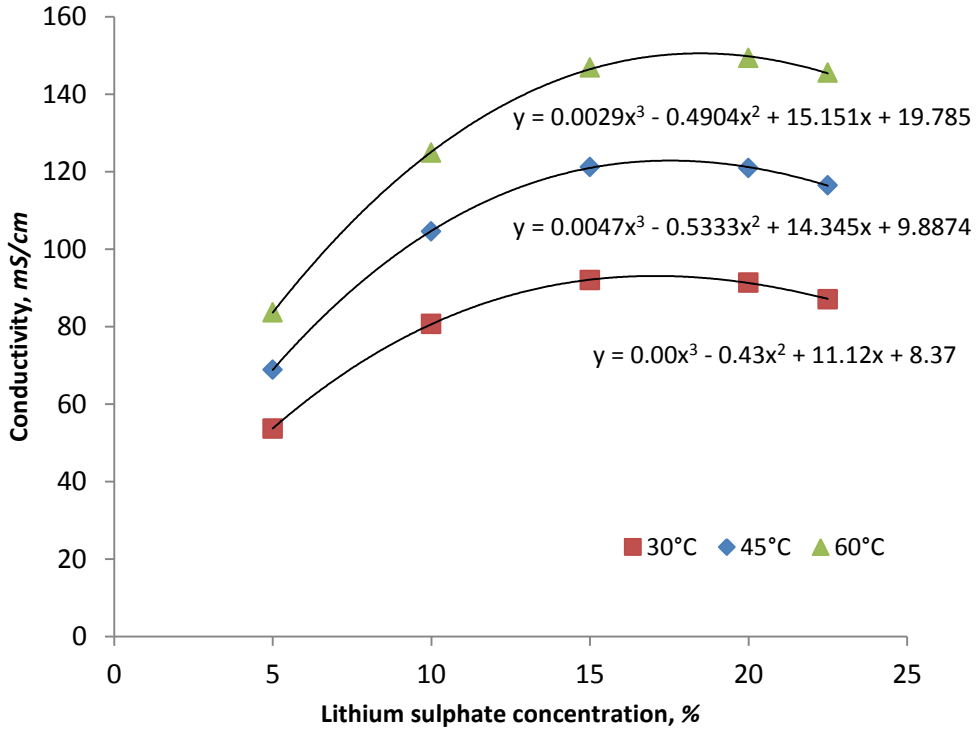

Figure 4.4 : Conductivity-concentration regression for anolyte (Li_2SO_4) solution.

After the determination of the optimum initial anolyte concentration level with the help of "preliminary conductivity measurements", "secondary conductivity measurements" of lithium sulphate-sulphuric acid mixtures having varying

concentrations were performed at 30°C in order to simulate the concentration change of the anolyte during electrolysis. The results are presented in Table 4.5.

Table 4.5 : Secondary conductivity measurements.

No	Li_2SO_4, %	H_2SO_4, %	pH	Conductivity, mS/cm
1	20.0	0	8.50	91.5
2	19.4	0.5	2.05	96.7
3	18.9	1	1.69	102.2
4	18.3	1.5	1.50	107.4
5	17.8	2	1.35	113.9
6	16.6	3	1.14	128.4
7	15.5	4	1.00	143.1
8	14.4	5	0.91	160.1

Both pH and conductivity values were correlated with lithium sulphate and sulphuric acid values with the help of MS Excel 2010 Data Analysis. The theory of multiple regression is given in Appendix A. Thus, regression analyses were performed with the values in Table 4.5 for the following regression equations;

$$\mathrm{pH} = \mathrm{C1} + \mathrm{C2} \times \alpha + \mathrm{C3} \times \beta \tag{4.3}$$

$$\mathrm{Cond}\ (\mathrm{mS.cm^{-1}}) = \mathrm{C4} + \mathrm{C5} \times \alpha + \mathrm{C6} \times \beta \tag{4.4}$$

where α and β are lithium sulphate and sulphuric acid concentrations (in %) respectively. The constants were found to be -1169972, 58498.72, 65572.25, -730809, 36544.8 and 40978 for C1, C2, C3, C4, C5 and C6, respectively. The adjusted R-square values for pH and conductivity equations were 0.996 and 0.994, respectively, which indicates a good correlation.

The established regression equations were tested in a separate batch electrolysis experiment. In this experiment, initial anolyte concentration was 20% lithium sulphate while initial catholyte concentration was 1% lithium hydroxide. 10 A current was applied during the experiment for 2.5 hours and every 30 minutes, conductivity-pH measurements were done and samples were taken from both electrolytes. The concentrations of lithium sulphate, sulphuric acid and lithium hydroxide were determined with the help of Li^+, H^+ and OH^- analysis via ICP and acid-base titrations. These concentrations were also predicted with the help of the measured pH-conductivity values and the previously established regression equations. The measured and predicted values are compared in Table 4.6. Table 4.6

shows that anolyte concentration prediction gives average error values of 6.0% and 19.5% for lithium sulphate and sulphuric acid concentration, respectively. Lithium sulphate error can be claimed to be acceptable, yet sulphuric acid prediction can yield high level of errors, which is attributed to the logarithmic relationship of pH with hydrogen ion concentration. On the other hand, lithium hydroxide can be predicted successfully with an average error value of 4.6%.

Table 4.6 : Comparison of the measured and predicted concentration values.

	Catholyte				Anolyte							
t, min	**Cond., mS/cm**	**LiOH**			**Cond., mS/cm**	**pH**	**Li2SO4**			**H2SO4**		
		Meas., %	Pred., %	Err., %			Meas., %	Pred., %	Err., %	Meas., %	Pred., %	Err., %
0	81.7	1.05	0.93	11.3	94.2	8.20	19.1	19.8	3.5	0.00	0.20	-
30	122.1	1.59	1.65	3.9	108.3	1.39	18.2	18.3	0.9	0.97	1.49	54.2
60	149.3	1.99	2.11	5.9	121.2	1.02	17.8	17.3	2.9	2.03	2.41	18.6
90	169.2	2.31	2.44	5.4	132.6	0.84	17.3	16.4	5.1	2.91	3.22	10.7
120	190.4	2.69	2.80	4.1	147.4	0.65	16.8	15.2	9.5	3.98	4.26	7.1
150	208.0	3.00	3.12	3.8	163.9	0.48	16.1	13.9	13.6	5.08	5.43	6.9

In order to be able to test if accuracy in concentration prediction can be increased further, some approaches were shown. In the first approach, lithium sulphate was defined as dependent variable, which was dependent on conductivity only since lithium sulphate concentration change was not greatly related with pH change. Moreover, sulphuric acid concentration was defined as;

$$\mathrm{C_{H2SO4}} = (\mathrm{C^0_{Li2SO4}} - \mathrm{C_{Li2SO4}}).\frac{\mathrm{M^0}}{\mathrm{M}} \tag{4.5}$$

where C_{H2SO4} and C_{Li2SO4} are concentrations (moles/kg) of sulphuric acid and lithium sulphate respectively, M is the total amount of solution (kg) while ^{0} superscript refers to the initial value of the related parameter. This relationship was formed considering the fact that sulphate concentration is constant in the case above, which requires that the total (molar) concentration of lithium sulphate and sulphuric acid at any time "t" will be equal to the initial concentration of lithium sulphate in moles. $\frac{M^0}{M}$ ratio was required to be able to take the mass change of the solution into consideration. The mass change was calculated according to;

$$\mathrm{M} = \mathrm{M^0} - \left(\frac{\mathrm{It}}{\mathrm{2F}} + \frac{\mathrm{It}}{\mathrm{F}}.\mathrm{T_w}\right).\mathrm{w_{H2O}} \tag{4.6}$$

where I is the current applied during electrolysis, t is time (seconds), T_w is the water transport number through membrane, F is Faraday, w_{H2O} is the molecular weight of water. The first term in brackets represents the mass change due to anodic water splitting reaction, the second term represents the mass change due to transport of water through membrane while other mass changes are neglected in this calculation. T_w is assumed constant as 6.8 according to the water transport number results in the following Section (Section 4.7). Lithium sulphate regression equation was found as (R_squared = 0.9995);

$$\alpha = 32.438 - 0.1681\text{cond} + 0.000347\text{cond}^2 \tag{4.7}$$

where α is lithium sulphate concentration (%) and *cond* is conductivity (mS/cm).

Table 4.7 : Anolyte concentration prediction according to Eq. 4.5-7.

Anolyte							
Cond.,mS/cm	**pH**	**Li2SO4**			**H2SO4**		
		Meas., %	Pred., %	Err., %	Meas., %	Pred., %	Err., %
94.2	8.20	19.1	19.7	3.0	0.00	0.0	-
108.3	1.39	18.2	18.3	0.7	0.97	1.3	31.0
121.2	1.02	17.8	17.2	3.6	2.03	2.4	17.0
132.6	0.84	17.3	16.2	5.9	2.91	3.3	14.8
147.4	0.65	16.8	15.2	9.6	3.98	4.5	12.8
163.9	0.48	16.1	14.2	11.8	5.08	5.7	11.3

As seen in Table 4.7, the errors in concentration prediction slightly decreased for lower concentration levels of sulphuric acid with an average error value of 5.8% and 17.4% for lithium sulphate and sulphuric acid, respectively.

In a second approach, lithium sulphate and sulphuric acid concentrations were accepted as dependent variables being functions of conductivity and pH while the interaction between independent parameters was taken into consideration, too. The regression equations produced with this approach are;

$$\alpha = 23.534 + 4.18 * \text{pH} - 0.0412 * \text{cond} - 0.0437 * \text{pH} * \text{cond} \tag{4.8}$$

$$\beta = -3.152 - 3.73 * \text{pH} + 0.0368 * \text{cond} + 0.0389 * \text{pH} * \text{cond} \tag{4.9}$$

Eq. (4.8) improved the prediction of lithium sulphate with an error range of 0.7-5.6% and an average error value of 3.6%. On the other hand, Eq. (4.9) does not seem to

have any contribution in the accuracy of the prediction of sulphuric acid concentration compared to the values in Table 4.6 with an average error value of 19.8%.

All these analyses showed that lithium hydroxide and lithium sulphate could be predicted with average error values as low as 3.6% and 4.6%. However, the average error value in the prediction of sulphuric acid was not able to be reduced below 17.4%. This is probably due to the fact that sulphuric acid concentration is mainly defined by pH parameter, which has logarithmic relationship with concentration and this logarithmic character can result in great deviations. On the other hand, lithium sulphate concentration can be mainly defined by conductivity parameter, which is more close to linearity. As for lithium hydroxide, since this species is the only concentration element in catholyte solution, conductivity value of catholyte is successful in expressing the lithium hydroxide concentration value.

Up to now, the conductivity/pH vs. concentration relation was investigated according to the scheme where around 20% lithium sulphate solution is electrolysed with no further feeding into the anolyte solution, which makes it possible to simulate the change in anolyte assuming that sulphate amount is constant. Now, the investigation will be conducted in a larger concentration matrix of lithium sulphate/ sulphuric acid mixtures. As seen in Table 4.8, pH and conductivity values of lithium sulphate (5-20%) and sulphuric acid (0-10%) mixtures were measured.

A regression analysis was carried out using data in Table 4.8 and the obtained equations were used in the prediction of the results of the previous test measurements. It was found that in order to reach more sensible results, pH equration can be handled in two separate equations (partial functions). Above pH≈1, logarithmic equations are better in the prediction of while below pH≈1 polynomial equations are better utilized. So, a partial functions system formed of;

$$\mathrm{ph} = 1.2012 - 0.7061 \log \beta \qquad (4.10.a)$$

$$\mathrm{ph} = 8.496 - 2.572\beta + 0.1830\beta^2 \qquad (4.10.b)$$

are used to define pH. Here pH was assumed to be a function of only sulphuric acid concentration, which is a sensible approach. On the other hand conductivity was defined as;

$$\mathrm{Cond} = 32.52 + 3.829\alpha + 31.62\beta + 0.508\beta^2 - 1.3256\alpha\beta \qquad (4.11)$$

Table 4.8 : Anolyte concentration measurements in a larger concentration range.

Li_2SO_4, %	H_2SO_4, %	ph	Cond., mS/cm
5,00	0,00	8,300	51,3
7,50	0,00	8,300	67,4
10,00	0,00	8,380	79,1
15,00	0,00	8,407	92,9
20,00	0,00	8,375	96,3
5,00	2,57	1,183	107,1
7,51	2,48	1,220	114,8
10,00	2,54	1,223	122,9
14,99	2,54	1,227	128,9
19,98	2,56	1,191	124,2
5,01	5,05	0,862	185,9
7,50	5,02	0,859	178,1
10,01	5,01	0,856	174,7
14,99	5,06	0,840	168,2
19,91	4,99	0,803	152,0
5,01	7,56	0,655	275,0
7,52	7,60	0,617	254,0
10,00	7,48	0,606	235,0
14,96	7,58	0,610	211,0
19,96	7,55	0,542	181,4
5,04	10,05	0,528	363,0
7,52	10,10	0,488	332,0
10,04	9,90	0,447	297,0
14,96	10,05	0,412	254,0
19,97	10,05	0,370	209,0

First, sulphuric acid concentration was found using (4.10.a-b). Then lithium sulphate concentration was determined using (4.11). These equations were utilized to predict the measurements of the test equation. However, no better results were reached compared to the previous analyses (average error values were 22.7% and 19.7% for sulphuric acid and lithium sulphate, respectively). Even, the results were worse for the case of lithium sulphate. So, it can be claimed that performing measurements in a narrower matrix (close to the range studied) is better in terms of the prediction of conductivity values. However, it should be noted that sulphuric acid prediction can be still expected to be a little bit erroneous.

4.7 General Membrane Behaviour in The Electrochemical Production of Lithium Hydroxide

4.7.1 Purpose

In this section of the study, it was aimed to investigate the general behaviour of Nafion®N-424 membrane in the electrochemical production of lithium hydroxide in a two-compartment membrane electrolysis cell under different process parameters (temperature, current density, catholyte concentration) and to compare the performance with similar previous studies. Moreover, optimum membrane electrolysis parameters for this process were recommended based on a production cost estimation realized using the results of this study.

4.7.2 Experimental

The materials-equipment required and the necessary pre-treatment procedures are described in Section 4.2 and Section 4.5.

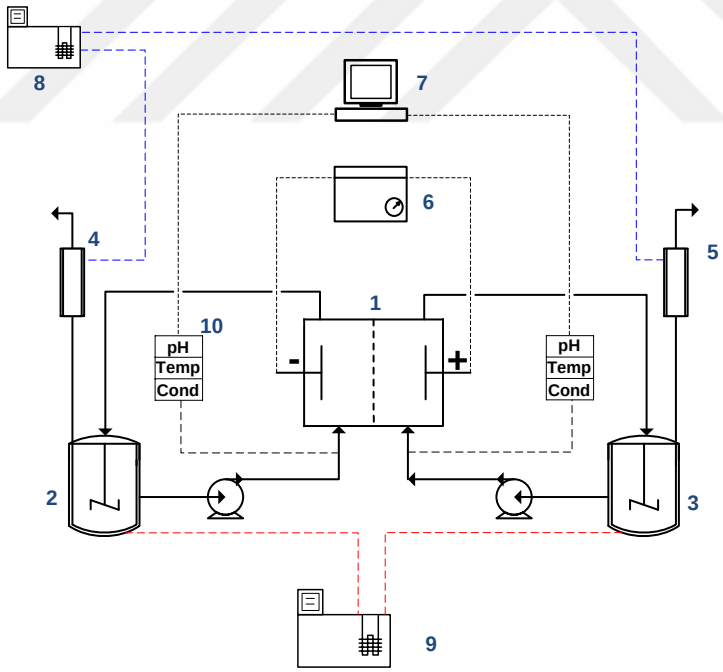

Figure 4.5 : The diagram of the experimental set-up for batch process (1: cell, 2-3: anolyte-catholyte reactors, 4-5: condensers, 6: power source, 7: computer, 8: cooling system, 9: heating system, 10: measuring devices).

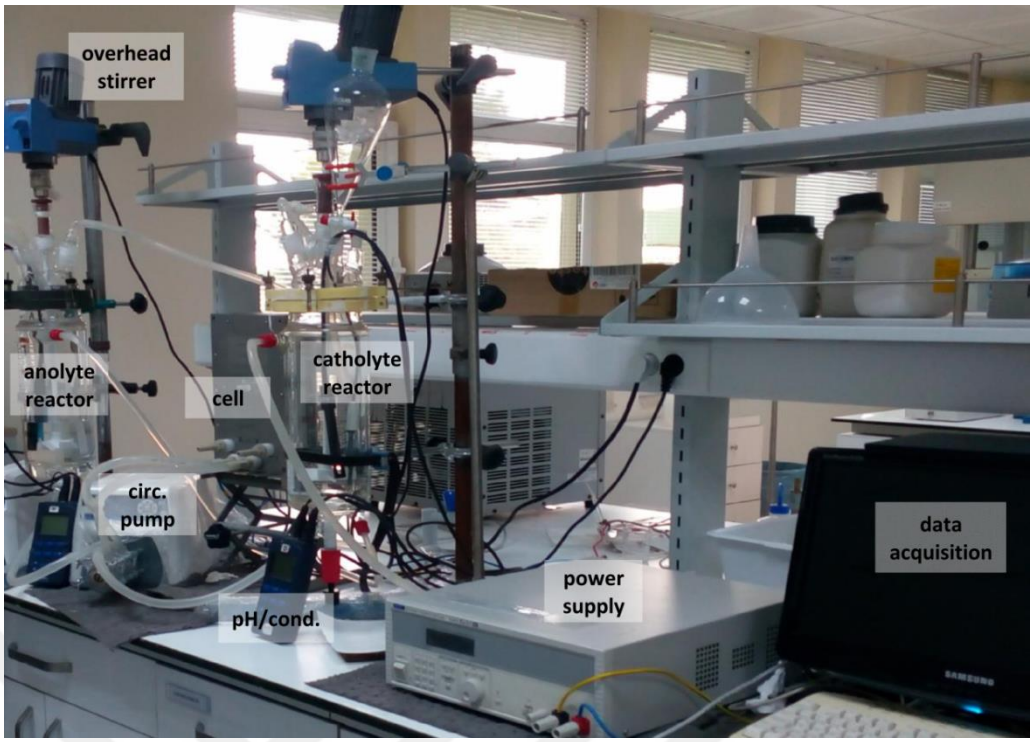

Figure 4.6 : Experimental set-up for batch process, view1.

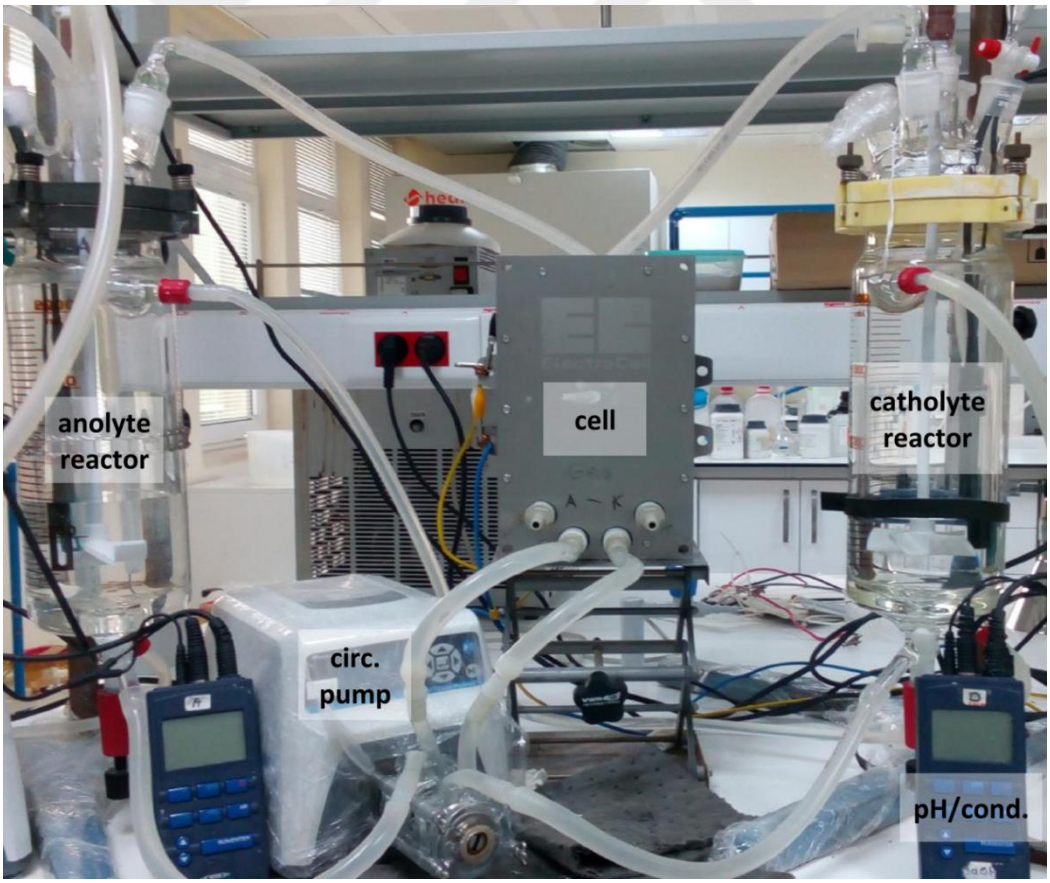

Figure 4.7 : Experimental set-up for batch process, view2.

The membrane electrolysis system mainly consisted of the following equipment: membrane cell, 1 L reactors with overhead stirrers for anolyte and catholyte solutions, chillers at the exit of electrolysis gases to condense water vapour, peristaltic pumps, pH and conductivity measuring devices, flexible tubing, power supply (rectifier) and computer for data acquisition and storage. Fig. 4.5 shows the diagram of the batch process experimental set-up used in this study while Figure 4.6 and 4.7 show the pictures of the set-up from different views.

The general procedure applied in batch membrane electrolysis experiments is as follows:

1) The synthesized-purified Li_2SO_4 solution was placed in the anolyte reactor while the prepared LiOH solution was placed in the catholyte reactor. The amount of the electrolyte was ca. 800 g each.

2) The peristaltic pumps circulating the anolyte and catholyte solutions from the reactors to the anode and cathode compartments of the electrolysis cell, respectively, were started. The temperatures of anolyte and catholyte reactors were adjusted. pH and conductivity meters, the values of which were recorded at certain intervals, were mounted.

3) For constant current operation, current was set to the desired value in the power supply. The experiment was started by supplying current to the cell. During the experiment, potential values were recorded thanks to the data cable connected to a computer.

4) After a certain time, the experiment was ended by cutting off current. Electrolyte solutions were drained and their weights were measured.

5) The initial and final samples of electrolytes were analysed with ICP-OES.

The experiments were performed at the following parameters, where two repeats were done:

- Nafion®N-424 membrane; Circulation flowrate of 500 mL/min; Temperature 30, 60°C; Anolyte initial concentration: 22% Li_2SO_4; Catholyte initial concentration: 4, 6, 8% LiOH; Current density of 4, 8, 12, 16 A/dm^2.

The main output of the experiments is "current efficiency", for lithium which is;

$$\mathrm{CE}\ (\%) = 100 \times \frac{\Delta \mathrm{Li}_{\mathrm{real}}}{\Delta \mathrm{Li}_{\mathrm{theory}}} \tag{4.12}$$

ΔLi_{real} *(g)* is the amount of lithium transferred from anode to cathode chamber, which is calculated with the help of the analysis of the initial and final electrolyte samples. ΔLi_{theory} *(g)* is the theoretical amount that is expected to be transferred according to Lithium change according to Faraday's laws of electrolysis, as derived from Eq. (2.30) is;

$$\Delta \mathrm{Li}_{\mathrm{theory}} = \frac{\mathrm{w_{Li}} \times \mathrm{I} \times \mathrm{t} \times 3600}{96484} \tag{4.13}$$

w_{Li} *(mole/g)* is the atomic weight of lithium, *I (A)* is the current applied and *t (h)* is the duration of electrolysis. The other important outputs are "electrolysis unit power consumption" (EPW) (derived from Eq. (2.55)) and "electrolysis production rate" (EPR), which are given as follows:

$$\mathrm{EPW} = \frac{\mathrm{V} \times \mathrm{I} \times \mathrm{t}}{\Delta \mathrm{Li}_{\mathrm{real}}} \tag{4.14}$$

$$\mathrm{EPR} = \frac{\Delta \mathrm{Li}_{\mathrm{real}}}{\mathrm{S} \times \mathrm{t}} \tag{4.15}$$

Here, *V (Volt)* is average potential and *S* (m^2) is membrane area.

4.7.3 Results

Current efficiency results are shown in Figures 4.8-9. The most remarkable factor affecting current efficiency seems to be LiOH concentration, the increase of which led to a reduction in current efficiency. This reduction was possibly due to the increasing back-transport of OH^- ions with the increase of LiOH concentration. (Davis, 2006; Turan et al, 2012a; Carlberg, 2015). Current density, however, was not observed to have a meaningful effect on current efficiency for the current density range studied. This was possibly due to the fact that limiting current was not reached during the experiments. Temperature, on the other hand, slightly enhanced current efficiency. This may be attributed to the increase of conductivity and decrease of viscosity, which all together improved the transport properties of lithium through membrane.

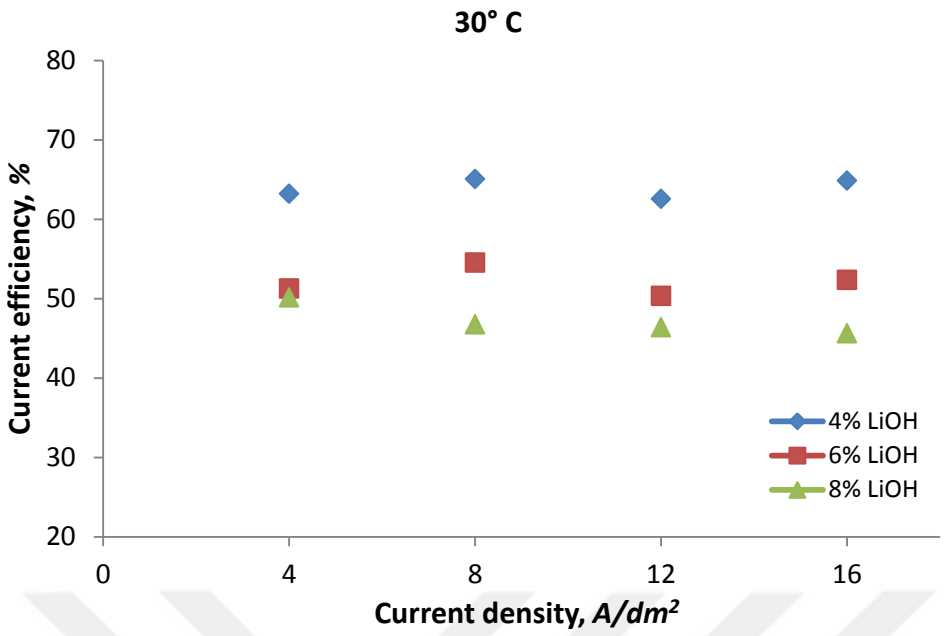

Figure 4.8 : Current efficiency results (30°C)

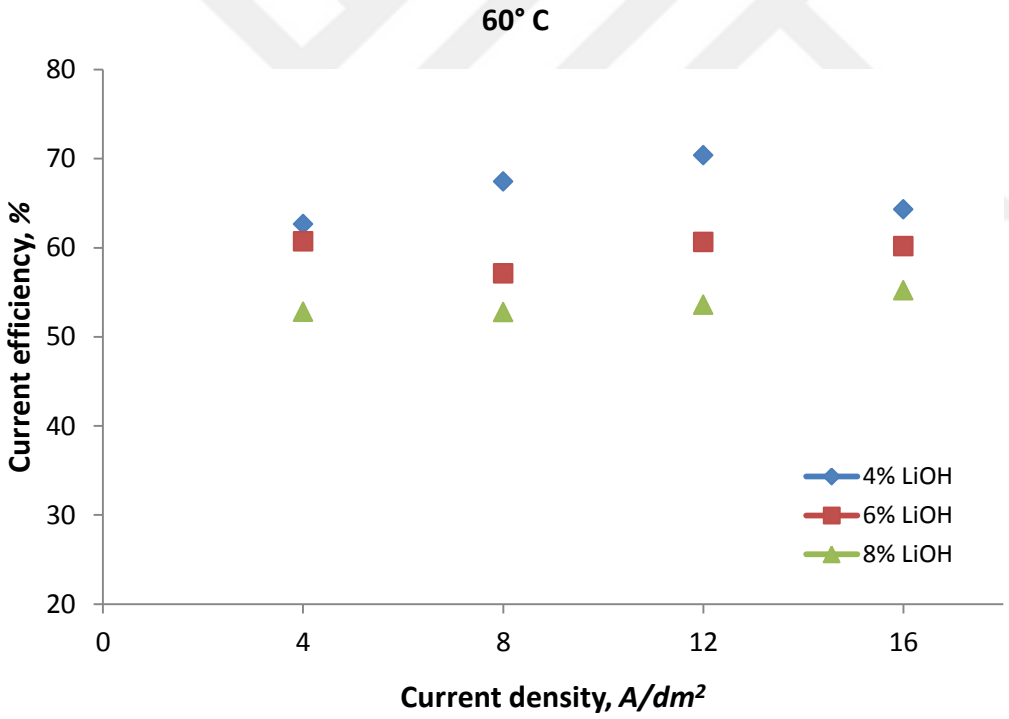

Figure 4.9 : Current efficiency results (60°C)

Electrolysis unit power consumption (EPW) results are shown in Fig. 4.10-11. It is clear that the increase of current density significantly increased power consumption. The increase of potential with increasing current due to Ohm's law (potential = current x resistance) is the main reason of power increase. However, there are two more possible reasons which may have caused this increase: i) decrease of current efficiency due to the increase of current density, ii) further increase of potential due to working around limiting current. Former is insignificant since current density did not have a meaningful effect on current efficiency as mentioned above. It was also found that the studied range was below limiting current. Nevertheless, the existence of limiting current can be better examined at a potential vs. current diagram. As seen in Figure 4.12, the increase of potential is linear, which suggests that limiting current was not reached within the current density range studied. Otherwise, one could expect an exponential increase of the potential if limiting current had been reached. It was also observed that the increase of LiOH concentration increased power consumption, which was due to the fact low current efficiencies were obtained at high LiOH concentrations. Furthermore, temperature increase, which led to the increase of conductivity, caused a decrease in cell potential, correspondingly a decrease in power consumption.

LiOH production rates are shown in Figure 4.13-14. It is clear that current density increased production rates almost linearly since the studied range is well below the limiting current as mentioned above. A reduction in LiOH concentration, as mentioned above, caused an increase in current efficiency, which resulted in an increase in production rate.

To sum up; the obtained values were in the range of 45-70% for current efficiency, 6.1-14.6 kWh/kg-LiOH for power consumption and 140-900 g LiOH/m^2membrane/h for production rate.

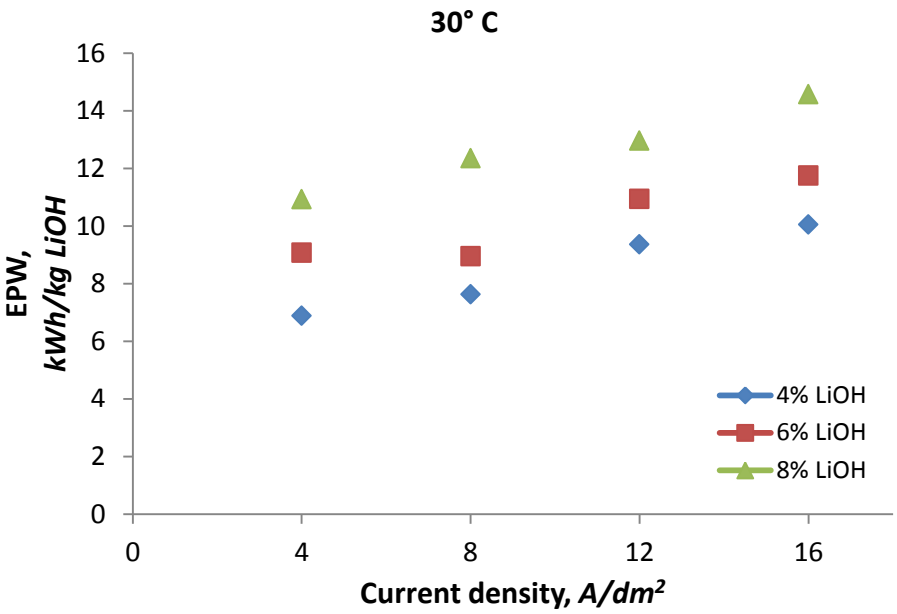

Figure 4.10 : Electrolysis unit power consumption results (30°C).

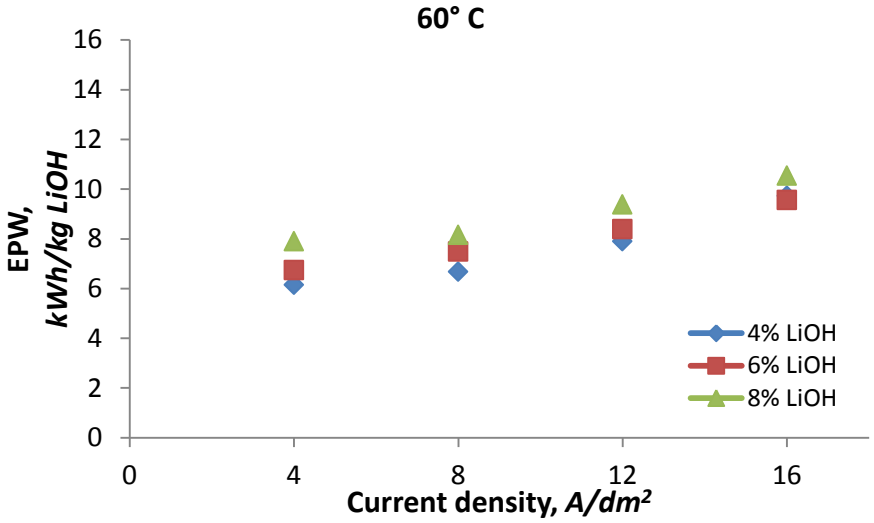

Figure 4.11 : Electrolysis unit power consumption results (60°C)

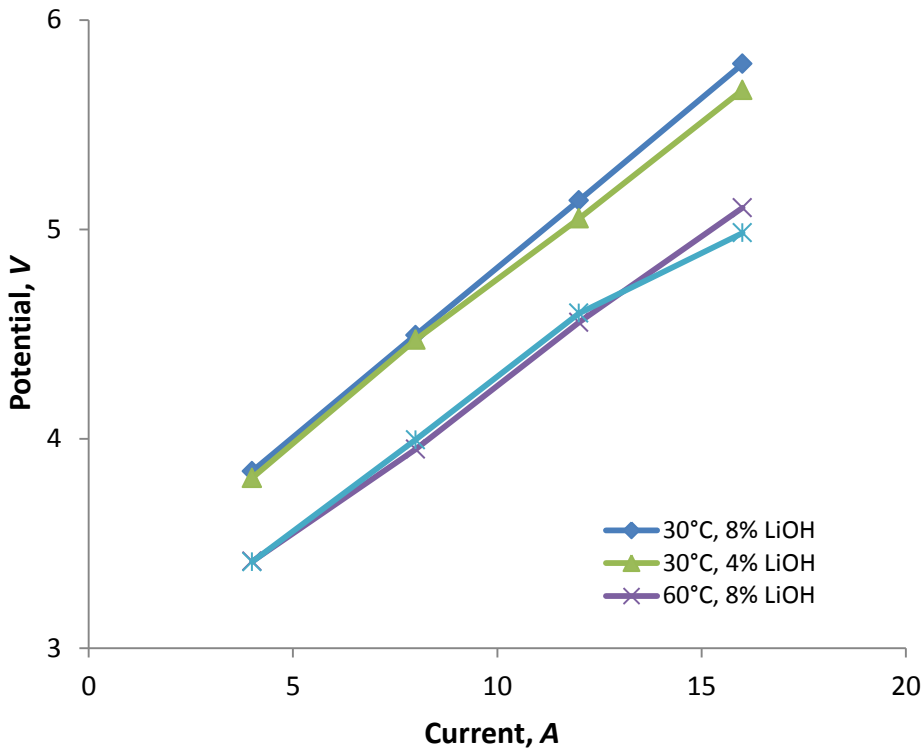

Figure 4.12 : Current-potential relation.

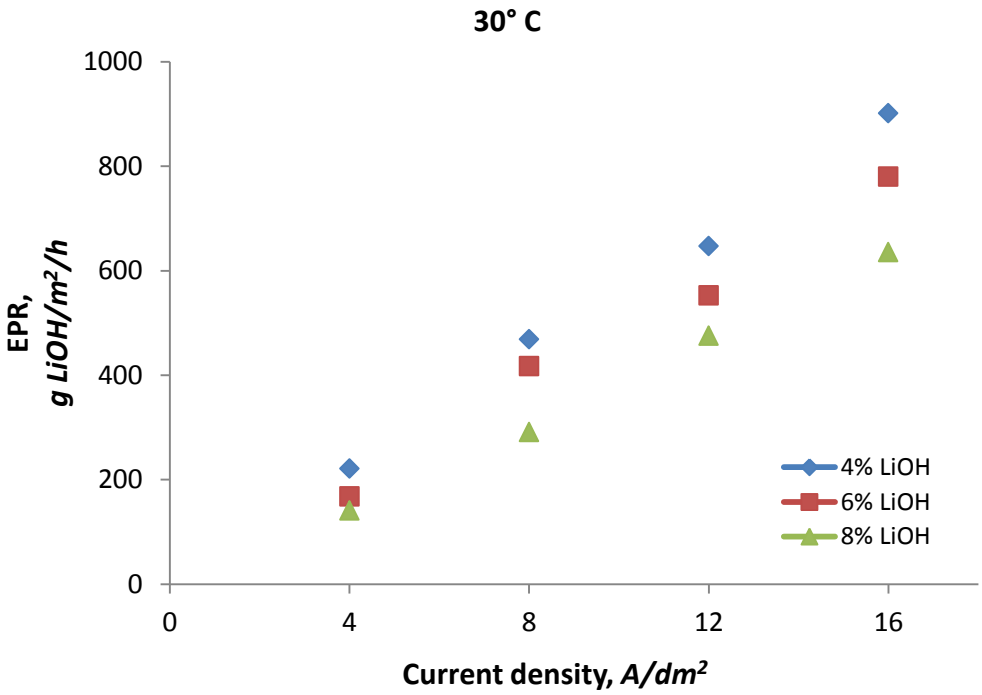

Figure 4.13 : LiOH production rate results (30°C).

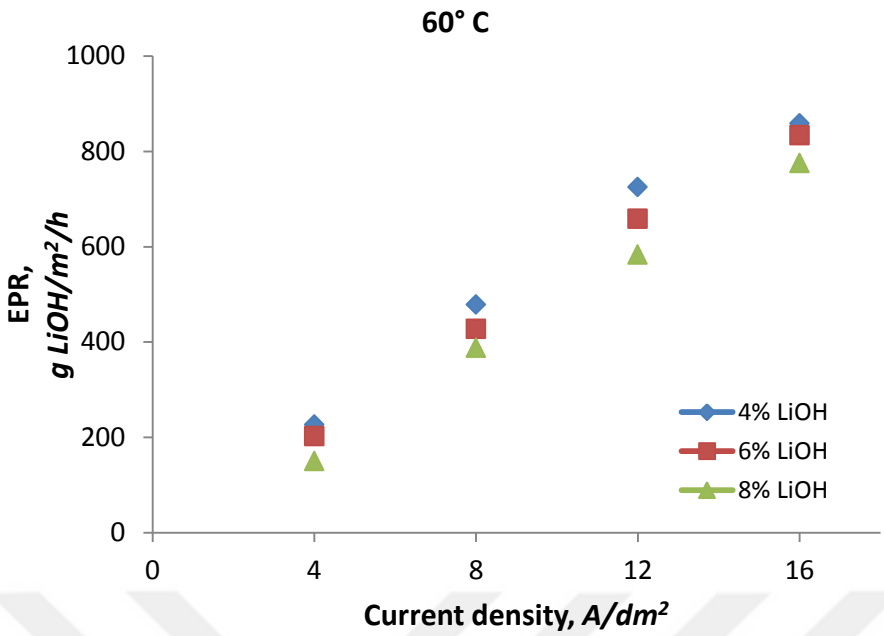

Figure 4.14 : LiOH production rate results (60°C).

The performance of N-424 membrane was compared with previous studies. In a previous study by Ryabtsev et al. (2004), where MK-40 membrane was used, it was seen that lower current efficiencies were obtained (at 4% LiOH, ca. 45% current efficiency; at ca. 8% LiOH, ca. 20% current efficiency). Thus it may be claimed that for this process, Nafion membrane is likely to be superior possibly due to a better rejection of hydroxides through the membrane. A detailed experimental comparative analysis was made in Section 4.9.

Furthermore, optimum membrane electrolysis parameters within the studied range were determined with the help of a comparative production cost estimation. In this cost estimation, heating, power and evaporation costs were calculated to produce 10% LiOH solution. Heating is required to heat the cell to the desired process temperature (30°C or 60°C). Power cost originates from the current supplied to electrolysis cell while any other power cost (pumping etc.) is neglected in this estimation. Finally, taking into consideration of the cost of evaporating lithium hydroxide solutions of different concentrations (4-8% LiOH) to a reference concentration (10% LiOH) is essential for a fair comparison. Further costs (crystallization, filtration, drying etc.) to produce lithium hydroxide monohydrate crystals were neglected since these costs would be the same for all conditions. The results were given in Table 4.9. In table 4.9, it is seen that experiment EM113, having the lowest total cost, presents the optimum working parameters (60°C, 8%

LiOH, 4 A/dm^2). This is due the fact high temperature and low current density lowers power costs while high LiOH concentration makes it possible to evaporate less water to obtain 10% LiOH solution. So it can be claimed that in order to be able to carry out this electromembrane process at low production cost levels, one should pick high temperature and low current density levels. However, working at lower current density values decreases reaction rate considerably, which requires comparatively larger cell stacks in order to obtain a certain production rate; that is to say as current density decreases, capital cost of an electrochemical plant increases. So, in order to be able to determine the optimum current density, capital costs should also be considered along with production costs, which is out of scope of this study.

Table 4.9 : Comparison of LiOH electro-membrane production costs.

Exp. no	Temp., °C	Li_2SO_4, %	LiOH, %	Current density, A/dm^2	Heating cost, €/tonne LiOH	Electrolysis power cost, €/tonne LiOH	Evaporation cost, €/tonne LiOH	Total cost, €/tonne LiOH
EM101	30	22	8	4	9	765	63	837
EM102	30	22	8	8	9	865	63	937
EM103	30	22	8	12	9	908	63	980
EM104	30	22	8	16	9	1020	63	1092
EM105	30	22	6	4	13	636	167	815
EM106	30	22	6	8	13	627	167	806
EM107	30	22	6	12	13	766	167	945
EM108	30	22	6	16	13	823	167	1002
EM109	30	22	4	4	19	482	375	876
EM110	30	22	4	8	19	534	375	928
EM111	30	22	4	12	19	655	375	1049
EM112	30	22	4	16	19	704	375	1098
EM113	60	22	8	4	28	553	63	644
EM114	60	22	8	8	28	570	63	661
EM115	60	22	8	12	28	656	63	747
EM116	60	22	8	16	28	737	63	828
EM117	60	22	6	4	38	472	167	676
EM118	60	22	6	8	38	524	167	728
EM119	60	22	6	12	38	587	167	791
EM120	60	22	6	16	38	669	167	874
EM121	60	22	4	4	56	430	375	861
EM122	60	22	4	8	56	467	375	898
EM123	60	22	4	12	56	553	375	985
EM124	60	22	4	16	56	681	375	1112

** Heating is from ambient (15°C) to electrolysis temperature. Steam (saturated, 6 bar) is used for heating and evaporation. % 80 steam efficiency is assumed. Evaporation has one effect. Utility costs are assumed as 20 €/ton steam and 0.07€/kWh*

4.8 Determination and Regression Modelling of Transport Numbers

4.8.1 Purpose

In the previous section (Section 4.7), the general behaviour of N-424 membrane during the electromembrane process of lithium sulphate was investigated. Now in this section, the aim is to further investigate the effect of ion concentrations (Li^+ and H^+ in anolyte, OH^- in catholyte) on transport numbers in order to examine the "acid/alkaline states of membranes" phenomenon as called by Jörissen and Simmrock (1991), which is described in detail in the literature review section. It is aimed to investigate the membrane electrolysis of Li_2SO_4 with this approach and to put forward a regression model equation, which will reflect the scientific reality observed in the membrane transport mechanism in a sensible manner. Also, in this section, continuous feed experiments were performed in addition to batch experiments, which brings the following benefits:

- In anolyte solution near zero acidity ($H^+ \rightarrow 0$) condition can be attained. So, the effect of acidity on the process can be better observed.
- This way, a constant concentration process was possible, which is required to reflect industrial process conditions.

4.8.2 Experimental

The materials-equipment required and the necessary pre-treatment procedures are described in Section 4.2 and Section 4.5. The experiments were performed using the following parameters:

- Nafion®N-424 membrane
- Circulation flowrate of 750 $mL.min^{-1}$;
- Temperature 30°C
- Current density of $10A.dm^{-2}$
- Anolyte initial concentration: 5, 10, 20% Li_2SO_4 + 0, 1, 5, 10% H_2SO_4

- Catholyte initial concentration: 1, 3, 7% LiOH

In the previous section (Section 4.7), it was found that current density did not significantly affect current efficiency (i.e. lithium transport number) within the studied range (4-16 $A.dm^{-2}$). Moreover, current-potential correlation was linear, which indicated that the studied range was well below the limiting current. Based on this experience, current density was not considered in the regression equation of this study and experiments were performed at constant current density of 10 $A.dm^{-2}$. Nevertheless, two additional experiments were performed at the same concentration level of one of the experiments yet at different current densities (5 and 15 $A.dm^{-2}$) in order to test the effect of current density on ion and water transport. In addition to all these, two more experiments were performed in order to test the accuracy of the regression equation in the prediction of lithium transport number.

The experimental procedure is similar to the one described in Section 4.7.2. However, dissimilarly, these experiment series were performed in two ways:

i) Via batch process; where no further feeding was done into reactors during the experiment after electrolytes were loaded into the reactors;

ii) Via continuous feed process, where substances were fed into the reactors during the experiment continuously in order to keep ion concentrations in the reactors at constant levels.

For the latter (continuous feed process), batch process procedure was valid, yet with some additions in the process as seen in Fig. 4.15 in blue highlights. The anolyte and catholyte feed add-ons for continuous process set-up are shown in Fig. 4.16.

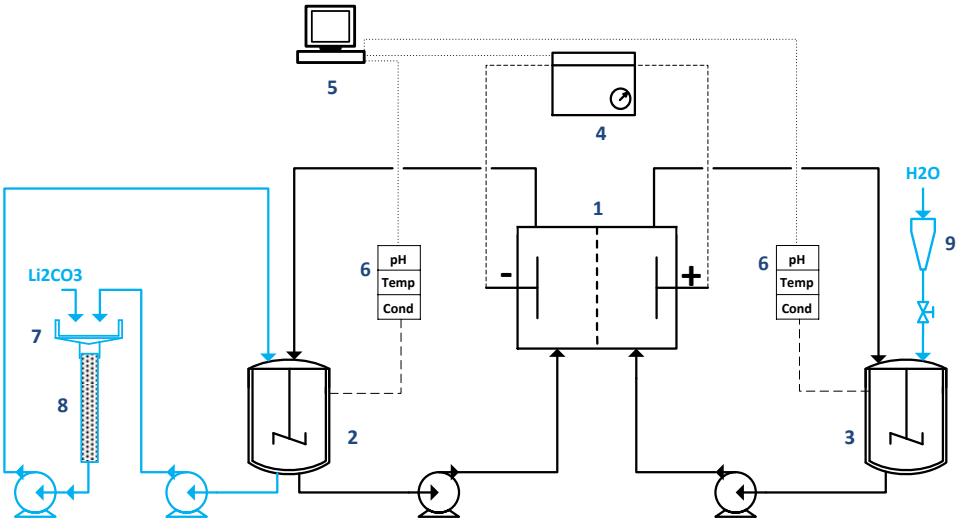

Figure 4.15 : The diagram of the experimental set-up for continuous process (blue lines are unique to continuous process, 1: cell, 2-3: anolyte-catholyte reactors, 4: DC power source, 5: computer, 6: pH/conductivity measuring devices, 7: büchner funnel, 8: resin column, 9: water feed funnel).

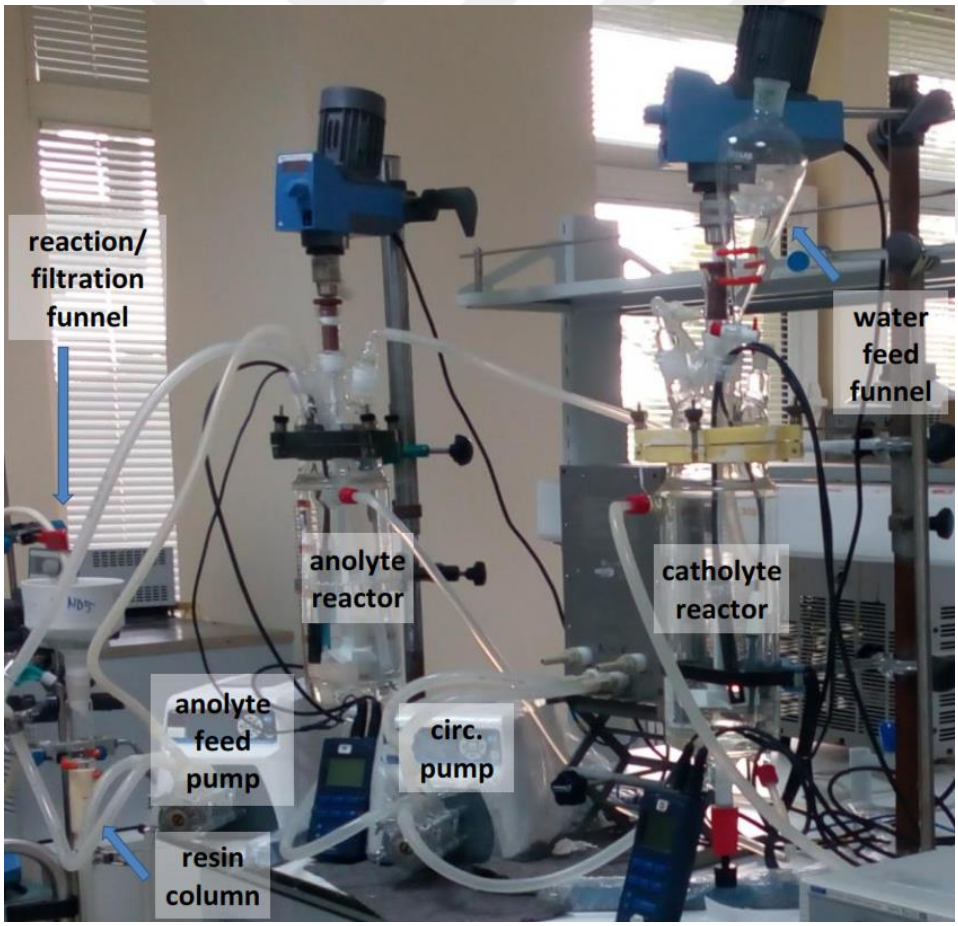

Figure 4.16 : Experimental set-up (continuous process).

For the continuous feed process, hydrogen ions produced by anodic reaction in anolyte reactor have to be neutralized by reacting with lithium carbonate (Eq. 3.29), which also helps to compensate the lithium ions transported to the catholyte chamber through membrane. So, as the process continues with a circulation of both electrolytes through the electro-membrane cell, some portion of the anolyte was withdrawn from anolyte reactor and pumped over a Büchner funnel, on which there is a paper filter. At the same time, solid lithium carbonate was fed over the funnel, where neutralization reaction occurs. The neutralized anolyte was filtered to an ion exchange resin column (Amberlite® IRC 748) for purification in terms of hardness. The purified solution was pumped from the column back to anolyte reactor. The effectiveness of the neutralization process was followed by pH measurements, where >2.5 pH was observed to be a satisfactory value, which makes it possible to obtain very low H^+ concentration values. In catholyte, concentration of lithium hydroxide increases due to membrane transport of Li^+ ions from anolyte chamber. That's why constant concentration level was obtained with the addition of water by water feed funnel. The flowrate of water was adjusted in such a way that the initial conductivity level was maintained. The amount of the fed water was measured, which was required for water transport number calculations.

The main output of the experiments is "transport number", which is the fraction of the current that is carried by a certain ion as described in detail in Section 2.1.5, Section 2.2.2.2 and Section 2.2.2.3. Transport number of lithium was calculated according to faradaic equations. Transport numbers of other ions were calculated with the help of Eq. (2.48) and with an approximation of the individual terms in the regression equation that was formed. Water transport number was calculated with the help of Eq. (2.92) and (3.18).

The experiments performed were used to put forward a regression equation. In this equation, transport number of lithium was calculated. Moreover, this equation made it possible to approximate transport numbers of hydrogen and hydroxyl ions. Two other additional test experiments, which had different concentrations than the ones used in regression analysis, were performed. Concentrations of ions during experiment, which are the dependent variables in the equation, were averaged using initial and final analysis of samples. The equation was evaluated according to R-

squared values and according to its success in the prediction of the results of the test experiments. All statistical analyses were performed with the help of MS Excel® 2010 Data Analysis add-on and Minitab® 17. The theory of multiple regression is given in Appendix A.

4.8.3 Results

4.8.3.1 Ion transport numbers

The results of the experiments are given in Table 4.10. Experiments 1-42 were used to establish a regression model equation while experiments 43 and 44 (Test 1, 2) were used to test the model. Experiments 45 and 46 were performed at the same concentration levels of experiment 31, yet at different current densities (15 and 5 $A.dm^{-2}$, respectively) in order to check the effect of current density, which had been found to have no significant effect on transport number of lithium in the studied range in the previous section (Section 4.7). Also, these two experiments helped to investigate the effect of current density on water transport.

Table 4.10 : Transport number results for N-424 membrane.

	Initial concentration, %			Average concentration of ions, *moles/kg solution*			T_{Li}			T_H	T_{OH}	T_{H2O}			Notes
Exp. No	**Li_2SO_4**	**H_2SO_4**	**LiOH**	**Li^+,** *(in anolyte)*	**H^+,** *(in anolyte)*	**OH^-,** *(in catholyte)*	*meas.*	*calclt.*	*% error*			*meas.*	*calclt.*	*% error*	
1	20	0	7	3,88	0,32	3,14	0,71	0,67	6	0,03	0,26	4,9	6,0	22	*Batch process*
2	20	0	1	3,83	0,48	0,81	0,85	0,81	5	0,10	0,05	6,8	6,6	3	
3	20	5	7	3,81	1,37	3,06	0,56	0,54	4	0,26	0,18	5,0	4,7	4	
4	5	0	7	0,73	0,31	2,97	0,39	0,41	6	0,15	0,46	6,0	6,3	5	
5	5	0	1	0,72	0,33	0,64	0,48	0,54	13	0,42	0,10	6,7	7,3	8	
6	5	5	7	0,89	1,20	2,89	0,18	0,18	0	0,57	0,24	4,6	4,7	2	
7	5	5	1	0,89	1,21	0,51	0,22	0,19	15	0,76	0,01	4,6	4,9	5	
8	20	0	3	3,74	0,43	1,56	0,73	0,79	7	0,10	0,16	6,2	6,6	7	
9	20	5	3	3,79	1,43	1,51	0,63	0,57	8	0,31	0,07	5,4	4,9	11	
10	5	0	3	0,74	0,33	1,41	0,45	0,50	12	0,29	0,26	6,9	7,0	1	
11	5	5	3	0,90	1,20	1,31	0,19	0,22	14	0,72	0,08	4,6	5,0	10	
12	20	10	3	3,64	2,32	1,45	0,47	0,48	2	0,47	0,06	3,9	3,9	1	
13	10	10	3	1,86	2,25	1,32	0,26	0,29	13	0,68	0,06	4,0	4,4	11	
14	5	10	3	0,92	2,14	1,25	0,10	0,07	29	0,85	0,05	3,6	3,5	3	
15	10	0	3	1,66	0,44	1,49	0,62	0,61	1	0,19	0,19	8,1	7,4	8	
16	10	5	3	1,79	1,32	1,40	0,40	0,41	1	0,51	0,08	5,9	5,8	2	
17	20	10	1	3,78	2,35	0,66	0,49	0,47	3	0,49	0,02	4,1	3,6	13	
18	10	10	1	1,87	2,25	0,53	0,25	0,31	25	0,74	0,02	3,9	4,4	14	
19	5	10	1	0,93	2,16	0,46	0,11	0,08	29	0,88	0,01	3,3	3,4	5	
20	10	0	1	1,66	0,46	0,73	0,68	0,66	3	0,25	0,07	8,4	7,7	8	
21	10	5	1	1,80	1,30	0,61	0,41	0,40	2	0,57	0,02	5,6	5,8	3	
22	20	10	7	3,73	2,31	3,03	0,44	0,44	1	0,39	0,17	4,1	3,8	7	
23	10	10	7	1,86	2,23	2,92	0,22	0,25	13	0,59	0,19	4,2	4,3	1	
24	5	10	7	0,93	2,15	2,86	0,09	0,06	33	0,73	0,19	3,8	3,4	12	
25	10	0	7	1,68	0,37	3,03	0,55	0,51	7	0,09	0,36	6,5	6,7	3	
26	10	5	7	1,78	1,33	2,96	0,39	0,35	11	0,40	0,21	5,7	5,4	6	
27	5	1	7	0,77	0,48	2,97	0,37	0,37	2	0,25	0,39	6,1	6,0	1	
28	10	1	7	1,72	0,56	3,03	0,52	0,50	4	0,16	0,32	6,5	6,5	0	
29	20	1	7	3,69	0,52	3,08	0,58	0,67	17	0,10	0,33	4,8	6,0	24	
30	5	1	3	0,77	0,49	1,38	0,41	0,46	12	0,40	0,19	7,3	6,7	9	
31	10	1	3	1,68	0,61	1,48	0,59	0,58	2	0,26	0,15	7,8	7,2	7	
32	20	1	3	3,60	0,62	1,55	0,71	0,76	8	0,16	0,13	5,6	6,5	16	
33	5	1	1	0,75	0,48	0,60	0,40	0,48	19	0,54	0,06	6,9	6,9	0	
34	10	1	1	1,69	0,61	0,71	0,60	0,62	3	0,34	0,05	7,4	7,4	0	
35	20	1	1	3,53	0,64	0,81	0,77	0,78	1	0,18	0,05	6,1	6,7	10	

Table 4.10 (continued) : Transport number results for N-424 membrane.

	Initial concentration, %			Average concentration of ions, *moles/kg solution*			T_{Li}			T_H	T_{OH}	T_{H2O}			Notes
Exp. No	**Li_2SO_4**	**H_2SO_4**	**LiOH**	**Li^+,** *(in anolyte)*	**H^+,** *(in anolyte)*	**OH^-,** *(in catholyte)*	*meas.*	*calclt.*	*% error*			*meas.*	*calclt.*	*% error*	
36	20	0	3	3,92	0,01	1,29	0,71	0,70	1	0,00	0,29	6,0	6,9	15	*Continuous process*
37	20	0	1	3,79	0,02	0,44	0,84	0,77	8	0,00	0,16	6,4	7,4	15	
38	20	0	7	3,84	0,02	2,78	0,52	0,59	14	0,00	0,48	5,6	6,3	12	
39	10	0	3	1,95	0,02	1,26	0,67	0,66	3	0,00	0,33	8,0	7,7	4	
40	10	0	1	2,03	0,02	0,48	0,85	0,74	13	0,00	0,15	9,1	8,2	9	
41	10	0	7	2,17	0,02	2,84	0,52	0,53	1	0,00	0,48	6,1	6,8	10	
42	5	0	7	1,14	0,01	2,87	0,56	0,47	16	0,00	0,44	6,3	6,6	4	
43	9,5	1,5	3,2	1,64	0,71	1,55	0,58	0,55	5	0,29	0,14	7,3	7,0	5	*TEST 1 & 2*
44	15,4	3,5	4,9	2,83	1,15	2,22	0,63	0,57	9	0,25	0,12	6,3	6,1	2	
45	10	1	3	1,69	0,69	1,54	0,59	0,56	5	0,27	0,14	6,9	7,0	2	*15 & 5 A/dm²*
46	10	1	3	1,69	0,61	1,53	0,61	0,58	5	0,24	0,15	7,1	7,2	1	

For the interpretation of the results, first of all, in order to be able to determine the significant effects and interactions, a multiple regression investigating two-way interactions and quadratic terms was performed. The regression analysis realized using Minitab® 17 produces two plots revealing the effect of factors. First is "main effects plot", which illustrate the individual effects of factors on the response. Second is "interaction plot", which shows how the interactions between two factors affect the response. The examination of the main effects plot reveals that Li^+ and H^+ have strong effect on transport number of lithium, T_{Li}, while the effect of OH^- is less compared to the other two parameters (Fig. 4.17.a). Also, the curvature in the main effects plot of lithium revealed that quadratic term of Li^+ could be significant too, which suggested that Li^2 term should take place in the regression model equation. Though relatively less significant, H^2 term could also be included in the model equation. Whether these two quadratic terms should really take place in the regression equation or not was decided according to the p-values (level of significance) they present when they are added to the model equation. As seen in Table 4.11, p-values of these terms are less than 0.05, which indicates that they are significant enough to take part in the equation.

Moreover, significant deductions could be made of interaction plots (Fig. 4.17.b) such as;

- Main effects plot show that the increase of H^+ concentration causes a significant decrease in T_{Li}. However, interaction plot reveals that the increase of H^+ concentration increases the significance of Li^+. This can be observed at H^+*Li^+ interaction plot, where it is seen that the increase of hydrogen ion concentration causes a wider span between low and high level graphs of lithium (Fig. 4.17.b) indicating an influence of hydrogen ion on how lithium concentration affects T_{Li}. This is an indirect effect, that is to say, increasing acidity suppresses the effect of OH^- ions, which in return, increases the significance of Li^+ concentration.

- The increase of Li^+ and OH^- concentrations decreases the effect of H^+ ions on T_{Li}. Li^+*H^+ and OH^-*H^+ interaction plots reveal that the increase of lithium and hydroxyl concentration narrows the span between low-high level graphs of hydrogen (Fig. 4.17.b) indicating an influence of lithium and hydroxyl ion on how hydrogen ion concentration affects T_{Li}. This is due to the decreasing competitive advantage of H^+ with the increase of the concentration of its opponents in membrane transport.

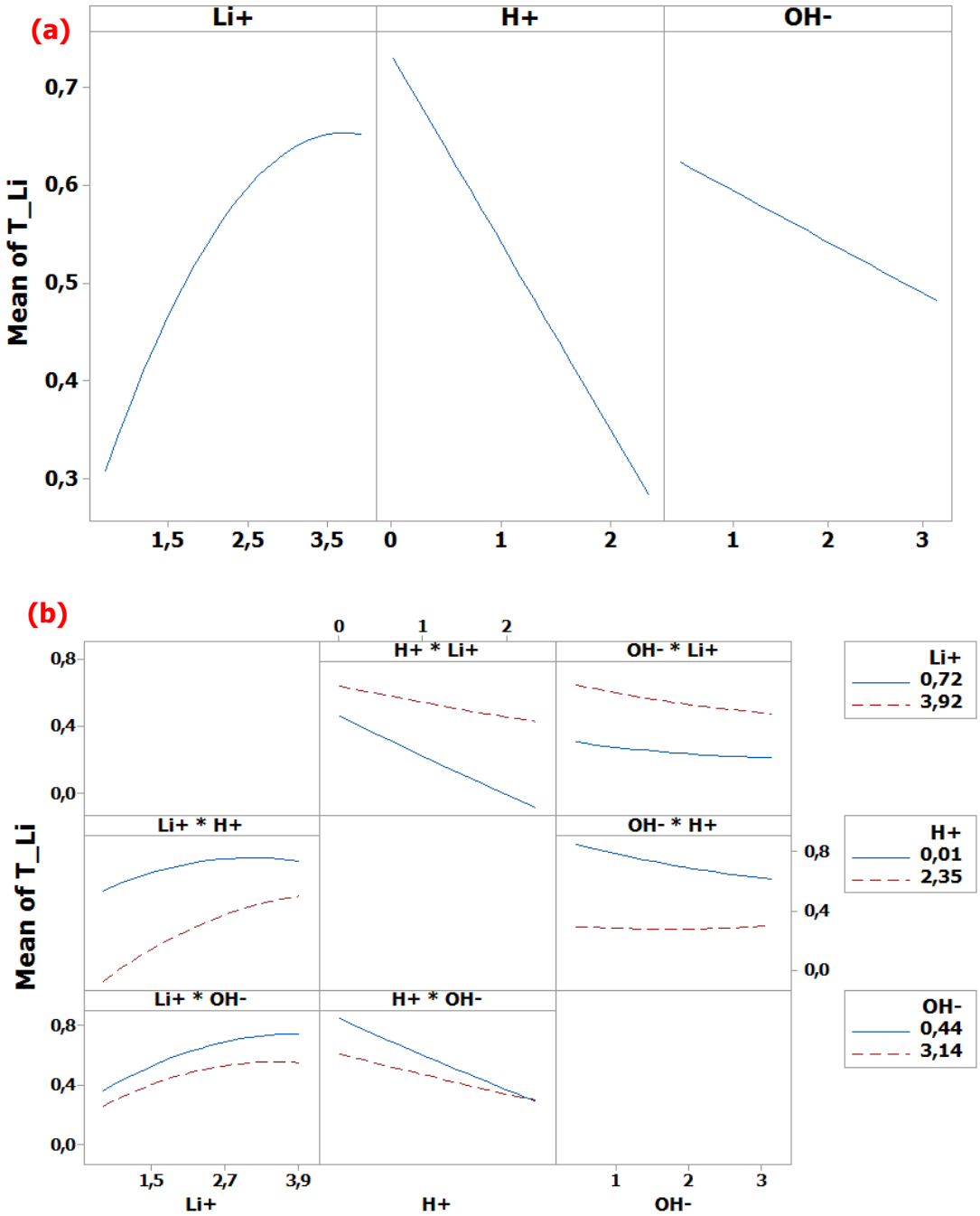

Figure 4.17 : (a) Main effects (b) Interaction plots for T_{Li}.

Another important illustration, which helps determine the significant interactions between parameters, is contour plot, which is a projection of a 3-D graph. From the contour plots of Li^+, H^+, OH^- v.s T_{Li}, (Fig. 4.18-20), the following deductions can be made:

- Fig. 4.18 shows that at very low acid concentrations, the change in Li^+ concentration does not seriously affect T_{Li}, while OH^- is effective at this relatively high pH levels. Increasing acid concentration diminishes the effect

of OH^-, yet, the increase of Li^+ concentration boosts the influence of OH^- ions. The latter is an indirect effect, i.e. increasing Li^+ concentration decreases the influence of H^+ ions on T_{Li}, which in return, increases the significance of OH^- concentration. As seen in Fig. 4.14.d-e, the colour lines are parallel to the x-axis (OH^- concentration), which indicates that OH^- increase does not affect the transport number of lithium in this region. However, as the concentration of lithium increases, it can be seen that the parallel lines get curved, which suggests that OH^- concentration becomes more significant with the increase of lithium concentration. The reason why this effect is not so clear in these two graphs (Fig. 4.14.d-e) is due to the fact that very high level of acid concentrations (5 and 10 %) suppresses the effect of OH ions in a large concentration interval of lithium.

- In Fig. 4.19, the influence of H^+/Li^+ ratio on the significance of OH^- is more clear, the increase of which decreases the effect of OH^- on T_{Li}.

- In Fig. 4.20, it is seen that at low H^+ concentrations, the increase of OH^- concentration causes a slight decrease in the significance of Li+ ions on T_{Li}. This is due to the decreasing competitive advantage of Li^+ with the increase of the concentration of OH^-.

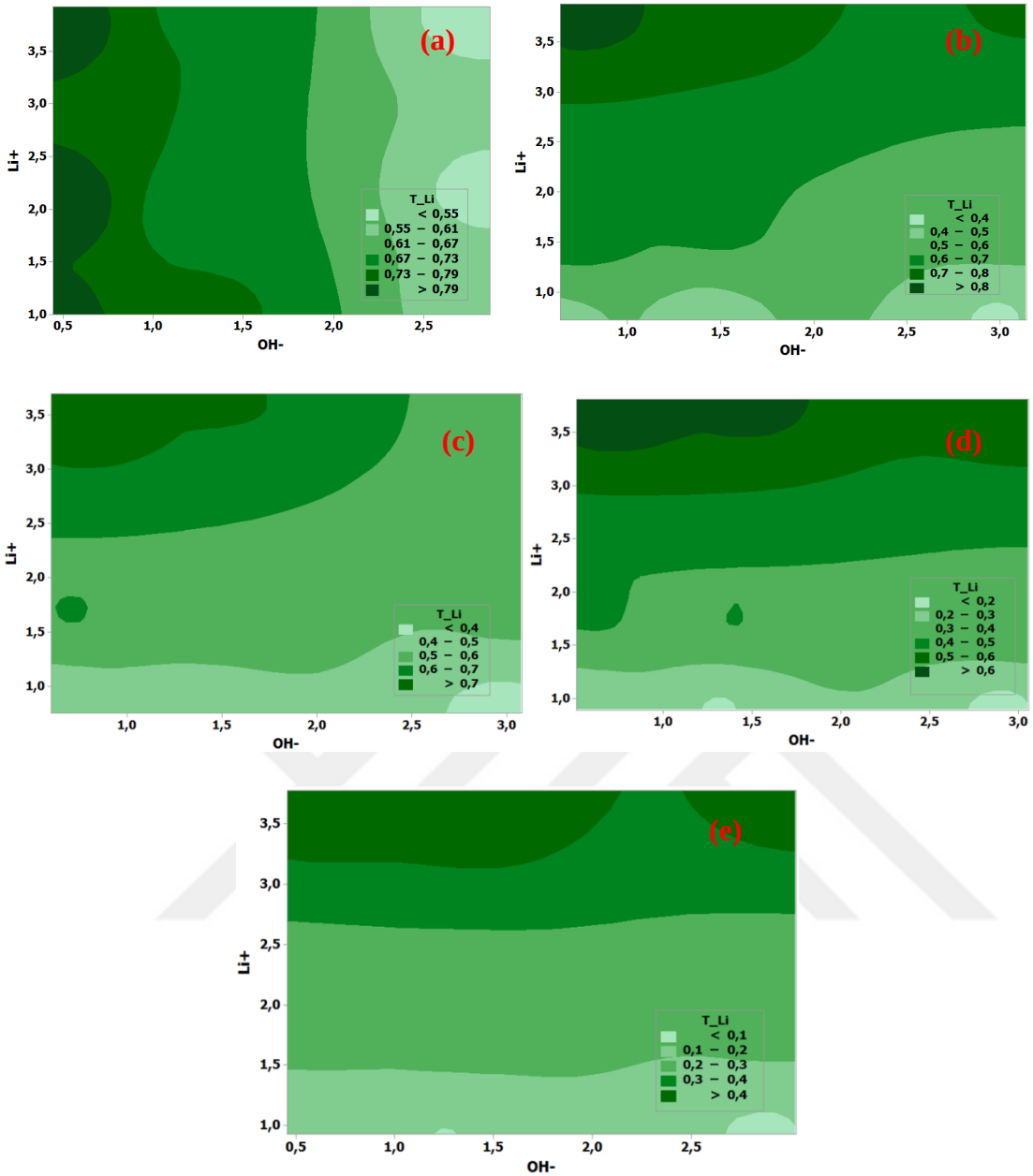

Figure 4.18 : Contour plots of x=OH^-, y=Li^+ (moles/kg) vs. T_{Li} at H_2SO_4 concent. of a) 0% (continuous process), b) 0% (batch), c) 1%, d) 5%, e) 10%.

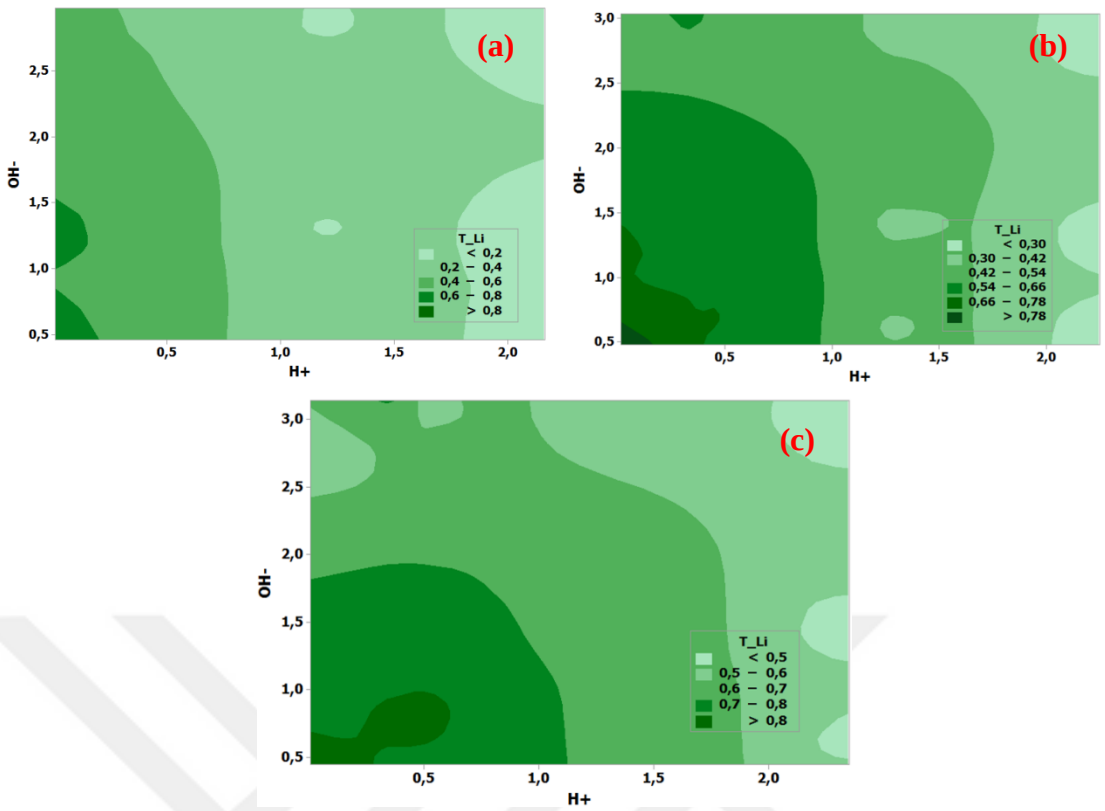

Figure 4.19 : Contour plots of x=H^+, y=OH^- (moles/kg) vs. T_{Li} at Li_2SO_4 concentrations of a) 5%, b) 10%, c) 20%.

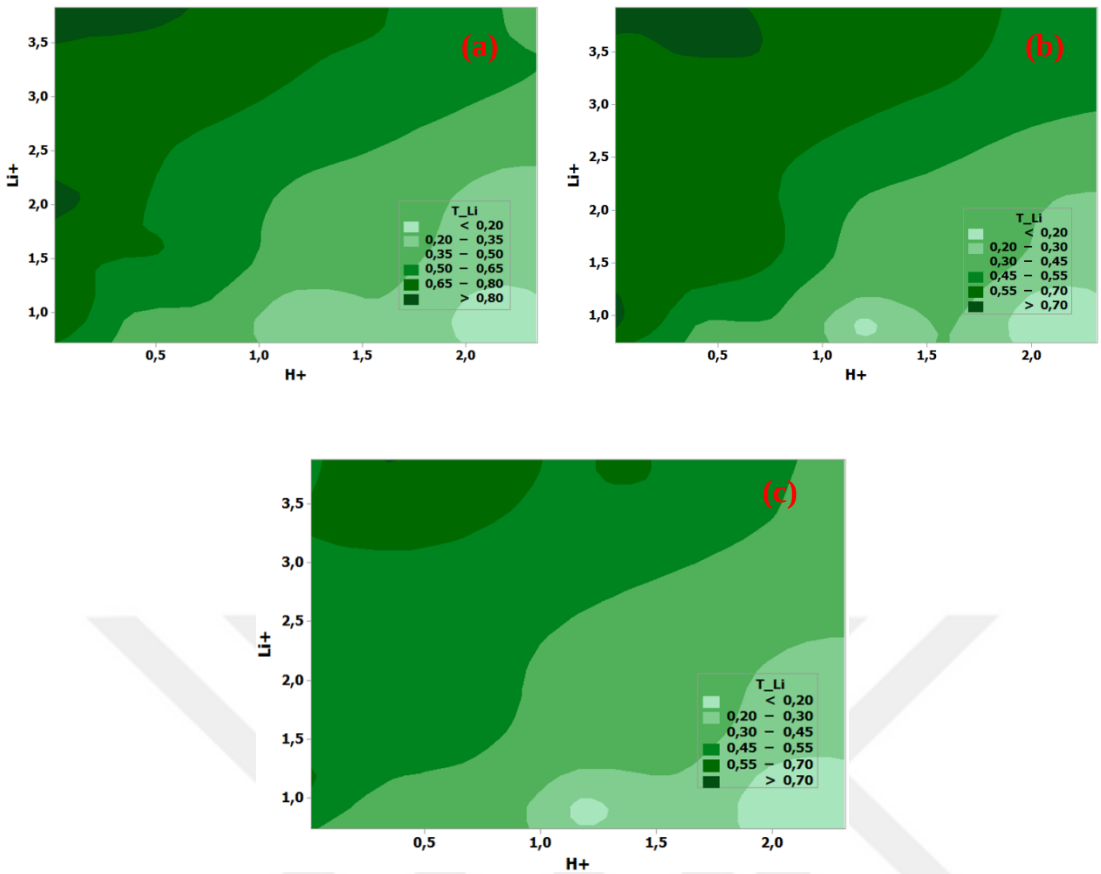

Figure 4.20 : Contour plots of x=H^+, y=Li^+ (moles/kg) vs. T_{Li} at LiOH concentrations of a) 1%, b) 3%, c) 7%.

All these deductions suggest that;

- $Li^+.H^+$ and Li^+/OH^- are the critical factors determining the significance of Li^+ concentration, the increases of which increase the influence of Li^+ on T_{Li}.
- H^+/Li^+ and H^+/OH^- are the critical factors determining the significance of H^+ concentration, the increases of which increase the influence of H^+ on T_{Li}.
- $OH^-.Li^+$ and OH^-/H^+ are the critical factors determining the significance of OH- concentration, the increases of which increase the influence of OH^- on T_{Li}.

These factors have to be embedded in the regression model equation in order to adjust the main effects in such a way that they will be able to reflect the actual mechanism in membrane transport. In other words, the main effects have to be multiplied with these factors in such a way that when this multiplier goes to zero, the significance of the related parameter approaches zero. Likewise, when this multiplier

goes to infinity, the significance of the related parameter becomes independent of this multiplier. Exponential terms are found to be appropriate multipliers, which have the potential to reflect this effect. So the model equation was found to be;

$$T_{Li} = k_0 + k_1.Li.\left[2 - \exp(-Li.H) - \exp\left(-\frac{Li}{OH}\right)\right] + k_2.Li^2.\left[2 - \exp(-Li.H) - \exp\left(-\frac{Li}{OH}\right)\right] + k_3.H.\left[2 - \exp\left(-\frac{H}{Li}\right) - \exp\left(-\frac{H}{OH}\right)\right] + k_4.H^2.\left[2 - \exp\left(-\frac{H}{Li}\right) - \exp\left(-\frac{H}{OH}\right)\right] + k_5.OH.\left[2 - \exp(-Li.OH) - \exp\left(-\frac{OH}{H}\right)\right] \quad (4.16)$$

where, T_{Li} is the transport number of lithium and *Li*, *H* and *OH* are concentrations of the related species in moles.kg^{-1}.

With a closer look at the model equation (4.16) for lithium transport number, one can see that when the exponential term in brackets goes to zero, the main effect will be dominant and be independent of other ions, while it is clear that as this value goes to 1, the total term in brackets will go to zero, diminishing the influence of the ion in question. As long as the exponential terms are calculated, the constants of this equation can be determined with multiple linear regression analysis. The first trial of multiple regression analysis with the data obtained from 45 experiments revealed that residuals were very high at 3 points. Regression analysis was repeated after omitting these 3 points, the results of which are given in Table 4.11.

Table 4.11 : Multiple regression analysis comparison of two equations for T_{Li}.

Regression Statistics					
	Multi R	*R^2*	*Adjst. R^2*	*Std. Error*	*Observ.*
Eq. A :	0,976	0,953	0,947	0,048	42
Eq. B :	0,987	0,975	0,970	0,035	34

ANOVA						
		df	*SS*	*MS*	*F*	*Signif. F*
Eq. A :	Regres.	5	1,695	0,339	147,26	6,4E-23
	Residual	36	0,083	0,002		
	Total	41	1,778			
Eq. B :	Regres.	5	1,31988	0,26398	214,048	2,1E-21
	Residual	28	0,03453	0,00123		
	Total	33	1,35441			

Coefficients					
		Coeffic.	*Std. Error*	*t Stat*	*P-value*
Eq. A :	k0	0,5834	0,0273	21,3696	4,8E-22
	k1	0,1224	0,0201	6,1003	5,1E-07
	k2	-0,0186	0,0047	-3,9329	3,7E-04
	k3	-0,3910	0,0349	-11,2114	2,7E-13
	k4	0,1054	0,0147	7,1740	1,9E-08
	k5	-0,0274	0,0040	-6,8978	4,5E-08
Eq. B :	k0	0,51346	0,02471	20,7783	1,5E-18
	k1	0,12583	0,01543	8,15452	7,1E-09
	k2	-0,01759	0,00359	-4,89963	3,6E-05
	k3	-0,30974	0,0285	-10,8697	1,5E-11
	k4	0,07281	0,01167	6,23674	9,7E-07
	k5	-0,02023	0,00336	-6,02127	1,7E-06

** Eq. A: derived from batch+cont. data; Eq. B: derived from batch data only.*

As seen in Table 4.11, this equation can represent the membrane transport successfully with an R_squared value of 0.953 (Eq. A). Also, this equation was tested with experiments which were out of the model. Lithium transport numbers of experiment no. 43 and 44 (Test 1 and Test 2 experiments) were calculated as 0.55 and 0.57 with error values of 4.9% and 8.8%, respectively. Moreover, in order to be able to increase the accuracy in prediction within a narrower range, a second equation was derived by multiple regression analysis using batch process data only. As seen in Table 4.9, the R_squared value increased to 0.975 (Eq. B). This is due to the fact that in continuous process -though the concentrations were tried to be kept constant- there might have occurred some fluctuations, which might have caused errors in measuring the average concentration of ions. However, since the very low acidity conditions, which could only be obtained in continuous processes, were not included in the second equation (Eq. B), this equation was poorer in the prediction of transport numbers, where anolyte had low acidity. So, one can choose which equation to use according to the concentration range expected to study.

The transport numbers of H^+ and OH^- are hard to measure since there exist multiple steps in their production/consumption such as; production due to electrodic reactions, transport through membrane, consumption due to neutralization with the transported H^+/OH^- ions. However, the regression equation established for T_{Li} can be readily utilized to calculate the other transport numbers along with Eq. (2.48), which assumes that the total transport number of ions should be equal to unity. So, the absolute values of H and Li terms in regression equation (4.16) were assumed to be directly related with the transport numbers, T_H and T_{OH}, respectively. With this approach, T_H and T_{OH} values were calculated and given in Table 4.10.

Permselectivity values of lithium, hydrogen and hydroxyl ions were calculated according to Eq. (2.90). Binary permselectivity relations are illustrated in Figure 4.21 at constant concentration of the third species. In 4.21.a, it is seen that membrane's permselectivity for lithium ion against hydrogen ion, $P^{Li/H}$, is low (under 1) in a large interval of concentration. Permselectivity can reach unity only when lithium concentration is very high and hydrogen concentration is very low. This is mainly due to hydrogen ion's unique way of transport through membrane (tunnelling mechanism), which is described in detail in the following section (Water transport number). The transport number regression equation (4.16) reflects this change in permselectivity with the help of *exp(-Li.H)* and *exp(-H/Li)* multipliers, which adjust the significance of lithium and hydrogen ions, respectively. Fig. 4.21.b shows membrane's permselectivity for lithium ion against to hydroxyl ion, $P^{Li/OH}$, where permselectivity is generally very high in favour of lithium ion, mainly due to Donnan exclusion of hydroxyl ions, as expected. What is more interesting is that as lithium ion concentration increases at constant acid concentration, the permselectivity of lithium ion decreases against hydroxyl ion. This is in line with the previous finding that increasing Li^+ concentration decreases the influence of H^+ on the transport number of lithium, which in return increases the significance of OH^- concentration. *exp(-Li.OH)* multiplier was added in the regression model in order to reflect this effect. In Fig. 4.21.c, it is seen that membrane's permselectivity for hydrogen ion against hydroxyl ion, $P^{H/OH}$, is generally much higher than unity and the increase in H+/OH- concentration ratio causes a further increase. This is again mainly due to hydrogen ion's high transport number. The transport number regression equation (4.16) reflects this change in permselectivity with the help of *exp(-H/OH)* and *exp(-*

OH/H) multipliers, which adjust the significance of hydrogen and hydroxyl ions, respectively.

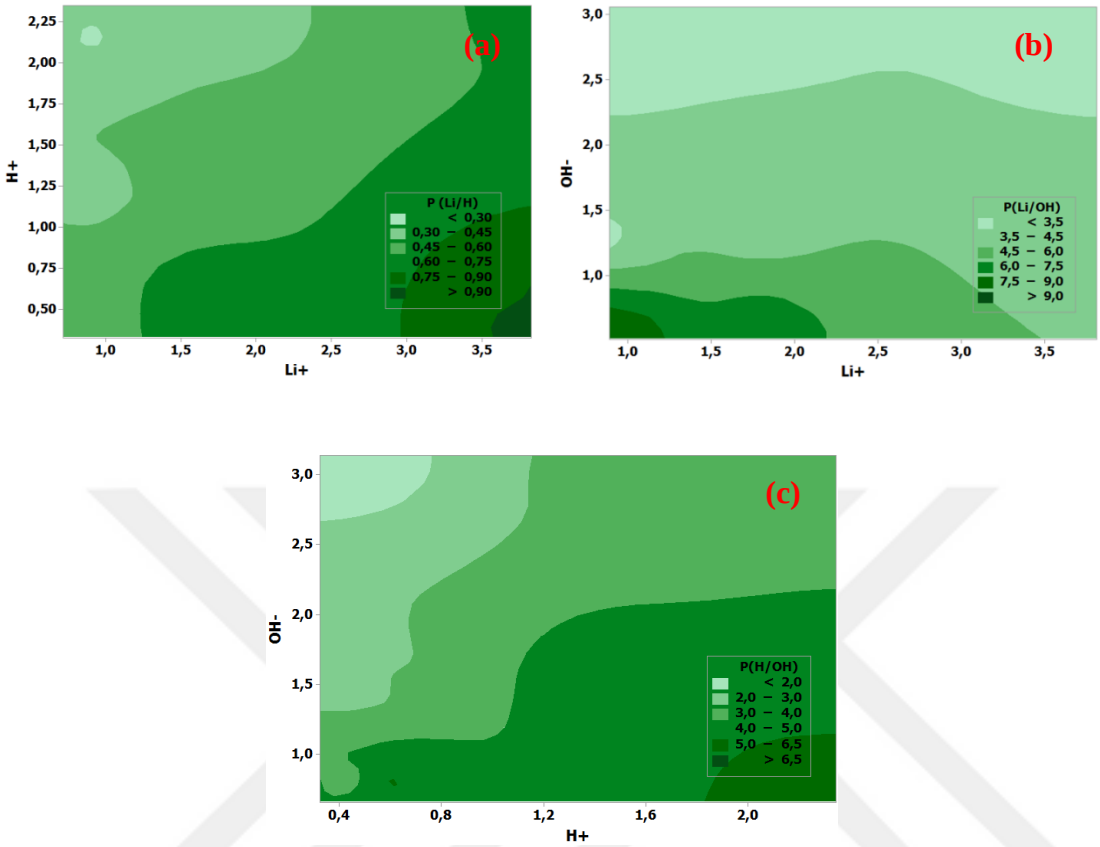

Figure 4.21 : Contour plots of permselectivity; a) x=Li^+, y=H^+ (moles/kg) vs. $P^{Li/H}$ (at 1% LiOH); b) x=Li^+, y=OH^- (moles/kg) vs. $P^{Li/OH}$ (at 5% H_2SO_4); c) x=H^+, y=OH^- (moles/kg) vs. $P^{H/OH}$ (at 20% Li_2SO_4).

4.8.3.2 Water transport number

The transport number of water, T_{H2O}, was calculated with the help of,

i) The amount of change of water in catholyte, $\Delta N^{c}_{H_2O}$, measured from the difference between initial and final catholyte volumes.

ii) T_H values calculated with the approximation mentioned above.

iii) Eq. (2.92).

The results are given in Table 4.8. It was observed that measured T_{H2O} values vary between ca. 4-9. Generally, the increase in Li^+ concentration causes an increase in

T_{H2O}, while H^+ and OH^- ions cause the decrease of water transport number. In order to be able to interpret the results, water transport mechanism has to be investigated.

Transport of water through membrane can occur via several mechanisms as described in Section 2.2.2.3. Of the three mechanisms; osmotic flux can be neglected. So only the effect of electro-osmotic flow and ion hydration was investigated here. In order to be able to determine the effect of electro-osmotic flow, experiments 45 and 46 were performed at the same concentration levels of experiment 31, yet at different current densities (15 and 5 $A.dm^{-2}$, respectively), which helps obtain different electrical potential gradients in the cell during the experiment. It was found that T_{H2O} does not change significantly between 5-15A, which suggests that electrical potential is not a required factor in the multiple regression analysis of T_{H2O}. So, ion hydration can be claimed to be the dominant factor in the determination of water transport number. Moreover, it should be noted that the relatively higher water transport number (7.8) of experiment 31 has possibly no significance and is probably due to experimental uncertainty. This is more apparent when one examines lithium transport number of these experiments, which are almost the same (0.59, 0.59 and 0.61). However, one would expect to find a significantly different lithium transport number for experiment 31 if the relatively higher water transport number of this experiment had any significance since cation transport number is closely related with water transport number as stated below.

In an ion hydration controlled mechanism, transport of water is directly related with the type of the transported species since different cations have different ion hydration numbers. For lithium, ion hydration number can be reported to be between 2 and 22, which is a quite large interval.

As for ion mobility, the greater the ion hydration number, the less is its mobility since ions carrying more water will have to move more slowly (e.g. $Li^+ < Na^+ < K^+$).

Transport of hydrogen ions, as described in detail in Section 2.2.2.3, occurs via a different mechanism called tunnelling or hopping transport. The same mechanism is also true for the transport of hydroxyl ions. These facts lead to two significant results: i) Their mobility is high, ii) they carry less water compared to common cations since their transport mechanism is not fully coupled with ion hydration.

These phenomena about water transport along with the fact that transport number of water is general between 4-8 in most electro-membrane processes [1] clearly explains the findings of this study both on cation transport and water transport;

- The uniqueness in hydrogen ion transport mechanism affects both cation transport numbers as well as water transport number.
- Transport number of lithium reduces significantly with the increase of hydrogen ions. As for hydroxyl ions, the increase of its concentration also creates a reduction in T_{Li}, yet much less compared to the effect of hydrogen ions due to ion exclusion.
- Water transport number increases with the increase of Li^+ concentration while decreases with the increase of H^+ and OH^- concentrations solely due to the differences in transport mechanism as mentioned above.

Since transport of water is very closely linked to the transport of cations, a regression equation, which had a similar structure with the one formed for lithium transport (Eq. (4.16)) was established. So, the following equation was obtained, with an R-squared value of 0.912;

$$T_{H_2O} = k_0 + k_1.\mathrm{Li}.\left[2 - \exp(-\mathrm{Li.H}) - \exp\left(-\frac{\mathrm{Li}}{\mathrm{OH}}\right)\right] + k_2.\mathrm{Li}^2.\left[2 - \exp(-\mathrm{Li.H}) - \exp\left(-\frac{\mathrm{Li}}{\mathrm{OH}}\right)\right] + k_3.\mathrm{H}.\left[2 - \exp\left(-\frac{\mathrm{H}}{\mathrm{Li}}\right) - \exp\left(-\frac{\mathrm{H}}{\mathrm{OH}}\right)\right] + k_4.\mathrm{H}^2.\left[2 - \exp\left(-\frac{\mathrm{H}}{\mathrm{Li}}\right) - \exp\left(-\frac{\mathrm{H}}{\mathrm{OH}}\right)\right] + k_5.\mathrm{OH}.\left[2 - \exp(-\mathrm{Li.OH}) - \exp\left(-\frac{\mathrm{OH}}{\mathrm{H}}\right)\right] \quad (4.17)$$

where, *k0, k1, k2, k3, k4* and *k5* are, 7.6160, 0.8007, -0.2133, -2.4044, 0.5366 and -0.2204respectively. This equation could successfully predict the water transport numbers of the model experiments with an average error value of 7%, while T_{H2O} of test experiments could be predicted with an average error value of 3%.

4.9 Comparison of the Transport Properties of Different Membranes

4.9.1 Purpose

In the previous section (Section. 4.8), a detailed investigation of a perfluorinated membrane (N-424) was carried out in terms of membrane transport properties during electromembrane process of lithium sulphate. In this section, the findings on N-424 will be compared with another homogeneous perfluorinated membrane (N-438) as well as a heterogeneous cation exchange membrane (MK-40). Similarly, regression analyses are carried out for N-438 and MK-40 membranes to model membrane transport.

4.9.2 Experimental

The materials-equipment required and the necessary pre-treatment procedures are described in Section 4.2 and Section 4.4. The experiments were performed at the following parameters:

- Nafion® N-438 and MK-40 membranes
- Circulation flowrate of 750 $mL.min^{-1}$;
- Temperature 30°C
- Current density of $10A.dm^{-2}$
- Anolyte initial concentration: 5, 20% Li_2SO_4 + 0, 5 H_2SO_4
- Catholyte initial concentration: 1, 7% LiOH

In addition to the experiments that were conducted at these concentration levels, another experiment (for each membrane) was performed at a concentration level which is different than these in order to test the regression equation with an experiment which was out of the model.

4.9.3 Results

4.9.3.1 Ion transport numbers

The measured transport numbers of lithium are given in Table 4.12. In this table, experiments 1-16 were used to establish a regression model equation while experiments 17-18 were used to test this equation.

Table 4.12 : Transport number results for N-438 and MK40 membranes.

		Initial concentration, *%*			Average concentration of ions, *moles/kg solution*			T_{Li}^{*}	T_{H}^{**}	T_{OH}^{**}	T_{H2O}^{***}	Notes
Memb.	**Exp. No**	**Li_2SO_4**	**H_2SO_4**	**LiOH**	**Li+,** *(in anolyte)*	**H+,** *(in anolyte)*	**OH-,** *(in catholyte)*					
N-438	1	20	0	1	3,59	0,56	0,91	0,81	0,10	0,08	6,3	*Used in regression model equation*
	2	20	0	7	3,68	0,28	3,05	0,57	0,02	0,42	4,6	
	3	20	5	1	3,62	1,47	0,84	0,64	0,32	0,04	4,7	
	4	20	5	7	3,64	1,41	3,05	0,52	0,24	0,24	4,3	
	5	5	0	1	0,69	0,35	0,69	0,43	0,37	0,20	6,2	
	6	5	0	7	0,71	0,34	2,92	0,39	0,09	0,52	6,2	
	7	5	5	1	0,88	1,22	0,57	0,22	0,75	0,03	4,1	
	8	5	5	7	0,87	1,23	2,86	0,18	0,49	0,33	4,6	
MK-40	9	20	0	1	3,72	0,38	0,75	0,59	0,08	0,32	4,6	
	10	20	0	7	3,78	0,22	2,98	0,39	0,01	0,59	3,9	
	11	20	5	1	3,72	1,41	0,74	0,57	0,35	0,08	4,5	
	12	20	5	7	3,82	1,23	2,97	0,29	0,26	0,45	2,4	
	13	5	0	1	0,76	0,32	0,67	0,45	0,31	0,24	5,3	
	14	5	0	7	0,80	0,27	2,95	0,35	0,07	0,57	4,2	
	15	5	5	1	0,87	1,15	0,53	0,20	0,77	0,04	3,6	
	16	5	5	7	0,87	1,16	2,90	0,18	0,50	0,32	3,4	
N-438	17	10,7	4,2	3,05	1,75	1,23	1,46	0,43	0,43	0,14	5,3	*Used for testing*
MK-40	18	10,7	4,2	3,05	1,76	1,20	1,48	0,41	0,42	0,18	4,8	

**measured.*
***calculated with an approximation from T_{Li} regression equation and Eq. (2.48).*
**** from Eq.(2.92) and (3.18) with the help of measured ΔN_{H2O} and calculated T_H values.*

N-438

For the interpretation of the results, first of all, in order to be able to determine the significant effects and interactions, a multiple regression investigating single terms and two-way interactions was performed. The effect of quadratic terms couldn't be considered here since limited number of points could produce misleading results. It

was found that Li^+ and H^+ has strong effect on T_{Li}, while the effect of OH^- is less but still a significant factor Fig. 4.22.a.

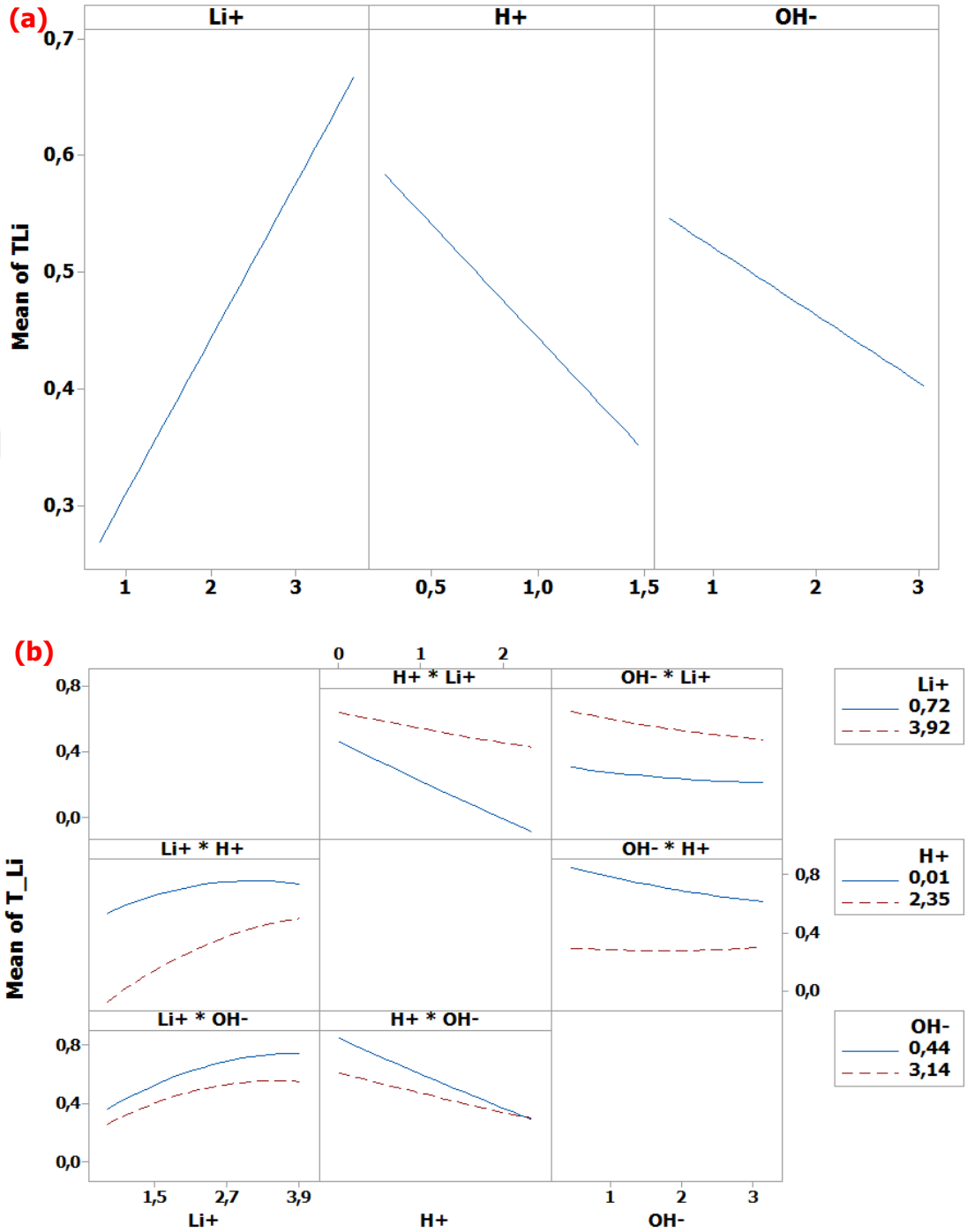

Figure 4.22 : (a) Main effects (b) Interaction plots for T_{Li} (N-438).

Moreover, significant deductions could be made of interaction plots Fig. 4.22.b such as;

- Main effects plot show that the increase of H^+ concentration causes a significant decrease in T_{Li}. However, interaction plot reveals that the increase of H^+ concentration increases the significance of Li^+. This is an indirect effect, that is to say, increasing acidity suppresses the effect of OH^- ions, which in return, increases the significance of Li^+ concentration.

- The increase of Li^+ and OH^- concentrations decreases the effect of H^+ ions on T_{Li}. This is due to the decreasing competitive advantage of H^+ with the increase of the concentration of its opponents in membrane transport.

Another important illustration, which helps determine the significant interactions between parameters, is contour plot, which is a projection of a 3-D graph. From the contour plots of Li^+, H^+, OH^- v.s T_{Li}, (Fig. 4.23), the following deductions can be made:

- Fig. 4.23.a-b shows that increasing acid concentration diminishes the effect of OH^-, yet the increase of Li^+ concentration boosts the influence of OH^- ions. The latter is an indirect effect, i.e. increasing Li^+ concentration decreases the influence of H^+ ions on T_{Li}, which in return, increases the significance of OH-concentration.

- In Fig. 4.23.c-d, the influence of H^+/Li^+ ratio on the significance of OH^- is more clear, the increase of which decreases the effect of OH^- on T_{Li}.

- In Fig. 4.23.e-f, it is seen that at low H^+ concentrations, the increase of OH^- concentration causes a slight decrease in the significance of Li^+ ions on T_{Li}. This is due to the decreasing competitive advantage of Li^+ with the increase of the concentration of OH^-.

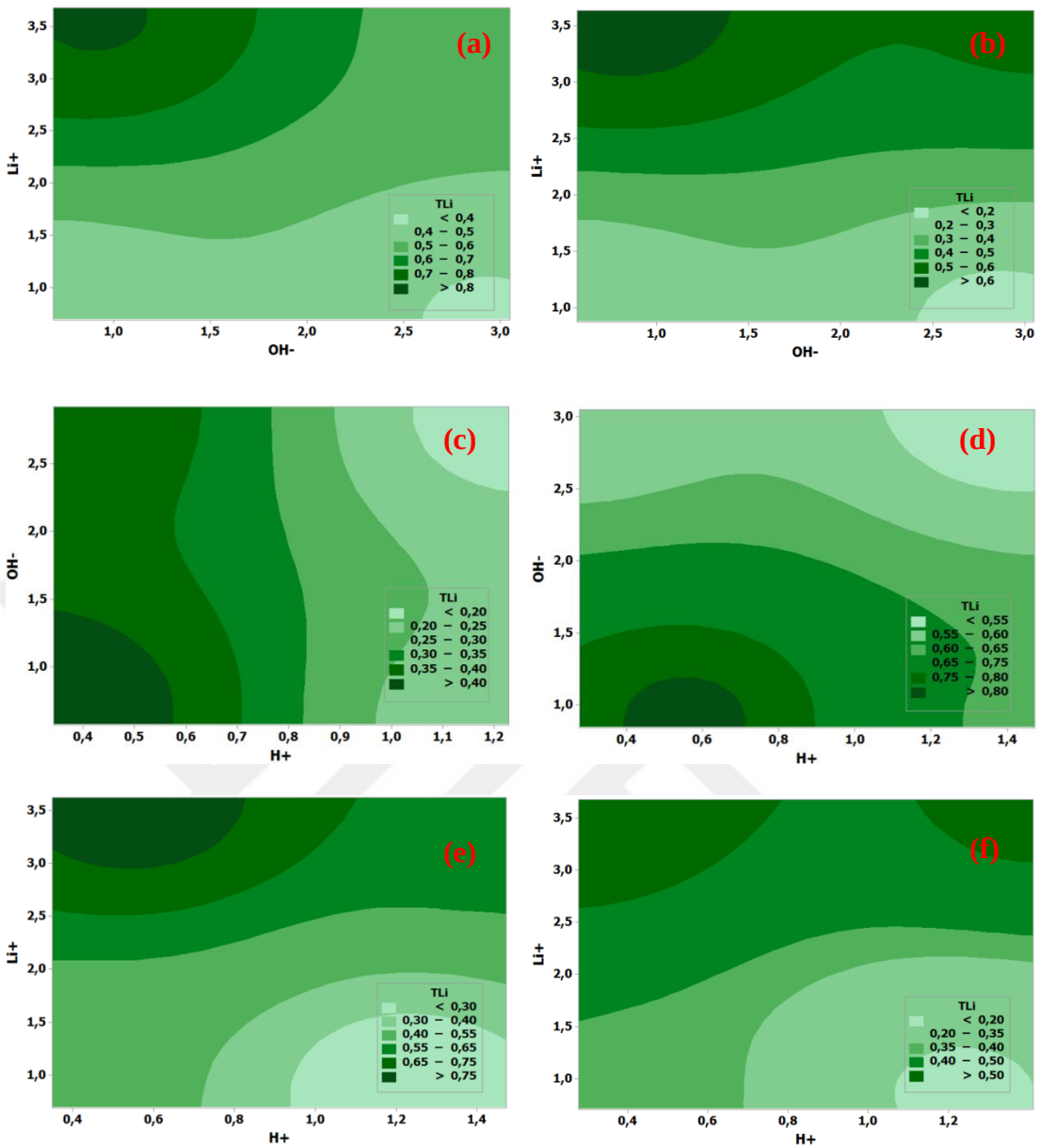

Figure 4.23 : Contour plots of T_{Li} of N-438 membrane for x=OH^-, y=Li^+ (moles/kg) at H_2SO_4 concentrations of a) 0%, b) 5%; for x=H^+, y=OH^- (moles/kg) at Li_2SO_4 concentrations of c) 5%, d) 20%; for x=H^+, y=Li^+ (moles/kg) at LiOH concentrations of e) 1%, f) 7%.

All these deductions suggest that;

- $Li^+.H^+$ and Li^+/OH^- are the critical factors determining the significance of Li^+ concentration, the increases of which increase the influence of Li^+ on T_{Li}.

- H^+/Li^+ and H^+/OH^- are the critical factors determining the significance of H^+ concentration, the increases of which increase the influence of H^+ on T_{Li}.

- $OH^-.Li^+$ and OH^-/H^+ are the critical factors determining the significance of OH^- concentration, the increases of which increase the influence of OH^- on T_{Li}.

These factors have to be embedded in the regression model equation in order to adjust the main effects in such a way that they will be able to reflect the actual mechanism in membrane transport. In other words, the main effects have to be multiplied with these factors in such a way that when this multiplier goes to zero, the significance of the related parameter approaches zero. Likewise, when this multiplier goes to infinity, the significance of the related parameter becomes independent of this multiplier. Exponential terms are found to be appropriate multipliers, which have the potential to reflect this effect. So, the model equation was proposed as;

$$T_{Li} = k_0 + k_1.\mathrm{Li}.\left[2 - \exp(-\mathrm{Li}.\mathrm{H}) - \exp\left(-\frac{\mathrm{Li}}{\mathrm{OH}}\right)\right] + k_2.\mathrm{H}.\left[2 - \exp\left(-\frac{\mathrm{H}}{\mathrm{Li}}\right) - \exp\left(-\frac{\mathrm{H}}{\mathrm{OH}}\right)\right] + +k_3.\mathrm{OH}.\left[2 - \exp(-\mathrm{Li}.\mathrm{OH}) - \exp\left(-\frac{\mathrm{OH}}{\mathrm{H}}\right)\right] \quad (4.18)$$

In addition to the equation above, the candidate model equations proposed to be tested for MK-40 (Eq. 4.10-12) were tested for N-438, too. The results are given in Table 4.13. It is seen in Table 4 that the equation proposed for N-438 membrane (Eq. 4.18) represents the membrane transport best with an R_squared value of 0.974. The coefficients of this equation are; 0.49790, 0.05945, -0.16251 and -0.02862 for k_0, k_1, k_2 and k_3, respectively. Average error values in the prediction of lithium transport numbers with this equation is 6.4% while the test experiment could be predicted with an error value of 12.0%.

Table 4.13 : Statistical test of proposed model equations.

Membrane	Equation no.	R_squared, R^2	% error in the prediction of T_{Li} of test experiment
N-438	4.18	0,974	12,0
	4.19	0,969	12,1
	4.20	0,974	13,8
	4.21	0,969	13,1
MK-40	4.18	0,810	21,5
	4.19	0,859	23,2
	4.20	0,809	24,0
	4.21	0,857	25,2

The transport numbers of H^+ and OH^- are hard to measure since there exist multiple steps in their production/consumption such as; production due to electrodic reactions, transport through membrane, consumption due to neutralization with the transported H^+/OH^- ions. However, the regression equation established for T_{Li} can be readily utilized to calculate the other transport numbers along with Eq. (2.48), which assumes that the total transport number of ions should be equal to unity. So, the absolute values of H and Li terms in regression equation of T_{Li} were assumed to be directly related with the transport numbers, T_H and T_{OH}, respectively. With this approach, T_H and T_{OH} values were calculated and given in Table 4.12.

MK-40

The same statistical evaluation was performed for MK-40 membrane. The same trend of main effects as in N-438 was observed. However, the effect of OH^- ions seem to be more powerful than N-438 suggesting a worse prevention of hydroxyl ion back-transport. Examination of interaction plots (Fig. 4.24) leads to the following conclusions;

- The increase of H^+ concentration causes a significant decrease in T_{Li}. However, interaction plot reveals that the increase of H^+ concentration increases the significance of Li^+. The increase of Li^+ concentration decreases the effect of H^+ ions on T_{Li}, which is due to the decreasing competitive advantage of H^+ with the increase of the concentration of its opponents in membrane transport. These were observed for N-438, too.

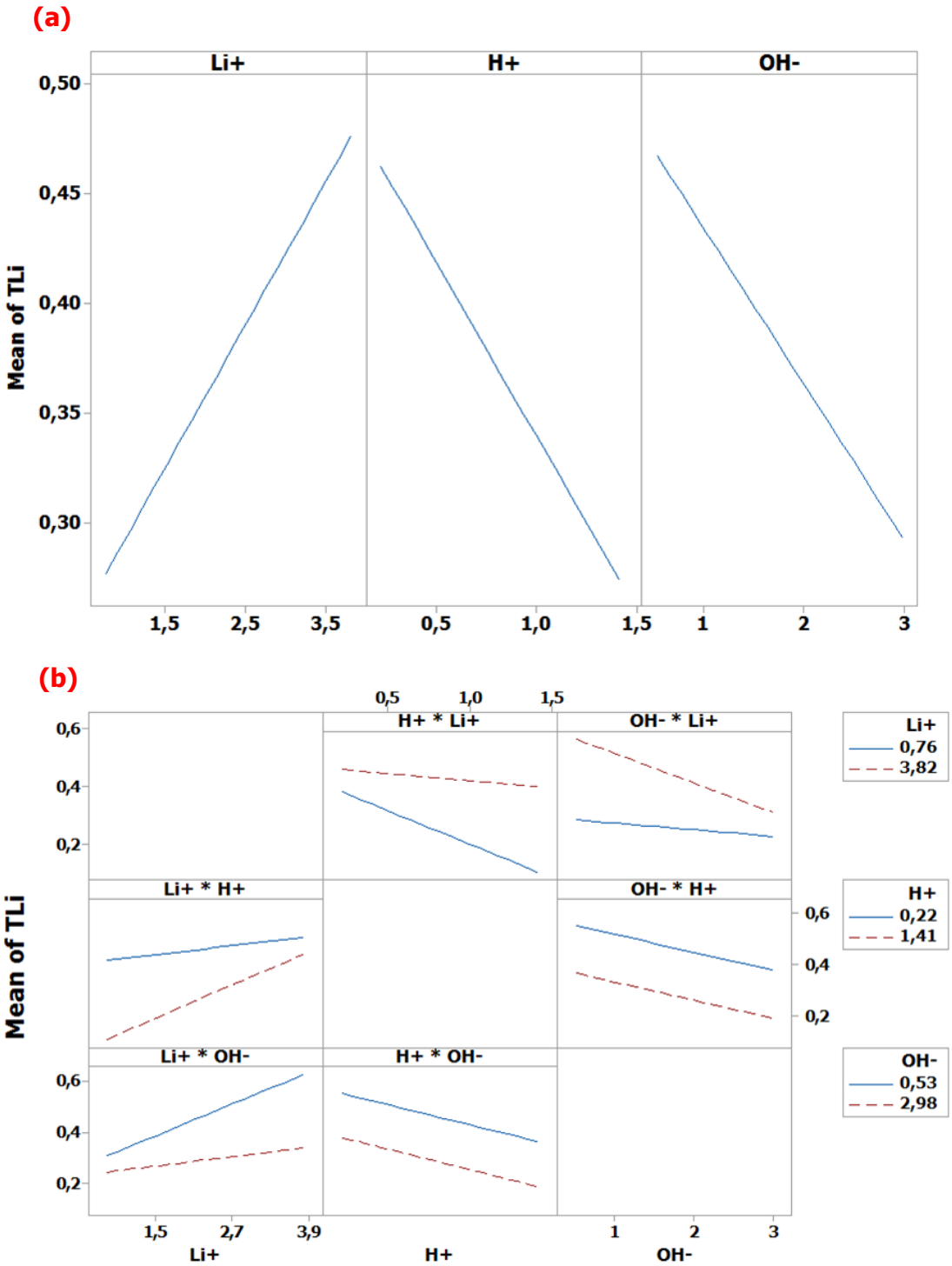

Figure 4.24 : (a) Main effects (b) Interaction plots for T_{Li} (MK-40).

The examination of the contour plots of Li^+, H^+, OH^- v.s T_{Li}, (Fig. 4.25) leads to the following conclusions:

- The trend of Fig. 4.25.a-b is a bit different from the similar graph of N-438. In this graph, it is seen that the effect of increasing acid concentration on the effect of OH^- is not that strong, which may suggest that the OH^-/H^+ term, which was embedded in the model equation of N-438 to arrange the

significance of OH^- concentration, can be neglected. However, in Fig. 4.25.c-d, the influence of H^+/Li^+ ratio on the significance of OH^- can be observed, the increase of which decreases the effect of OH^- on T_{Li}. In Fig. 4.25.e-f, though weaker, the same effect on the effectiveness of Li^+ observed for N-438 can be claimed to exist.

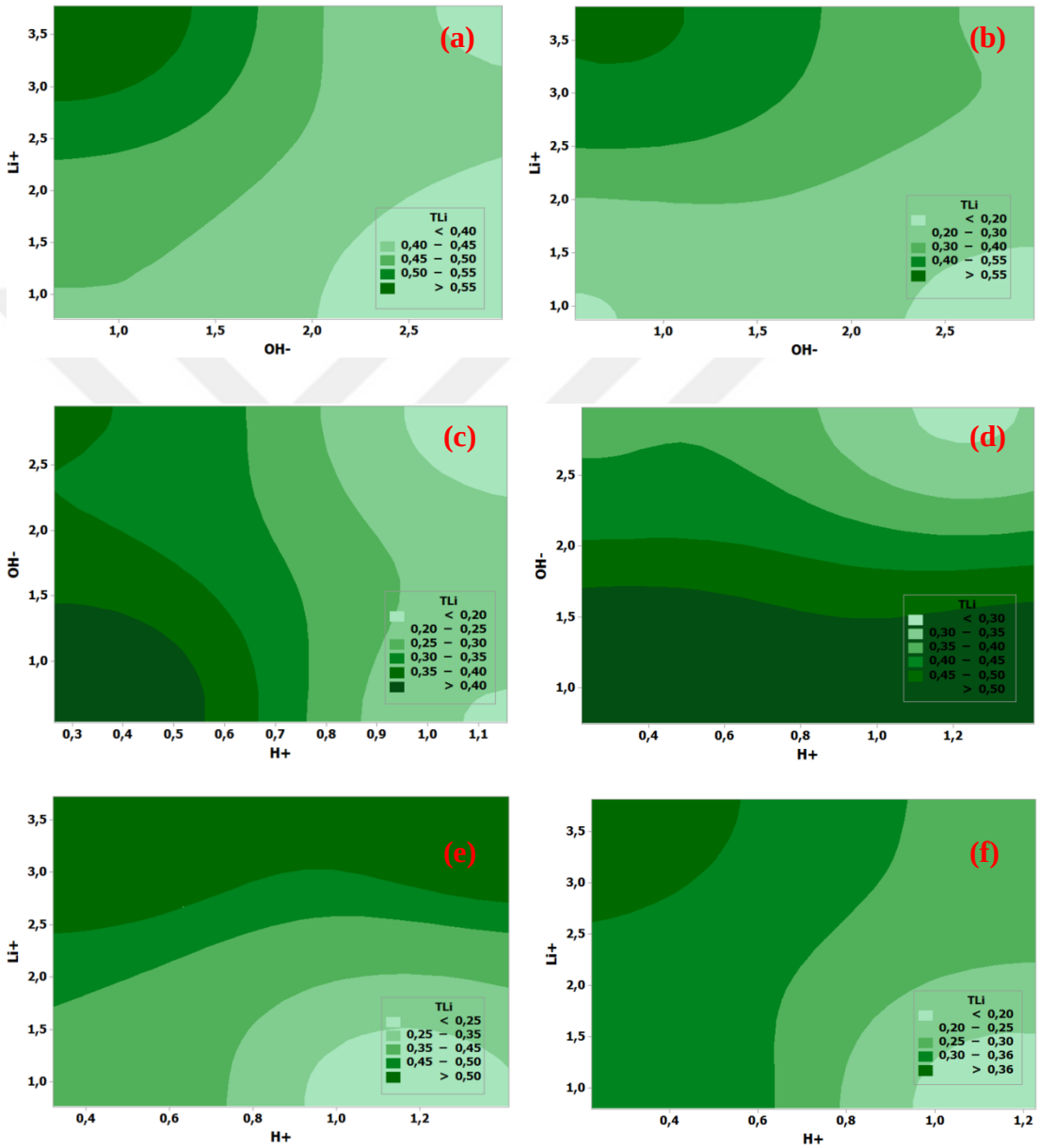

Figure 4.25 : Contour plots of T_{Li} of MK-40 membrane for x=OH^-, y=Li^+ (moles/kg) at H_2SO_4 concentrations of a) 0%, b) 5%; for x=H^+, y=OH^-(moles/kg) at Li_2SO_4 concentrations of c) 5%, d) 20%; for x=H^+, y=Li^+ (moles/kg) at LiOH concentrations of e) 1%, f) 7%.

These evaluations lead to the following conclusions;

- $Li^+.H^+$ and Li^+/OH^- are the critical factors determining the significance of Li^+ concentration, the increases of which increase the influence of Li^+ on T_{Li}.

- H^+/Li^+ is the critical factor determining the significance of H^+ concentration, the increase of which increases the influence of H^+ on T_{Li}. However, the effect of H^+/OH^- has to be tested in regression analysis.

- $OH^-.Li^+$ is the critical factor determining the significance of OH^- concentration, the increase of which increases the influence of OH^- on T_{Li}. However, the effect of OH^-/ H^+ has to be tested in regression analysis.

These factors, as mentioned for N-438, are embedded in the regression model equation in exponential forms. However, in order to be able to reflect the effect of H^+/OH^- parameter correctly, as discussed above, three more models were tested in addition to Eq. (4.18), i.e.;

$$T_{Li} = k_0 + k_1.\mathrm{Li}.\left[2 - \exp(-\mathrm{Li.H}) - \exp\left(-\frac{\mathrm{Li}}{\mathrm{OH}}\right)\right] + k_2.\mathrm{H}.\left[1 - \exp\left(-\frac{\mathrm{H}}{\mathrm{Li}}\right)\right] + \\ + k_3.\mathrm{OH}.\left[2 - \exp(-\mathrm{Li.OH}) - \exp\left(-\frac{\mathrm{OH}}{\mathrm{H}}\right)\right] \quad (4.19)$$

$$T_{Li} = k_0 + k_1.\mathrm{Li}.\left[2 - \exp(-\mathrm{Li.H}) - \exp\left(-\frac{\mathrm{Li}}{\mathrm{OH}}\right)\right] + k_2.\mathrm{H}.\left[2 - \exp\left(-\frac{\mathrm{H}}{\mathrm{Li}}\right) - \\ \exp\left(-\frac{\mathrm{H}}{\mathrm{OH}}\right)\right] + + k_3.\mathrm{OH}.\left[1 - \exp(-\mathrm{Li.OH})\right] \quad (4.20)$$

$$T_{Li} = k_0 + k_1.\mathrm{Li}.\left[2 - \exp(-\mathrm{Li.H}) - \exp\left(-\frac{\mathrm{Li}}{\mathrm{OH}}\right)\right] + k_2.\mathrm{H}.\left[1 - \exp\left(-\frac{\mathrm{H}}{\mathrm{Li}}\right)\right] + \\ + k_3.\mathrm{OH}.\left[1 - \exp(-\mathrm{Li.OH})\right] \quad (4.21)$$

The results are given in Table 4.13. It is seen that in all proposed equations for MK-40, R_squared values are relatively low and error values in the prediction of T_{Li} of test experiment are relatively high. This is attributed mainly to the heterogeneous structure of MK-40, which possibly creates a more chaotic transport mechanism and so makes it hard to put forward a regression model representing ion transport in terms of concentrations only. As indicated and illustrated in the study of Martí-Calatayud et al., the structure of heterogeneous membranes includes zones which are rich in inert binder, thus complicating the connection between the conducting channels available for the ion transport (counter-ion pathway) (Martí-Calatayud et al,

2014). On the other hand, homogeneous membranes present a much smoother counter-ion pathway. Moreover, the fact that heterogeneous membranes are much thicker (which is valid for N-438 and MK-40 comparison) makes the transport pathway even more complicated for these membranes. Nevertheless, the model equation representing ion transport through MK-40 membrane best was selected from Table 4.13. Despite not presenting the best (lowest) error value, Eq. (4.19) was picked since it introduces the best R_squared value by far. R_squared value of this equation is 0.859 while the coefficients are 0.50140, 0.02018, -0.28634 and -0,02976; for k_0, k_1, k_2 and k_3, respectively. Average error values in the prediction of lithium transport numbers with this equation is 16.7% while the test experiment could be predicted with an error value of 23.2%.

Transport numbers of hydrogen and hydroxyl ions, T_H and T_{OH}, were calculated according to the method explained for N-438 and given in Table 4.12.

4.9.3.2 Water transport numbers

The transport number of water, T_{H2O}, was calculated with the help of, i) the amount of change of water in catholyte, $\Delta N^c_{H_2O}$, measured from the difference between initial and final catholyte volumes, ii) T_H values calculated with the approximation mentioned above, iii) Eq. (3.18).

The transport numbers measured in experiments are given in Table 4.12. The average water transport numbers are 5.1 and 4.1 for N-438 and MK-40 membranes, respectively. Generally, the increase in Li^+ concentration causes an increase in T_{H2O}, while H^+ and OH^- ions cause the decrease of water transport number.

The interpretation of the results of water transport can be easily made with the investigation of water transport mechanism, which was explained in detail in Section 4.8.3.2 for water transport through N-424 membrane. The same analysis is valid for N-438 and MK-40 membranes. The general findings are;

- The uniqueness in hydrogen ion transport mechanism affects both cation transport numbers as well as water transport number.

- Transport number of lithium reduces significantly with the increase of hydrogen ions. As for hydroxyl ions, the increase of its concentration also creates a reduction in T_{Li}. The reduction in less compared to the effect of hydrogen ions due to ion exclusion in case of perfluorinated membrane (N-438), which presents a more successful ion exclusion. However, the reduction is more significant in case of MK-40 due to its heterogeneous structure.

- Water transport number increases with the increase of Li^+ concentration while decreases with the increase of H^+ and OH^- concentrations due to the differences in transport mechanism as mentioned above.

- The fact that MK-40 exhibits a relatively lower average water transport number is attributed to the fact transport number of hydrogen and hydroxyl ions are generally higher than those of N-438 since these ions carry less water compared to lithium ion.

Since transport of water is very closely linked to ion transport as explained above, a regression equation, which had a similar structure with the one formed for lithium transport was established for both membranes. So, the following equations were established for N-438 and MK-40 membranes, respectively;

$$T_{H_2O} = k_0 + k_1.\mathrm{Li}.\left[2 - \exp(-\mathrm{Li}.\mathrm{H}) - \exp\left(-\frac{\mathrm{Li}}{\mathrm{OH}}\right)\right] + k_2.\mathrm{H}.\left[2 - \exp\left(-\frac{\mathrm{H}}{\mathrm{Li}}\right) - \exp\left(-\frac{\mathrm{H}}{\mathrm{OH}}\right)\right] + +k_3.\mathrm{OH}.\left[2 - \exp(-\mathrm{Li}.\mathrm{OH}) - \exp\left(-\frac{\mathrm{OH}}{\mathrm{H}}\right)\right] \quad (4.22)$$

$$T_{H_2O} = k_0 + k_1.\mathrm{Li}.\left[2 - \exp(-\mathrm{Li}.\mathrm{H}) - \exp\left(-\frac{\mathrm{Li}}{\mathrm{OH}}\right)\right] + k_2.\mathrm{H}.\left[1 - \exp\left(-\frac{\mathrm{H}}{\mathrm{Li}}\right)\right] + +k_3.\mathrm{OH}.\left[2 - \exp(-\mathrm{Li}.\mathrm{OH}) - \exp\left(-\frac{\mathrm{OH}}{\mathrm{H}}\right)\right] \quad (4.23)$$

For N-438 membrane, the coefficients of Eq. (4.22) are 6.91413, -0.02971, -1.31911 and -0,17452 for k_0, k_1, k_2 and k_3, respectively. R_squared value is 0.7654, which does not indicate a very good correlation. On the other hand, the water transport value of the test experiment can be predicted with an error value of 10.7%, which is acceptable.

For MK-40 membrane, the coefficients of Eq. (4.23) are 5.74965, -0.09395, -2.15306 and -0.20392 for k_0, k_1, k_2 and k_3, respectively. R_squared value is 0.7651, which is better than that of N-438. On the other hand, the water transport value of the test

experiment can be predicted with an error value of 21.1%, which is higher than that of N-438.

4.9.3.3 Comparison of membrane performances

For a comparative membrane performance evaluation, transport number and permselectivity results are illustrated in Figures 4.26-32. The concentration parameters of the experiments used for comparison of the membranes are given in Table 4.14. For a fair comparison, regression analysis for N-424 was repeated omitting the quadratic terms as in N-438 and MK-40 membranes.

Table 4.14 : The parameters of the experiments used for comparison.

	Initial concentration, *%*		
Exp. No	**Li_2SO_4**	**H_2SO_4**	**LiOH**
1	20	0	1
2	20	0	7
3	20	5	1
4	20	5	7
5	5	0	1
6	5	0	7
7	5	5	1
8	5	5	7

As the figures about transport numbers are examined (Fig 4.26-28), it is seen that transport number of lithium is generally higher for perfluorinated homogenous N-424 and N-438 membranes than heterogeneous MK-40 membrane. Moreover, hydrogen ion transport number does not change greatly according to the membrane used. However, transport number of hydroxyl ion differs according to the membrane, especially according to the membrane type (homogeneous/heterogeneous) used. These results suggest that; though hydrogen concentration is very effective in the distribution of transport numbers due to its highly dominant unique membrane transport mechanism as explained elaborately in the previous chapters, hydrogen ion transport number does not change greatly according to the membrane used. So it could be claimed that hydrogen ion transport is not affected significantly from the membrane type. This is probably due to the fact that hydrogen ion's advantageous way of transport makes it possible that hydrogen transport is not significantly restricted by membrane properties such as water content, fixed charge density and

especially the distribution and ratio of hydrophilic domains through which ions and water are transported.

On the other hand, the change of hydroxyl ion transport number according to the membrane type, especially according to the membrane structure (homogeneous/heterogeneous) is attributed to the differences in Donnan exclusion performance (Fig 4.28). Donnan exclusion effect usually decreases with the decrease of ion exchange capacity, which leads to the increase of co-ions inside membrane. However, apart from the ion exchange capacity, the structure of the membrane is of utmost importance in the determination of co-ion exclusion performance. The increase of membrane heterogeneity causes the fraction of micropores filled with solution become larger, which leads to the introduction of more co-ions into the membrane (Grabowski, 2010). In other words, the existence of regions which exhibit zero-selectivity behaviour increases the back migration of hydroxyl ions, which are not exposed to Donnan exclusion in these regions (Gregor, 1957). That's why heterogeneous MK-40 membrane exhibited higher hydroxyl ion transport values than the other homogeneous membranes despite its higher ion exchange capacity. This is in line with literature data, where homogeneous membranes having lower ion exchange capacities compared to heterogeneous membranes are reported to have higher permselectivies for counter-ions (Ecbobar and Schafer, 2010).

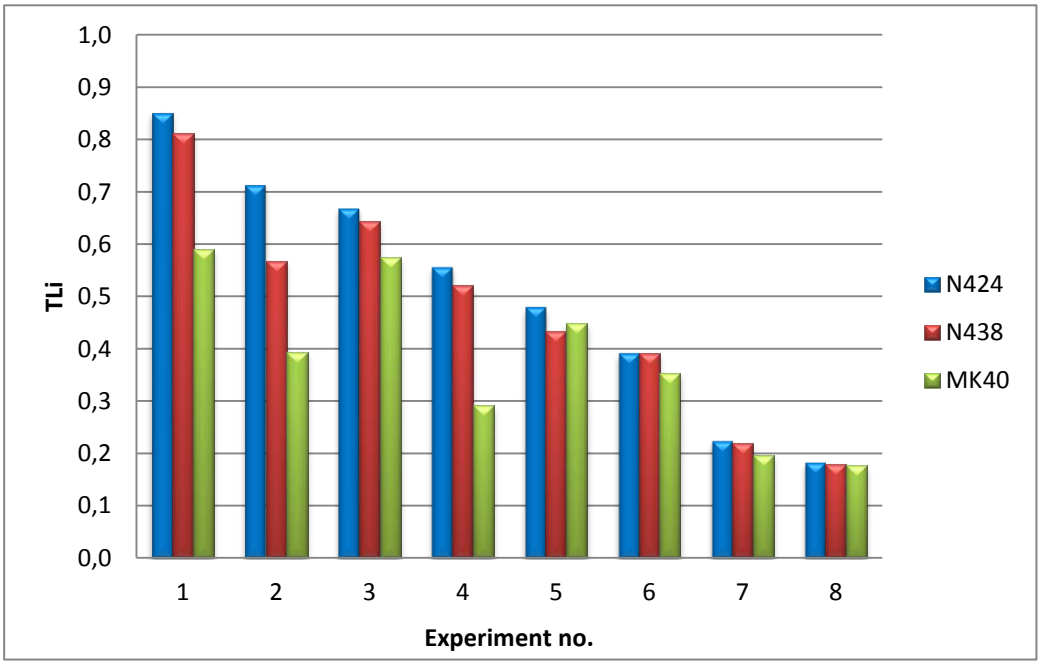

Figure 4.26 : Lithium ion transport numbers (T_{Li}) of the three membranes.

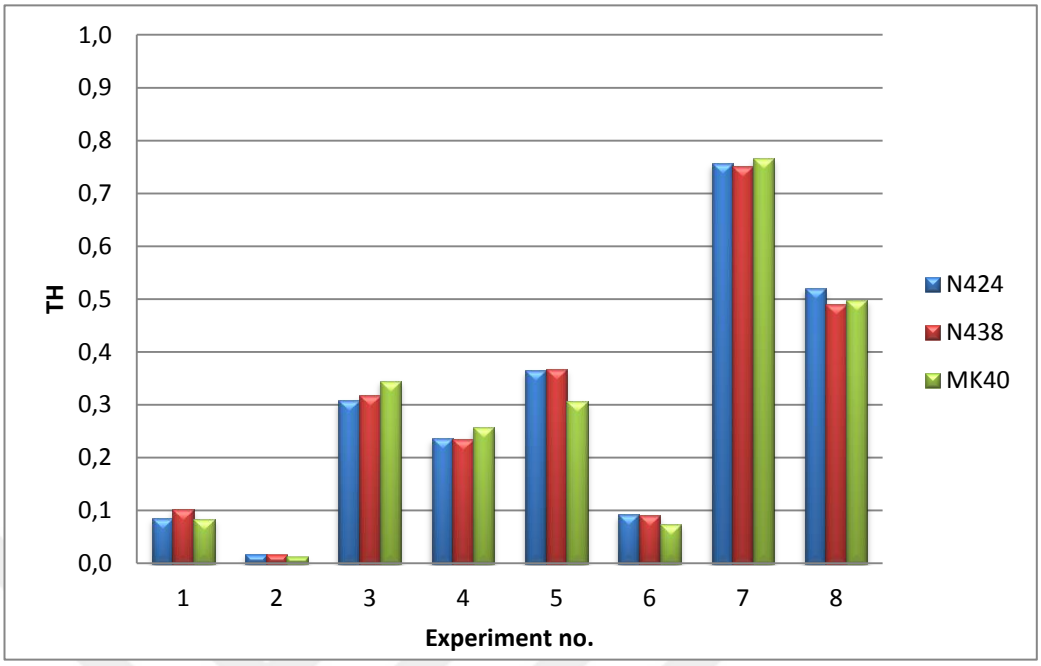

Figure 4.27 : Hydrogen ion transport numbers (T_H) of the three membranes.

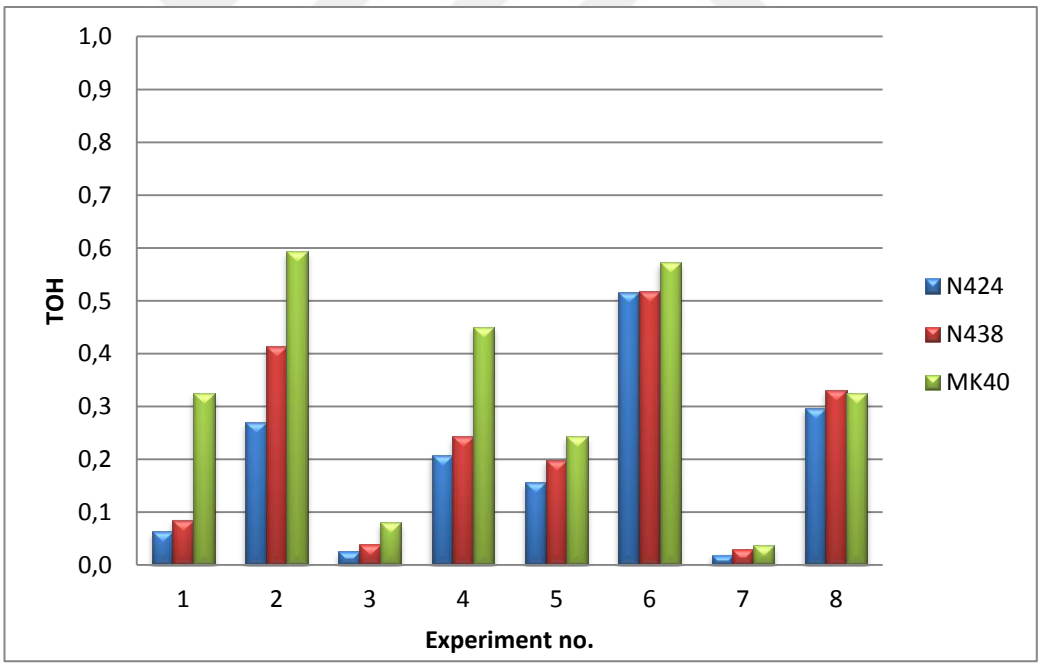

Figure 4.28 : Hydroxyl ion transport numbers (T_{OH}) of the three membranes.

The change in transport number of water according to the membrane type is closely linked with the differences in transport numbers of ions (Fig. 4.29). As explained in detail above, hydrogen and hydroxyl ions carry less water compared to lithium ion. So, water transport number in case of MK-40 membrane is generally lower than the other two membranes since lithium ion transport number is generally low for MK-40

membranes. Particularly, the high hydroxyl ion transport number is responsible for the relatively low water transport number obtained during experiments with MK-40 membrane.

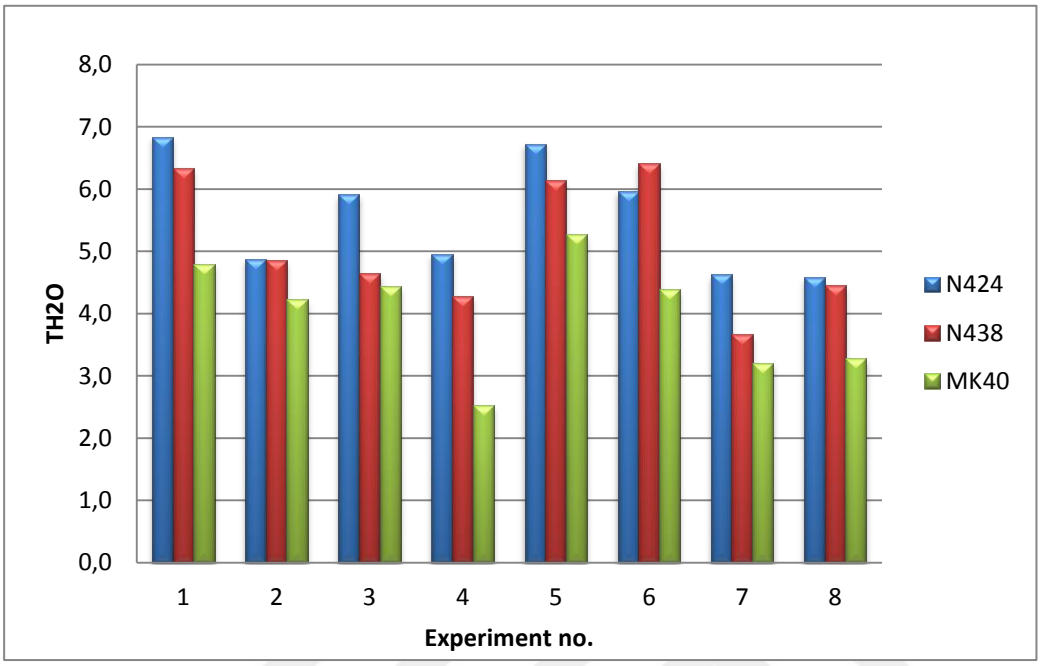

Figure 4.29 : Water transport numbers (T_{H2O}) of the three membranes.

Binary permselectivity relations for three membranes are illustrated in Figure 4.30-32 at constant concentration of the third species. In Fig 4.30, it is seen that membrane's permselectivity for lithium ion against hydrogen ion, $P^{Li/H}$, is generally highest for N-438, lowest for MK-40 membranes. In Fig 4.31, membrane's permselectivity for lithium ion against hydroxyl ion, $P^{Li/OH}$, is generally highest for N-424, lowest for MK-40 membranes. As for membrane's permselectivity for hydrogen ion against hydroxyl ion, $P^{H/OH}$, it is generally highest for N-424, lowest for MK-40 membranes. All these results suggest that MK-40 membrane is poorer in performance in terms of preventing back-transport of hydroxyl ions, as well as competition of lithium ions with hydrogen ions in membrane transport. Moreover, slightly higher $P^{Li/OH}$ values of N-424 compared to N-438 indicate a better Donnan exclusion for N-424.

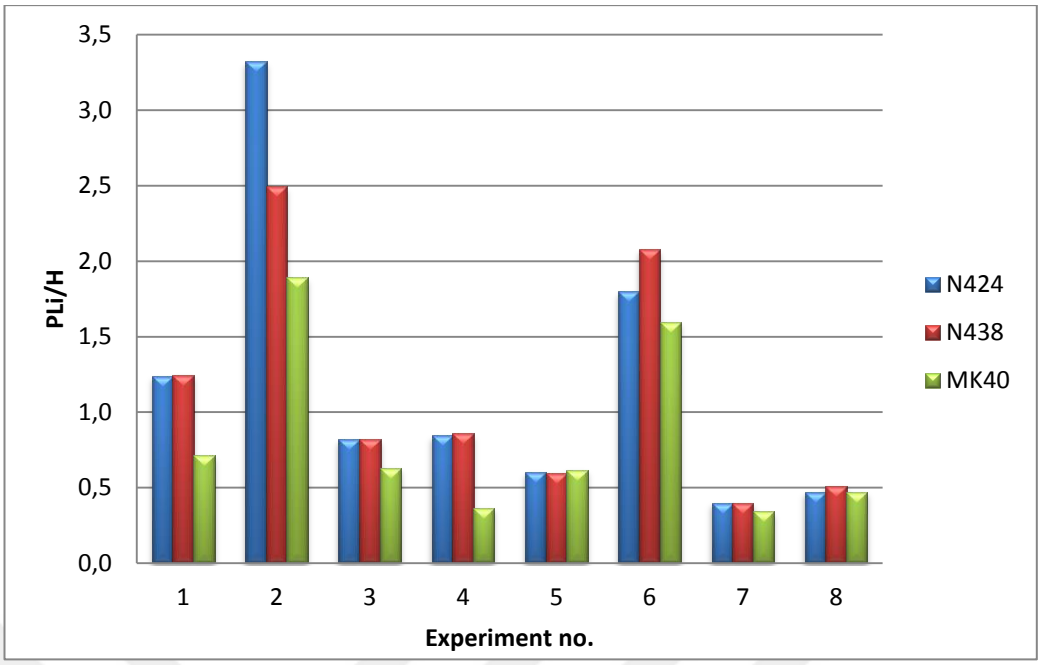

Figure 4.30 : Lithium ion permselectivity against hydrogen ion ($P^{Li/H}$) of the three membranes.

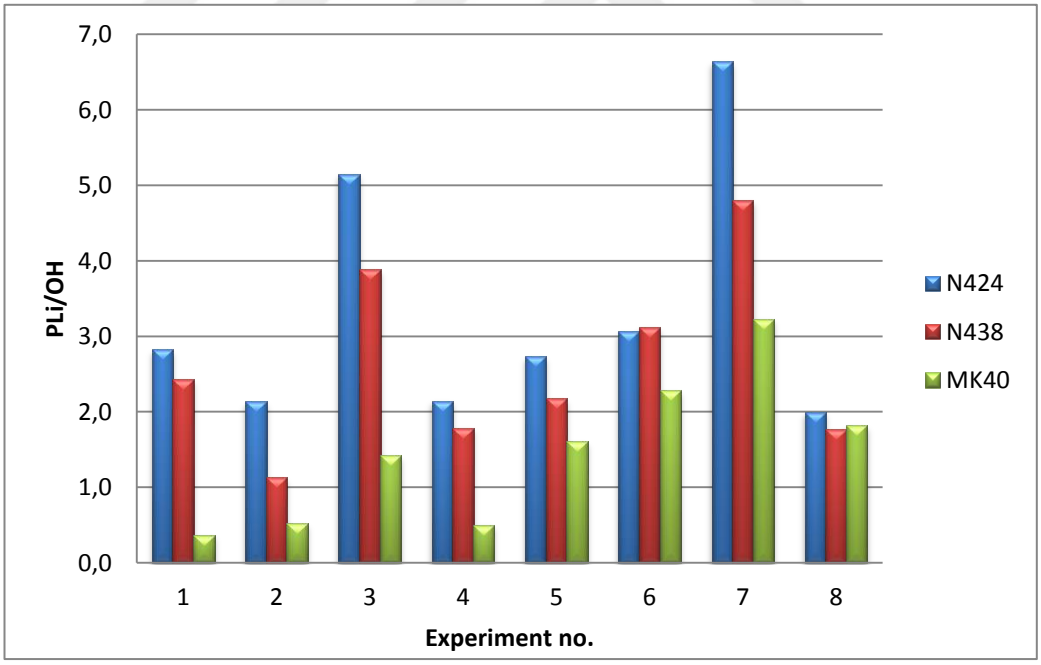

Figure 4.31 : Lithium ion permselectivity against hydroxyl ion ($P^{Li/OH}$) of the three membranes.

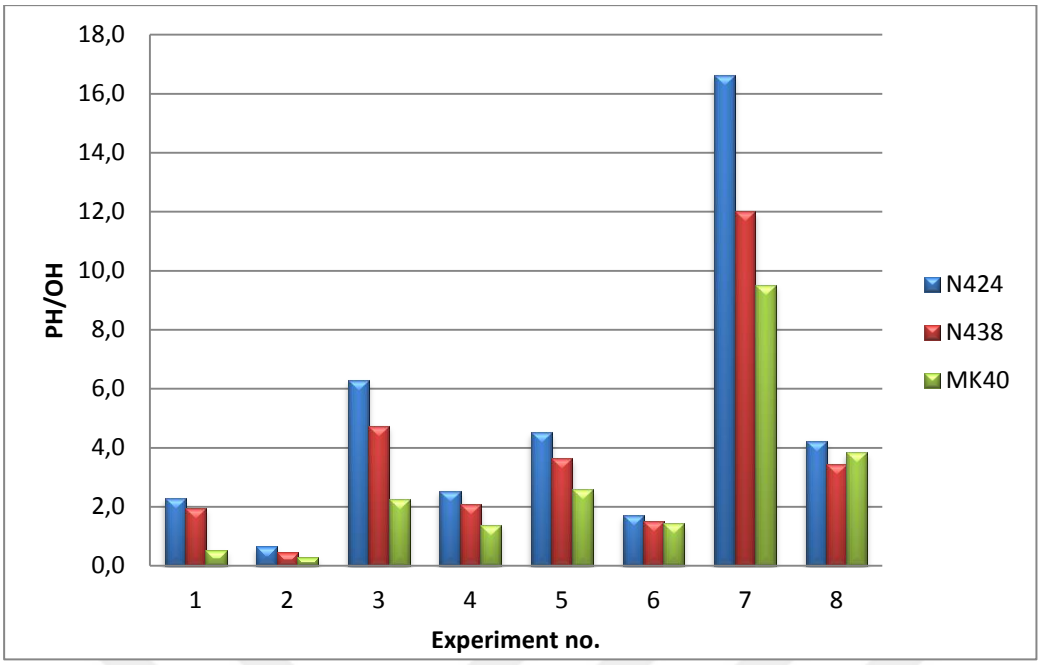

Figure 4.32 : Hydrogen ion permselectivity against hydroxyl ion ($P^{H/OH}$) of the three membranes.

Average cell voltage values during membrane electrolysis process are shown in Fig. 4.33. It is seen that there is not a significant difference in values both according to the experiment carried and according to the membrane type used. This suggests that most of the overall resistance originates from the electrolyte solutions. Moreover, it can be claimed that even the lowest conductivity values are enough to conduct electricity well and does not create a limiting resistance, which controls the overall resistance and so which affects the overall voltage. However, there is a small increase in the heterogeneous MK-40 membrane compared to the other two. This relatively higher voltage values can be attributed to the heterogeneity of MK-40, which causes extra resistance due to the following reasons;

- Tortuosity or the path length of ion transfer through the membrane is increased in heterogeneous membranes
- The stagnant inert phase of heterogeneous membranes with minimal or no ionogenic groups is always less conducive to transport of ions

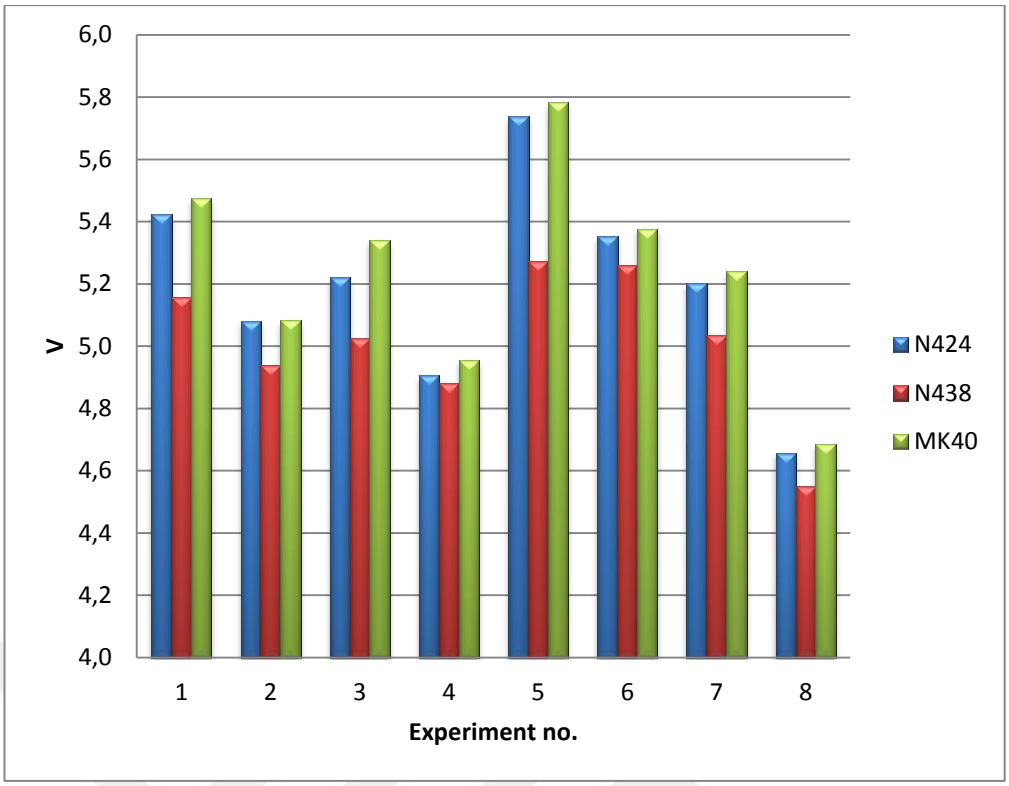

Figure 4.33 : Average cell voltage (V) during electrolysis.

5. CONCLUSIONS

In this study, electro-membrane salt splitting process to produce lithium hydroxide using lithium sulphate in a two-compartment membrane electrolysis cell was investigated by means of determining significant parameters affecting on the process and understanding the membrane transport behaviour during electrolysis.

First, concentration-conductivity regression equations were determined in order to be able to predict instantaneous anolyte and catholyte concentrations during membrane electrolysis with the help of conductivity-pH values and without the need of analysing the electrolytes. The measured values were compared with the predicted values with the help of the established regression equation and it was found that anolyte concentration prediction gives average error values of 6.0% and 19.5% for lithium sulphate and sulphuric acid concentration, respectively. Lithium sulphate error was found acceptable, yet sulphuric acid prediction was found to be a bit erroneous, which was attributed to the logarithmic relation of pH with hydrogen ion concentration. On the other hand, lithium hydroxide could be predicted successfully with an average error value of 4.6%. So, during an electromembrane process, lithium hydroxide concentration can be monitored and controlled using catholyte conductivity data and the equation produced in this study. As for anolyte solution, it can be said that numerical values obtained by the regression equations produced are not quite reliable. However, it can still be claimed that ph/conductivity data and the regression equation produced in this study can be helpful at least for the estimation of the order of anolyte concentration.

Then, general membrane behaviour was investigated in the electrochemical production of lithium hydroxide in a two-compartment membrane electrolysis cell under different process parameters (temperature, current density, catholyte concentration). The most important factor affecting on current efficiency was found to be LiOH concentration, the increase of which led to a reduction in current efficiency and that was attributed to the increasing back-transport of OH- ions with the increase of LiOH concentration. Current density did not exhibit a significant

effect on current efficiency for the current density range studied. This was possibly due to the fact that limiting current was not reached during the experiments. Temperature slightly improved current efficiency possibly due to increasing transport properties with increasing fluidity. Electrolysis unit power consumption (EPW) increased with the increase of current density due to the increasing potential with the increase of current according to Ohm's law. Power consumption also increased with the increase of LiOH concentration due to low current efficiencies obtained at high LiOH concentrations. Furthermore, temperature increase, which led to the increase of conductivity, caused a decrease in cell potential, correspondingly a decrease in power consumption. A cost estimation targeting to obtain 10% LiOH solution revealed that the experiment with 60°C, 8% LiOH and 4 A/dm^2 operating conditions presented the optimum working parameters to produce lithium hydroxide within the studied range. This was due the fact high temperature and low current density lowers power costs while high LiOH concentration makes it possible to evaporate less water to obtain 10% LiOH solution.

In the next stage of the study, the effect of ion concentrations (Li^+ in anolyte, H^+ in anolyte and OH^- in catholyte) on transport numbers was further examined in order to examine the interactions between ions and to put forward a regression model equation, which will reflect the scientific reality observed in the membrane transport mechanism. In this step, batch and continuous membrane electrolysis experiments were carried out. The main findings were as below:

- A detailed analysis of the interactions between parameters revealed that - other than the individual concentrations terms (Li+ and H+ in anolyte, OH- in catholyte)- the following critical factor pairs were effective in determining the significance of a specific ion concentration on the transport number of lithium; "$Li^+.H^+$ and Li^+/OH^-" ratios for Li^+ ion, "H^+/Li^+ and H^+/OH^-" ratios for H^+ ion and "$OH^-.Li^+$ and OH^-/H^+" ratios for OH^- ion.

- With this finding on interactions, a multiple regression equation adjusted by exponential forms of the critical factor pairs to reflect the effect of these interactions between individual terms was established. This equation gave an R-squared value of 0.953 and was helpful in predicting transport numbers of lithium with an average error value of 8.9%. The R-squared value of the equation increased even higher to 0.975 when only batch data was taken into consideration. This regression equation

was also helpful in predicting transport numbers of H^+ and OH^- ions with an approximation. Transport number of water was fitted in a similar regression equation having an R-squared value of 0.912. Experiments, which were kept out of the model, were used to test these equations. The transport number of these tests could be successfully predicted with average error values of 7% and 3% for lithium and water respectively.

- It was found that the uniqueness in hydrogen ion transport mechanism affected both cation transport numbers as well as water transport number. Transport number of lithium reduced significantly with the increase of hydrogen ions. As for hydroxyl ions, the increase of its concentration also created a reduction in transport number of lithium (T_{Li}), yet much less compared to the effect of hydrogen ions due to ion exclusion. Water transport number increased with the increase of Li^+ concentration while decreased with the increase of H^+ and OH^- concentrations due to the differences in transport mechanism. These findings were compatible with literature data.

- Binary permselectivity values of lithium, hydrogen and hydroxyl ions were determined at constant concentration of the third species and were found to be in line with the other findings on membrane transport behaviour. Membrane's permselectivity for lithium ion against hydrogen ion, $P^{Li/H}$, was under unity in a large interval of concentration ratios since hydrogen ion's unique way of transport through membrane suppressed lithium's influence very strongly. As for $P^{Li/OH}$ values, permselectivity was generally very high in favour of lithium ion thanks to Donnan exclusion. Moreover, $P^{Li/OH}$ decreased with the increase of Li^+ concentration, actually with the suppression of H^+ transport. As for membrane's permselectivity for hydrogen ion against hydroxyl ion, $P^{H/OH}$ values were found to be generally much higher than unity suggesting a strong selectivity for hydrogen ion.

In the last stage of the study, the previous findings obtained with the usage of homogeneous Nafion® N-424 membrane was compared with another perfluorinated membrane (N-438) as well as a heterogeneous cation exchange membrane (MK-40) by carrying out similar regression analyses to model membrane transport. The main findings are as below:

- N-438 membrane showed similar performance as that of N-424 membrane. On the other hand, the heterogeneous structure of MK-40 resulted in a different and mostly a poorer performance,

- Multiple regression equations were formed for each membrane in the similar manner as done for N-424 membrane in the previous section. The fact that R_squared value of MK-40 was relatively lower (0.859) compared to those of other membranes (0.975, 0.974) was attributed mainly to the heterogeneous structure of MK-40, which possibly creates a more chaotic transport mechanism due to its complicated counter-ion pathway compared to the smooth pathway of homogeneous membranes and so makes it hard to put forward a regression model representing ion transport in terms of concentrations only.

- Comparison of the performances revealed that transport number of lithium was generally higher for perfluorinated homogenous N-424 and N-438 membranes than heterogeneous MK-40 membrane. Besides, hydrogen ion transport number did not change greatly according to the membrane used. However, transport number of hydroxyl ion differed according to the membrane type (homogeneous/heterogeneous) used. These results suggested that; though hydrogen concentration was very effective in the distribution of transport numbers due to its highly dominant unique membrane transport mechanism, hydrogen ion transport number did not change greatly according to the membrane used. So it could be claimed that hydrogen ion transport was not affected significantly from the membrane type. This was probably due to the fact that hydrogen ion's advantageous way of transport made it possible that hydrogen transport was not significantly restricted by membrane properties such as water content, fixed charge density and especially the distribution and ratio of hydrophilic domains through which ions and water are transported.

- On the other hand, the change of hydroxyl ion transport number according to the membrane type, especially according to the membrane structure (homogeneous/heterogeneous) was attributed to the differences in Donnan exclusion effect, which is a function of ion exchange capacity, solution concentration and the structure of the membrane (membrane heterogeneity). That's why heterogeneous MK-40 membrane exhibited higher hydroxyl ion transport values than the other homogeneous membranes despite its higher ion exchange capacity, which was in line with literature data.

- The change in transport number of water according to the membrane type was closely linked with the differences in transport numbers of ions. Since hydrogen and hydroxyl ions carry less water compared to lithium ion, water transport number in case of MK-40 membrane was generally lower than the other two membranes, which exhibited higher lithium ion transport numbers.

One of the most outstanding contributions of this study is that "acid-alkaline states of membranes" phenomena (Jörissen and Simmrock, 1991) was further examined with a detailed investigation of the interactions between ions and the results of this investigation was successfully expressed quantitatively with the help of regression equations.

Moreover, lithium sulphate membrane electrolysis process was modelled as a both batch and continuous process in Chapter 3. In this modelling, basic faradaic equations, which define the production of hydrogen/oxygen gases as well as the transport of species through membrane were utilized. The relationships developed in this chapter, once coupled with the regression equations established as a result of experimental studies for the prediction of transport numbers, are able to model the whole electromembrane process. This is one of the most significant contributions of this study, i.e., one can predict the process outcomes (concentrations, efficiencies etc.) reached at any time "t" without the need of performing experiments.

Further investigations can be performed using a three-compartment electromembrane cell, where H_2SO_4, Li_2SO_4 and LiOH are in separate compartments with the help of anion and cation exchange membranes. This process can be more advantageous by means of keeping hydrogen ions away in a separate chamber, which enhances lithium's competition power in membrane transport against hydrogen ions. However, this system can bring forward some disadvantages as well such as acquiring lower efficiencies resulting from hydrogen leakages, producing bases of lower maximum concentrations, higher cell voltages and higher energy consumption. So, these advantages/disadvantages of the three-compartment system can be investigated in a separate study and the results can be compared with those of two-compartment systems.

REFERENCES

Ahmed, M. I., Chang, H. T., Selman, J. R. and Holsen, T. M. (2002). Electrochemical chromic acid regeneration process fitting of membrane transport properties. *J. Membrane Sci., 197*, 63-74.

Aidley, D. J. and Stanfield, P. R. (1996). *Ion channels: Molecules in action*. New York: Cambridge University Press.

An, L., Zhao, T. S., Chai, Z. H., Tan, P. and Zeng, L. (2014). Mathematical modeling of an anion-exchange membrane water electrolyzer for hydrogen production. *Int. J. Hydrogen Energ., 39*, 19869-19876.

Ata, N., Yazicigil, Z. and Oztekin, Y. (2008). The electrochemical investigation of salts partition with ion exchange membranes. *J. Hazard. Mater., 160*, 154-160.

Azotom Co. (n.d.). Monopolar Membranes. Retrieved March 14, 2016 from http://azotom.ru/monopolyarnye-membrany

Bagotsky, V. S. (2006). *Fundamentals of Electrochemistry*. New Jersey: John Wiley & Sons Inc.

Bakery, R. W. (2004). *Membrane Technology and Applications*. West Sussex: John Wiley & Sons Inc.

Bockris, J. O'M. and Reddy, A. K. N. (2002). *Modern Electrochemistry, Volume 1: Ionics*. West Sussex: John Wiley & Sons Inc.

Bouma, R. H. B., Checchetti, A., Chidichimo, G. and Drioli, E. (1997). Permeation through a heterogeneous membrane: the effect of dispersed phase. *J. Membrane Sci., 128*, 141-149.

Calatayud, M. C. M. (2014). *Study of the transport of heavy metal ions through cation-exchange membranes applied to the treatment of industrial effluents*. (PhD Thesis). Polytechnic University of Valencia, Engineering and Industrial Production Programme, Valencia.

Carlberg, A. H. (2015). *Modelling of Membrane in a Sodium Sulfate Electrochemical Splitting Cell*. (MSc Thesis). Chalmers University of Technology, Department of Chemistry and Chemical Engineering, Gothenburg.

Ceynowa, J. (1981). Hydrogen-ion transport numbers in cation exchange membrane determined by emf method. *Polymer, 23*, 203-206.

Chandran, R. R. and Chin, D. T. (1986). Reactor analysis of a chlor-alkali membrane cell. *Electrochim. Acta, 31*, 39-50.

Chapotot, A., Pourcelly, G. and Gavach, C. (1994). Transport competition between monovalent and divalent cations through cation-exchange membranes. Exchange isotherms and kinetic concepts. *J. Membrane Sci., 96*, 167-181.

Choi, J. H., Kim, S. H. and Moon, S. H. (2001). Heterogeneity of Ion-Exchange Membranes: The Effects of Membrane Heterogeneity on Transport Properties. *J. Colloid Interf. Sci., 241*, 120-126.

Davis, S. M. (2006). *Electrochemical splitting of sodium sulfate*. (MSc Thesis).Georgia Institute of Technology, The School of Chemical Engineering, Atlanta.

Donnan, F. G. (1932). Exact thermodynamics of membrane equilibrium. *Z. Phys. Chem. A, 162*, 346-360.

Dupont Co. (2006). *Product Bulletin 97-01: General Information on Nafion® Membrane for Electrolysis*. Fayetteville: Dupont Co.

Dupont Co. (2010). *Product Bulletin 98-00: N-424 membrane Product Information*. Fayetteville: Dupont Co.

Electrocell Co. (n.d.). EC Electro MP-Cell product sheet. Retrieved April 20, 2016 from http://www.electrocell.com/fileadmin/pdf/MPC-brochure.pdf.

Elbeyli, İ. Y., Turan, A. Z. and Kalafatoğlu, İ. E. (2015). The electrochemical production of boric acid. *J. Chem. Technol. Biot.*, 90, 1855-1860.

Eliseeva, T. V., Shaposhnik, V. A., Krisilova,, E. V. and Bukhovets, A. E. (2009). Transport of basic amino acids through the ion-exchange membranes and their recovery by electrodialysis. *J. Membrane Sci., 241*, 86-90.

Elmidaoui, A., Elattar, A., Pismenskaia, N., Gavach, C., and Porcelli, G. (1998). Comparison of transport properties of monovalent anions through anion exchange membranes. *J. Membr. Sci., 43*, 249-261.

Elmidaoui, A., Chay, L., Tahaikt, M., Sahli, M. A. M, Taky, M., Tiyal, F., Khalidi, A. and Hafidi, R. A. (2004). Demineralisation of beet sugar syrup, juice and molasses using an electrodialysis pilot plant to reduce melassigenic ions.*Desalination, 165*, 435.

Ersöz, M., Güğül, I. H., Çimen, A., Leylek, B. and Yıldız, S. (2001). The Sorption of Metals on the Polysulfone Cation Exchange Membranes. *Turk. J. Chem., 25*, 39-48.

Ecbobar, I. and Schafer, A. (2010). *Sustainable Water for the Future: Water Recycling versus Desalination*. Amsterdam: Elsevier.

Firdaous, L., Malériat, J. P., Schlumpf, J. P. and Quéméneur, F. (2007). Transfer of Monovalent and Divalent Cations in Salt Solutions by Electrodialysis. *Separ. Sci. Technol., 42*, 931-948.

Geise, G. M., Cassady, H. J., Paul, D. R., Logan, B. E. and Hickner, M. A. (2014). Specific ion effects on membrane potential and the permselectivity of ion exchange membranes. *Phys. Chem. Chem. Phys., 16*, 21673-21681.

Genders, D. (1995). Electrochemical salt splitting, *Watts New Quarterly Newsletter, 1*, 1-8.

Goodridge, F. and Scott, K. (1995). *Electrochemical Process Engineering*. New York: Springer.

Grabowski, A. (2010). *Electromembrane Desalination Processes for Production of Low Conductivity Water*. Berlin: Logos Verlag.

Gregor, H. P. (1957). Interpolymer ion-selective membranes. *Proceedings of the Symposium on Saline Water Conversion '57*. National Academy of Sciences, Washington, 4-6 November.

Guo, H., You, F., Yu, S., Li, L. and Zhao, D. (2015). Mechanisms of chemical cleaning of ion exchange membranes: A case study of plant-scale electrodialysis for oily wastewater treatment. *J. Membrane Sci., 496*, 310-317.

Güler, E. (2014). *Anion exchange membrane design for reverse electrodialysis*. (PhD Thesis). University of Twente, Enschede.

Hamani, H., Bouamrane, R., Kameche, M., Innocent, C. and Derriche, Z. (2013). Transport number and current–voltage of a cation exchange membrane equilibrated in aqueous and organic solutions. *Phys. Chem. Liq., 51*, 265-280.

Hwang, G. J., Ohya, H. and Nagai, T. (1999). Ion exchange membrane based on block copolymers. Part III; preparation of cation exchange membrane. J. Membrane Sci., 156, 61-65.

Inamuddin, I. and Luqman, M. (2012). *Ion exchange technology 1 - Theory and materials*. New York: Springer.

Ion Power Co. (n.d.). Nafion Membrane N-438. Retrieved February 20, 2016 from http://www.nafionstore.com/store/products/88/Nafion-Membrane-N438-Teflon-Fabric-Reinforced

Jajali, A. A., Mohammadi, F. and Ashrafizadeh, S. N. (2009). Effects of process conditions on cell voltage, current efficiency and voltage balance of a chlor-alkali membrane cell. *Desalination, 237*, 126-139.

Jensen, J. O., Bandur, V., Bjerrum, N. J., Jensen, S. H., Ebbesen, S., Mogensen, M. Tophøj, N. and Yde, L. (2008). *Pre-Investigation of water electrolysis* (Report No: PSO-F&U 2006-1-6287). Denmark: DTU.

Jobson, J. D. (1999). *Applied Multivariate Data Analysis*. New York: Springer.

Jörissen, J. and Simmrock, K. H. (1991). The behaviour of ion exchange membranes in electrolysis and electrodialysis of sodium sulphate.*J. Appl. Electrochem.*, 21, 869-876.

Judd, S. and Jefferson, B. (2003). *Membranes for Industrial Wastewater Recovery and Re-use*. Oxford: Elsevier.

Kamienski, C. W., McDonald, D. P., Stark, M. W. and Papcun, J. R.(2004). Lithium and Lithium Compounds. In *Kirk-Othmer Encyclopedia of Chemical Technology*.

Kaveh, N. S., Ashrafizadeh, S. N. and Mohammadi, F. (2008). Development of an artificial neural network model for prediction of cell voltage and current efficiency in a chlor-alkali membrane cell. *Chem. Eng. Res. Des., 86*, 461-472.

Kim, Y. (2010). *Ionic Separation in Electrodialysis: Analyses of Boundary Layer, Cationic Partitioning, and Overlimiting Current*.(PhD Thesis). The University of Texas at Austin, The Graduate School, Austin.

Kim, Y., Walker, W. S. and Lawler, D. F. (2012). Competitive separation of di- vs. mono-valent cations in electrodialysis: Effects of the boundary layer properties. *Water Res., 46*, 2042-2056.

Korngold, E., Belayev, N., Aronov, L. and Oren, Y. (2006). Conversion of dipotassium malate to malic acid by electromembrane processes. *Desalination, 195*, 153-159.

Kortüm, G. (1957). *Lehrbuch der Elektrochemie*. Weinheim: Verlag Chemie.

Koter, S. and Kultys, M. (2008). Electric transport of sulfuric acid through anion-exchange membranes in aqueous solutions. *J. Membrane Sci., 318*, 467-476.

Koter, S and Warszawski A. (2000). Electromembrane processes in environment protection. *Pol. J. Environ. Stud., 9*, 45-56.

Krol, J. J. (1997). *Monopolar and bipolar ion exchange membranes - Mass transport limitations*.(PhD Thesis). University of Twente, Enschede.

Lee, J. S., Quan, N. D., Hwang, J. M., Lee, S. D., Kim, H., Lee, H. and Kim, H. S. (2006). Polymer electrolyte membranes for fuel cells. *J. Ind. Eng. Chem., 12*, 175-183.

Liberti, L. and Helfferich, G. (1983).*Mass Transfer and Kinetics of Ion Exchange*. The Hague: Martinus Nijhoff Publishers.

Liu, N., Zhao, X., Wang, Y. and Fei, W. (2010). Electrolytic Regeneration of Decarbonising Potassium Carbonate Solution. *Chinese J. Chem. Eng., 18*, 583-543.

Manabe, A., Kashiwase, M., Hashimoto, T., Hayashida, T., Kato, A., Hirao, K., Shimomura, I. and Nagashima, I. (2013). Basic study of alkaline water electrolysis. *Electrochim. Acta, 100*, 249-256.

Marder, L., Bittencourt, S. D., Ferreira, J. Z. and Bernardes, A. M. (2016). Treatment of molybdate solutions by electrodialysis: The effect of pH and current density on ions transport behavior. *Sep. Purif. Technol., 167*, 32-36.

Martí-Calatayud, M. C., Buzzi, D. C., García-Gabaldón, M., Bernardes, A. M., Tenório, J. A. S. and Pérez-Herranz, V. (2014). Ion transport through homogeneous and heterogeneous ion-exchange membranes in single salt and multicomponent electrolyte solutions. *J. Membrane Sci., 466*, 45-57.

Molnar, C. J. and Drio, M. M. (1977). Effects of brine purity on chlor-alkali membrane cell performance, *Proceedings of The Electrochemical Society Fall Meeting*, Atlanta, Georgia, October.

Nagarele, R. K., Gohil, G. S. and Shahi, V. K. (2006). Recent developments on ion-exchange membranes and electro-membrane processes. *Adv. Colloid Interfac.,119*, 97-130.

Newman, J. and Thomas-Alyea, K. E.,(2004). *Electrochemical Systems*. New Jersey: John Wiley & Sons Inc.

Noble, R. D. and Stern, S. A. (1995). *Membrane Separations Technology Principles and Applications*. Amsterdam: Elsevier.

Novikova, S. A., Volodina, E. I., Pis'menskaya, N. D., Veresov, A. G., Stenina, I. A. and Yaroslavtsev, A. B. (2005). Ionic Transport in Cation-Exchange Membranes MK-40 Modified with Zirconium Phosphate. *Russ. J. Electrochem+, 41*, 1070-1076.

Numes, S. P. and Peinemann, K. V.(2001). *Membrane Technology in the Chemical Industry*. Weinheim: Wiley-VCH.

O'Brien, T. F., Bommaraju, T. V. and Hine, F. (2005). *Handbook of Chlor Alkali Technology*. New York: Springer.

Ogata, Y., Kojima, T., Uchiyama, S., Yasuda, M. and Hine, F. (1989). Effects of the Brine Impurities on the Performance of the Membrane-Type Chlor-Alkali Cell. *J. Electrochem. Soc., 136*, 91-95.

Okada, T. (1999a). Theory for water management in membranes for polymer electrolyte fuel cells Part 1. The effect of impurity ions at the anode side on the membrane performances. *J. Electroanal. Chem., 465*, 1-17.

Okada, T. (1999b). Theory for water management in membranes for polymer electrolyte fuel cells: Part 2. The effect of impurity ions at the cathode side on the membrane performances. *J. Electroanal. Chem., 465*, 18-29.

Okada, T., Arimura, N., Satou, H., Yuasa M. and Kikuchi, T. (2005). Membrane transport characteristics of binary cation systems with Li^+ and alkali metal cations in perfluorosulfonated ionomer. *Electrochim. Acta, 50*, 3569-3575.

Okada, T., Kjelstrup-Ratkje, S., Moller-Holst, S., Jerdal, L. O., Friestad, K., Xie, G. and Holmen, R. (1996). Water and ion transport in the cation exchange membrane systems $NaCl-SrCl_2$ and $KCl-SrCl_2$. *J. Membrane Sci., 111*, 159-167.

Okada, T., Moller-Holst, S., Gorseth, O. and Kjelstrup, S. (1998). Transport and equilibrium properties of Nafion membranes with H^+ and Na^+ ions. *J. Electroanal. Chem., 442*, 137-145.

Okada, T., Ratkje, S. K. and Hanche-Olsen, H. (1992). Water transport in cation exchange membranes. *J. Membrane Sci., 66*, 179-192.

Okada, T., Satou, H., Okuno, M. and Yuasa M. (2002). Ion and Water Transport Characteristics of Perfluorosulfonated Ionomer Membranes with H^+ and Alkali Metal Cations. *J. Phys. Chem. B, 106*, 1267-1273.

Okada, T., Xie, G., Gorseth, O., Kjelstrup, S., Nakamura, N. and Arimura, T. (1998). Ion and water transport characteristics of Nafion membranes as electrolytes. *Electrochim. Acta, 43*, 3741-3747.

Pabby, A. K., Rizvi, S. S. H. and Sastre, A. M. (2009). *Handbook of Membrane Separations; Chemical, Pharmaceutical, Food, and Biotechnological Applications*. Boca Raton: CRC Press.

Petrucci, R. H., Herring, F. G., Madura, J. D. and Bissonnette, C. (2011). *General Chemistry - Principles and Modern Applications*. Toronto: Pearson.

Pletcher, D. and Walsh, F. C.(1990). *Industrial Electrochemistry*. New Jersey: Kluwer.

Porter, M. C. (1990). *Handbook of Industrial Membrane Technology*. New Jersey: Noyes Pub.

Rácz, R. and Ilea, P. (2013) Electrolytic recovery of Mn3O4 and Zn from sulphuric acid leach liquors of spent zinc–carbon–MnO2 battery powder. *Hydrometallurgy, 139*, 116-123.

Rakib, M., Moçoteguy, Ph., Viers, Ph., Petit, E. and Durand, G. (1999a). Behaviour of Nafion 350 membrane in sodium sulfate electrochemical splitting: continuous process modelling and pilot scale tests. *J. Appl. Electrochem., 29*, 1439-1448.

Rakib, M., Moçoteguy, Ph., Viers, Ph., Petit, E. and Durand, G. (1999b). Two-compartment membrane electrolysis of sodium sulphate: sodium and hydrogen ions transport and water transfer through Nafion® 350 membrane, ICOM '99, Toronto, Canada, June 12-18.

Rohm and Haas Co. (2006). *Amberlite IRC748 Industrial Grade Chelating Resin for Metals Removal*. Philadelphia: R&H Co.

Ryabtsev, A. D., Nemkov, N. M., Kotsupalo, N. P. and Serikova, L. A. (2004). Preparation of High-Purity Lithium Hydroxide Monohydrate from Technical-Grade Lithium Carbonate by Membrane Electrolysis. *Russ. J. Appl. Chem+, 77*, 1108-1116.

Saito, M., Arimura, N., Hayamizu, K. and Okada, T. (2004). Mechanisms of Ion and Water Transport in Perfluorosulfonated Ionomer Membranes for Fuel Cells. *J. Phys. Chem. B, 108*, 16064-16070.

Saito, M., Hayamizu, K. and Okada, T. (2005). Temperature Dependence of Ion and Water Transport in Perfluorinated Ionomer Membranes for Fuel Cells. *J. Phys. Chem. B, 109*, 3112-3119.

Sata, T. (2004). *Ion Exchange Membranes – Preparation, Characterization, Modification and Application*. Cambridge: RSC.

Sata, T. Sata, T. and Yang, W. (2002). Studies on cation-exchange membranes having permselectivity between cations in electrodialysis. *J. Membrane Sci., 206*, 31-60.

Savari, S., Sachdeva, S. and Kumar, A. (2008). Electrolysis of sodium chloride using composite poly(styrene-co-divinylbenzene) cation exchange membranes. *J. Membrane Sci., 310*, 246-261.

Scoma, A., Varela-Corredor, F., Bertin, L., Gostoli, C. and Bandini, S. (2016). Recovery of VFAs from anaerobic digestion of dephenolized Olive Mill Wastewaters by Electrodialysis. *Sep. Purif. Technol., 159*, 81-91.

Scott, K. and Hughes, R.(1996). *Industrial membrane separation technology*. Tullamore: Springer.

Serre, E., Rozoy, E., Pedneault, K., Lacour, S. and Bazinet, L. (2016). Deacidification of cranberry juice by electrodialysis: Impact of membrane types and configurations on acid migration and juice physicochemical characteristics. *Sep. Purif. Technol., 163*, 228-237.

Shibli, S. M. A. and Noel, M. (1993). Evaluation of transport properties of cation exchange membranes for application in alkali concentrators. *J. Appl. Electrochem., 23*, 1147-1150.

Strathmann, H. (2004). *Ion-Exchange Membrane Separation Processes*. Amsterdam: Elsevier.

Strathmann, H. (2010). Electromembrane Processes: Basic Aspects and Applications. In E. Drioli, L. Giorno (Eds.), *Comprehensive Membrane Science and Engineering* (1st ed., Vol. 2, pp. 391-429). Amsterdam: Elsevier.

Tanaka, Y. (2007). *Ion Exchange Membranes Fundamentals and Applications*. Amsterdam: Elsevier.

Timashev, S. (1991). *Physical Chemistry of Membrane Processes*. West Sussex: Ellis Horwood.

Tuomi, S., Santasalo-Aarnio, A., Kanninen, P. and Kallio, T. (2013). Hydrogen production by methanol-water solution electrolysis with an alkaline membrane cell. *J. Power Sources, 229*, 32-35.

Tuckerman, M. E., Marx, D. and Parrinello, M. (2002). The nature and transport mechanism of hydrated hydroxide ions in aqueous solution. *Nature, 417*, 925-929.

Tuckerman, M. E., Chandra, A. and Marx, D. (2005). Structure and Dynamics of OH^-(aq). *Acc. Chem. Res., 39*, 925-158.

Turan, A. Z., Elbeyli, İ. Y. and Kalafatoğlu, İ. E. (2012a). Membrane Electrolysis of Borax Pentahydrate ($Na_2B_4O_7.5H_2O$). *J. Electrochem. Soc.*, 159, 149-153.

Turan, A. Z., Elbeyli, İ. Y., Bahar, T. and Kalafatoğlu, İ. E. (2012b). The performance of Nafion®424 in the membrane electrolysis of borax solution. *J. Ind. Eng. Chem., 18*, 1102-1106.

Tzanetakis, N., Taama, W. M. and Scott, K. (2003). Comparative performance of ion exchange membranes for salt splitting. *Filtr. Separat., 40*, 33-39.

Tzanetakis, N., Taama, W. M. and Scott, K. (2005). Salt splitting in a three-compartment membrane electrolysis cell. *Filtr. Separat., 39*, 30-38.

Volkov, V. I., Pavlov, A. A. and Sanginov, E. A. (2011). Ionic transport mechanism in cation-exchange membranes studied by NMR technique. *Solid State Ionics, 188*, 124-128.

Wendt, H. and Kreysa, G. (1999). *Electrochemical Engineering*. Berlin: Springer.

Wietelmann, U. and Steinbild, M. (2014). Lithium and Lithium Compounds. *In Ullmann's Encyclopedia of Industrial Chemistry*.

Wilhelm, F. G. (2001). *Bipolar Membrane Electrodialysis*. (PhD Thesis). University of Twente, Enschede.

Xie, G. and Okada, T. (1996). Pumping effects in water movement accompanying cation transport across Nafion 117 membranes. *Electrochim. Acta, 41*, 1569-1571.

Yazicigil, Z. (2007). Salt splitting with cation-exchange membranes. *Desalination, 212*, 70-78.

Zabolotsky, V.I. and Nikonenko, V.V. (1993). Effect of structural membrane inhomogeneity in transport properties.*J. Membrane Sci., 79*,181–198.

Zoski, C. G. (2007). *Handbook of Electrochemistry*. Amsterdam: Elsevier.

APPENDICES

APPENDIX A: Multiple Regression Model

APPENDIX A: Multiple Regression Model

An important scope of this study is to model membrane transport numbers of ions and water a multiple regression analysis. That's why the theory of this statistical method is described in this section.

Multiple regression is a statistical approach between a dependent variable and more than one independent variables. The general form of multiple regression equation is(Jobson, 1999);

$$y_i = \beta_0 + \beta_1 x_{i1} + \beta_2 x_{i2} + \cdots + \beta_p x_{ip} + u_i \qquad \text{(A 1.1)}$$

where *y* is the dependent variable, *x* terms are independent variables, *p* is the number of dependent variables, *i* is the number of observations, β is regression coefficient and *u* is unobserved error term. A sample of *n* observations gives the following set of equations;

$$y_1 = \beta_0 + \beta_1 x_{11} + \beta_2 x_{12} + \cdots + \beta_p x_{1p} + u_1 \qquad \text{(A 1.2a)}$$

$$y_2 = \beta_0 + \beta_1 x_{21} + \beta_2 x_{22} + \cdots + \beta_p x_{2p} + u_2 \qquad \text{(A 1.2b)}$$

$$y_n = \beta_0 + \beta_1 x_{n1} + \beta_2 x_{n2} + \cdots + \beta_p x_{np} + u_n \qquad \text{(A 1.2c)}$$

This set of equations can be written in the following matrix form;

$$\mathbf{y} = \mathbf{X\beta} + \mathbf{u} \qquad \text{(A 1.3)}$$

Least squares method can be utilized to estimate the parameter vector $\boldsymbol{\beta}$. The function that determines $\boldsymbol{\beta}$ with the minimization of the sum of squares is;

$$\zeta^2 = \sum_{i=1}^{n} (y_i - \beta_0 - \beta_1 x_{i1} - \beta_2 x_{i2} - \cdots - \beta_p x_{ip})^2 = (\mathbf{y} - \mathbf{X\beta})'(\mathbf{y} - \mathbf{X\beta}) \qquad \text{(A 1.4)}$$

The summations in Eq. (A 1.4) are calculated as below;

$$\sum_{i=1}^{n} y_i = n\beta_0 + \beta_1 \sum_{i=1}^{n} x_{i1} + \beta_2 \sum_{i=1}^{n} x_{i2} + \cdots + \beta_p \sum_{i=1}^{n} x_{ip} \qquad \text{(A 1.5)}$$

$$\sum_{i=1}^{n} x_{i1} y_i = \beta_0 \sum_{i=1}^{n} x_{i1} + \beta_1 \sum_{i=1}^{n} {x_{i1}}^2 + \beta_2 \sum_{i=1}^{n} x_{i1} x_{i2} + \cdots \beta_p \sum_{i=1}^{n} x_{i1} x_{ip} \qquad \text{(A 1.6)}$$

$$\sum_{i=1}^{n} x_{i2}y_i = \beta_0 \sum_{i=1}^{n} x_{i2} + \beta_1 \sum_{i=1}^{n} x_{i1}x_{i2} + \beta_2 \sum_{i=1}^{n} {x_{i2}}^2 + \cdots \beta_p \sum_{i=1}^{n} x_{i2}x_{ip} \qquad \text{(A 1.7)}$$

.

.

.

$$\sum_{i=1}^{n} x_{ip}y_i = \beta_0 \sum_{i=1}^{n} x_{ip} + \beta_1 \sum_{i=1}^{n} x_{i1}x_{ip} + \beta_2 \sum_{i=1}^{n} x_{i2}x_{ip} + \cdots \beta_p \sum_{i=1}^{n} {x_{ip}}^2 \qquad \text{(A 1.8)}$$

The normal equations can also be written in matrix notation as;

$$\mathbf{X'y} = \mathbf{X'X\beta} \qquad \text{(A 1.9)}$$

where;

$$\mathbf{X'y} = \begin{bmatrix} \sum_{i=1}^{n} y_i \\ \sum_{i=1}^{n} x_{i1}y_i \\ \sum_{i=1}^{n} x_{i2}y_i \\ \vdots \\ \sum_{i=1}^{n} x_{ip}y_i \end{bmatrix}_{(p+1)x1} \qquad \text{(A 1.10)}$$

$$\mathbf{X'X} = \begin{bmatrix} n & \sum_{i=1}^{n} \mathrm{x}_{i1} & \sum_{i=1}^{n} \mathrm{x}_{i2} & & \sum_{i=1}^{n} \mathrm{x}_{ip} \\ \sum_{i=1}^{n} \mathrm{x}_{i1} & \sum_{i=1}^{n} \mathrm{x}_{i1}{}^{2} & \sum_{i=1}^{n} \mathrm{x}_{i1}\mathrm{x}_{i2} & \cdots & \sum_{i=1}^{n} \mathrm{x}_{i1}\mathrm{x}_{ip} \\ \sum_{i=1}^{n} \mathrm{x}_{i2} & \sum_{i=1}^{n} \mathrm{x}_{i1}\mathrm{x}_{i2} & \sum_{i=1}^{n} \mathrm{x}_{i2}{}^{2} & \cdots & \sum_{i=1}^{n} \mathrm{x}_{i2}\mathrm{x}_{ip} \\ \vdots & \vdots & \vdots & \cdots & \vdots \\ \sum_{i=1}^{n} \mathrm{x}_{ip} & \sum_{i=1}^{n} \mathrm{x}_{i1}\mathrm{x}_{ip} & \sum_{i=1}^{n} \mathrm{x}_{i2}\mathrm{x}_{ip} & & \sum_{i=1}^{n} \mathrm{x}_{ip}{}^{2} \end{bmatrix}_{(\mathrm{p}+1)\mathrm{x}(\mathrm{p}+1)} \qquad \text{(A 1.11)}$$

The solution vector **b** is denoted by;

$$\mathbf{b} = (\mathbf{X'X})^{-1}\mathbf{X'y} \qquad \text{(A 1.12)}$$

CURRICULUM VITAE

Name Surname: Abdullah Zahid Turan

Place and Date of Birth: Giresun/Turkey, 26.01.1984

E-Mail: azturan@gmail.com

EDUCATION:

B.Sc.: Chemical Engineering, Istanbul Technical University, 2007

M.Sc.: Chemical Engineering, Istanbul Technical University, 2009

PROFESSIONAL EXPERIENCE AND REWARDS:

09.2009-present: Sr. Researcher, TÜBİTAK Marmara Research Centre.

PUBLICATIONS, PRESENTATIONS AND PATENTS ON THE THESIS:

▪ **Turan, A.Z.**, Ünveren, E. and Bulutcu, A.N., 2016. The prediction of membrane transport numbers in the salt splitting of lithium sulphate, J. Electrochem Soc., 163, F969-978, doi: 10.1149/2.0201609jes.

▪ **Turan, A.Z.** et. al., 2015. The behaviour of Nafion®424 membrane in the electrochemical production of lithium hydroxide, J. Chem. Technol. Biot., Accepted article published: 18 November 2015.

OTHER PUBLICATIONS, PRESENTATIONS AND PATENTS:

▪ Elbeyli, İ.Y., **Turan, A.Z.,** and Kalafatoğlu, İ.E., 2015. The Electrochemical Production of Boric Acid, J. Chem. Technol. Biot., 90, 1855-1860.

▪ **Turan, A.Z.,** Elbeyli, İ.Y., and Kalafatoğlu, İ.E., 2012. Membrane Electrolysis of Borax Pentahydrate (Na2B4O7.5H2O), J. Electrochem. Soc., 159(9), 149-153.

▪ **Turan, A.Z.,** Elbeyli, İ.Y., Bahar, T. and Kalafatoğlu, İ.E., 2012. The performance of Nafion®424 in the membrane electrolysis of borax solution, J. Ind. Eng. Chem., 18, 1102-1106.

▪ Haykiri-Acma, H., **Turan, A.Z.,** Yaman, S. and Kucukbayrak, S., 2010.

Controlling the excess heat from oxy-combustion of coal by blending with biomass, Fuel Process. Technol., 91, 1569-1575.

▪ Ozdemir, O., Turan, M., **Turan, A.Z.,** Faki, A. and Engin, A.B., 2009. Feasibility analysis of color removal from textile dyeing wastewater in a fixed-bed column system by surfactant-modified zeolite (SMZ), J. Hazard. Mater., 166, 647-654.

▪ Engin, A.B., Özdemir, Ö.,Turan, M. and **Turan, A.Z.,** 2008. Color removal from textile dyebath effluents in a zeolite fixed bed reactor: Determination of optimum process conditions using Taguchi method, J. Hazard. Mater., 159, 348-353.

▪ Faki, A., Turan, M., Ozdemir O. and **Turan, A.Z.,** 2008. Analysis of Fixed-Bed Column Adsorption of Reactive Yellow 176 onto Surfactant-Modified Zeolite, Ind. Eng. Chem. Res., 47, 6999–7004.

▪ **Turan, A.Z.,** Elbeyli, İ. Y., and Kalafatoğlu, İ.E. “Membrane Electrolysis of Borax Pentahydrate”, 17th International Symposium on Boron, Borides and Related Materials, Sept. 11-17 2011, İstanbul.